The Dissertation Committee for Erika Caro Gomez Certifies that this is the approved version of the following dissertation:

IDENTIFICATION OF PROTECTIVE RICKETTSIAL ANTIGENS FOR VACCINE DEVELOPMENT

Committee:

Gustavo Valbuena, M.D., Ph.D., Chair

Jere McBride, Ph.D.

Gregg N. Milligan, Ph.D.

Leonard Moise, Ph.D.

Lynn Soong, M.D., Ph.D.

Robin Stephens, Ph.D.

David W. Niesel, Ph.D.

Dean, Graduate School of Biomedical Sciences

IDENTIFICATION OF PROTECTIVE RICKETTSIAL ANTIGENS FOR VACCINE DEVELOPMENT

by

Erika Caro Gomez, B.S., M.S.

Dissertation

Presented to the Faculty of the Graduate School of

The University of Texas Medical Branch

in Partial Fulfillment

of the Requirements

for the Degree of

Doctor of Philosophy

The University of Texas Medical Branch

June 18, 2014

Dedication

To my beloved family that always encouraged me to pursue my dreams.

Acknowledgements

I am grateful to all the gifted individuals that help me to accomplish this work. First, I want to acknowledge my mentor Gustavo Valbuena who gave me the opportunity to join his lab and participate in this challenging, inspiring and interesting journey. To all members of the Valbuena lab Paula, Marilyn, Mike, Cesar and Bruno for their support and interesting conversations about science and life, specially to Angelica and Yenny who besides helping me during long experiment journeys also offered me their friendship and make really enjoyable my experience at UTMB. I am also grateful to Sandra and Evandro my fellow friends at the GSBS for their support.

I want to sincerely thank to all members of my supervisory committee, Dr. Jere McBride, Dr. Gregg Milligan, Dr. Lenny Moise, Dr. Lynn Soong and Dr. Robin Stephens, for their valuable feedback and timely advice.

Finally, I would like to acknowledge the James W. McLaughlin and Vale-Asche Fellowship for generously supporting my graduate work.

IDENTIFICATION OF PROTECTIVE RICKETTSIAL ANTIGENS FOR VACCINE DEVELOPMENT

Publication No._____

Erika Caro Gomez, Ph.D.
The University of Texas Medical Branch, 2014

Supervisor: Gustavo Valbuena

The genus *Rickettsia* contains some of the most lethal pathogens known to man, including *Rickettsia prowazekii*, a select agent that could be used as a biological weapon. Although *Rickettsia* spp. cause important diseases of public health importance and there is a need to develop countermeasures for biodefense, there are no commercially available vaccines. Resistance to rickettsial infections and cross-protective immunity between typhus and spotted fever group rickettsiae are attributed to the induction of antigen-specific T cells, particularly $CD8^+$ T cells. Defining specific T-cell antigens and correlates of protective cellular immunity are critical steps towards vaccine development for *Rickettsia*. However, these are major gaps in this field that are impeding progress towards a vaccine. In this investigation, I developed and validated an *in silico* algorithm that allowed the identification of five novel *R. prowazekii* vaccine antigen candidates recognized by $CD8^+$ T cells. The novel rickettsial vaccine candidate antigens, RP884, RP778, RP739, RP598, and RP403, protected mice against a lethal challenge with typhus group *R. typhi* and spotted fever group *R. conorii*, which demonstrates a level of cross-

protective immunity against these molecularly distinct pathogenic rickettsial groups. Moreover, considering that surviving a natural rickettsial infection results in long-lived immunity, I characterized the primary and memory $CD8^+$ T cell response after a rickettsial challenge using phenotypic markers for activation and measured effector molecules that could be used to validate the level of cellular immunity induced by novel antigens. Based on the studies presented herein, four correlates of protection against *R. typhi* infection in animals immunized with protective rickettsial antigens are proposed: 1) production of IFN-γ by antigen experienced $CD3^+CD8^+CD44^{high}$ cells, 2) production of Granzyme B by $CD27^{low}CD43^{low}$ antigen-experienced $CD8^+$ T cells, 3) generation of memory-type $CD8^+$ T cells [Memory Precursor Effector Cells (MPECs), as well as $CD127^{high}CD43^{low}$, and $CD27^{high}CD43^{low}$ $CD8^+$ T cells], and 4) generation of effector-like memory $CD8^+$ T cells ($CD27^{low}CD43^{low}$). Together, these findings validate a reverse vaccinology approach as a strategy to identify protective rickettsial antigens that induce cellular immunity. In addition, this work demonstrates the feasibility of developing a subunit vaccine that triggers T-cell-mediated cross-protection between phylogenetically distant *Rickettsia* spp. Finally, the proposed correlates could be useful for the validation and assessment of the quality of the $CD8^+$ T cell responses induced by novel antigens with potential use in a vaccine against *Rickettsia*.

TABLE OF CONTENTS

LIST OF TABLES

LIST OF FIGURES

LIST OF APPENDIX

LIST OF ABBREVIATIONS

%OPT	Percentage of the optimal score value for RANKPEP predictions
µl	micro litter
ABSL3	Animal biosafety level-3
ANNs	Artificial neural networks
ANOVA	Analysis of variance
APC	Antigen presenting cell
ATCC	American Type Culture Collection
BLASTp	Basic local alignment search tool for proteins
BSL3	Biosafety level-3
CCR	Chemokine receptor which recognize C-C chemokines
CD	Cluster of differentiation
CDC	Centers for Disease Control
CFSE	5-(and 6)-Carboxyfluorescein diacetate succinimidyl ester
CXCL	Chemokine (C-X-C motif) ligand
CXCR	Chemokine receptor which recognize C-X-C chemokines
DAMPS	Danger-associated molecular patterns
DC	Dendritic cell
DNA	Deoxyribonucleic acid
Dpi	days post-infection
EECs	Early effector cells
ELI	Expression library immunization
ELISpot	Enzyme linked immunosorbent spot
ER	Endoplasmic reticulum
BGS	Bovine growth serum
FITC	Fluorescein isothiocyanate
FMO	Fluorescent minus one, flow cytometry control
gltA	Citrate synthase-encoding gene
HEPES	Hydroxyethyl piperazineethanesulfonic acid
HLA	Human leukocyte antigen system

Hpi	Hours post-infection
i.p.	Intraperitoneally
i.v.	Intravenously
IACUC	Institutional Animal Care and Use Committee
ICAM-1	Intercellular adhesion molecule 1
ICS	Intracellular cytokine staining
ID_{50}	Infectious dose 50%
IDO	Indoleamine-pyrrole 2,3-dioxygenase
IFA	Indirect fluorescent antibody assay
IFN	Interferon
IgG	Immunoglobulin G
IL	Interleukin
i.m.	Intramusculary
iNOS	Inducible nitric oxide synthase
KLRG1	Killer cell lectin-like receptor subfamily G member 1
LD_{50}	Lethal dose 50% or median lethal dose
ldhal6b	L-lactate dehydrogenase A-like 6B
LFA-1	Lymphocyte function-associated antigen 1
Luc2	Firefly luciferase reporter gen *luc2*
MenB	Meningococcal B
MFT	Multifunctional T cell
MGB	Minor groove binder
MHC	Major histocompatibility complex
MPECs	Memory precursor effector cells
MVA	Modified vaccinia Ankara virus
NFkB	Nuclear factor kappa-light-chain-enhancer of activated B cells
NK	Natural killer cells
NLR	Nucleotide-binding oligomerization domain receptors
OmpA	Outer membrane protein A
OmpB	Outer membrane protein B
ORF	Open reading frame

ORFeome	Collection of open reading frames
PAMPS	Pathogen-associated molecular patterns
PBS	Phosphate-buffered saline
PE	R-Phycoerythrin
Q-PCR	Quantitative real-time polymerase chain reaction
RLR	Retinoic-acid-inducible protein 1-like receptors
SEM	Standard error of the mean
Sca	Surface cell antigen
SLECs	Short-lived effector cell
SPG	Sucrose-phosphate-glutamate buffer
TAP	Transporter associated with antigen processing
TB	Tuberculosis
T_{CM}	T central memory cell
TCR	T cell receptor
T_{EM}	T effector memory cell
Th1	Type 1 T helper cells
TLR	Toll-like receptor
TNF	Tumor necrosis factor
TNFR	Tumor necrosis factor receptor superfamily
UCOE	Ubiquitous chromatin opening element
VCAM-1	Vascular cell adhesion molecule 1

CHAPTER 1: Introduction and Background

RICKETTSIA

Biology and Life Cycle

Rickettsiae are small (0.3–0.5×0.8–1.0 μm) arthropod-borne obligately intracellular Gram-negative bacteria that primarily infect endothelial cells [1]. They are members of the genus *Rickettsia* within the family Rickettsiaceae in the order Rickettsiales. Rickettsiae are divided in four groups based on their biological, genetic and antigenic characteristics [2,3]:

1. Spotted fever group (SFG) *Rickettsia* include organisms highly pathogenic to humans such as tick-borne *R. rickettsii* (Rocky Mountain spotted fever, RMSF), *R. conorii* (Mediterranian spotted fever), and *R. parkeri* (mild spotted fever rickettsiosis found in North and South America) among others [4].
2. Typhus group *Rickettsia* has only two members: 1) *R. typhi*, agent of flea-borne murine or endemic typhus, which is probably one of the most prevalent and neglected rickettsiosis [5]; and 2) highly pathogenic *R. prowazekii*, agent of louse-borne epidemic typhus, which remains on the CDC's list of biothreat select agents that has been previously developed as a bioweapon [6, 7]. In addition, *R. prowazekii* is also the causative agent of Brill-Zinsser disease, the only known rickettsiosis that can present as a relapsing form years after the primary infection in asymptomatic carriers [8].

3. Transitional group *Rickettsia* include pathogenic *R. akari* (rickettsialpox), *R. australis* (Queensland tick typhus), and *R. felis.*
4. Ancestral group which include non-pathogenic *R. bellii* and *R. canadensis.*

Table 1.1 Summarizes the classification of recognized *Rickettsia* spp.

Table 1.1 Classification of *Rickettsia*[a]

Group	Organism	Disease
Spotted Fever	*R. rickettsii*	Rocky Mountain spotted fever
	R. conorii	Mediterranean spotted fever
	R. africae	African tick-bite fever
	R. parkeri	Spotted fever rickettsiosis
	R. slovaca	Tick-borne lymphadenopathy
	R. sibirica	Lymphangitis
	R. heilongjiangensis	Far-Eastern spotted fever
	R. massiliae	Spotted fever rickettsiosis
	R. honei	Flinders Island spotted fever
	R. japonica	Japanese spotted fever
	R. montanensis	Non pathogenic?
	R. peacockii	Non pathogenic?
	R. rhipicephali	Non pathogenic?
Typhus	*R. prowazekii*	Epidemic typhus
	R. typhi	Murine typhus
Ancestral	*R. bellii*	Unknown
	R. canadensis	Unknown
Transitional	*R. akari*	Rickettsialpox
	R. australis	Queensland tick typhus
	R. felis	Flea-borne spotted fever

[a] Adapted from D. H. Walker and N. Ismail, "Emerging and re-emerging rickettsioses: endothelial cell infection and early disease events.," Nat. Rev. Microbiol., vol. 6, no. 5, pp. 375–386, May 2008.

Rickettsia have small genomes (1.1 to 1.3 Mb), and due to its obligately intracellular niche, have undergone a process of reductive evolution and thus developed a dependence on the host cell for several biosynthetic metabolic pathways [9–12]. In fact, a number of these synthetic pathways have been replaced by transport systems [9]. Interestingly, rickettsiae have a close phylogenetic and evolutionary relationship with the origin of modern mitochondria, and there is a remarkable similarity at the functional level such as the ATP synthesis pathway [11].

Comparative genome analyses have defined the level of genetic similarity between rickettsiae of different groups. Comparisons among *R. prowazekii*, *R. typhi* and *R. conorii* genomes have indicated that these pathogens share 775 genes. Furthermore, it has been estimated that *R. conorii* and *R. typhi* genomes contain about 800 of the 834 ORFs predicted for *R. prowazekii* [9, 10]. Genes shared among *Rickettsia* are mainly related to metabolic and cellular processes, while genomic variations and species-specific genes have been associated with their ability to infect and adapt to a range of diverse hosts including mammals, ticks, fleas, lice, and mites; moreover it is suspected that some of these genetic variations might represent species- or strain-specific virulence factors [11]. As a consequence of this scenario, it has been proposed that the conserved metabolic pathways and transport mechanisms which allow *Rickettsia* to acquire nutrients inside host cells could represent potential vaccine or therapeutic targets [11].

In nature, rickettsiae are maintained effectively in a zoonotic cycle that involves rickettsemic rodents and their ectoparasites. This is documented in the case of *R. prowazekii* [13] and/or transovarial and trans-stadial transmission in ticks as observed

with SFG *Rickettsia* [3]. Thus, transmission to humans is accidental and is not essential to maintain the natural cycle of any *Rickettsia* spp.

In humans, the vascular endothelium is the primary target of rickettsial infections, followed by mononuclear phagocytes and hepatocytes [14]. Rickettsial entry into the mammalian cell requires the binding of outer membrane protein B (OmpB or sca5) to cell receptor, Ku70, a component of the DNA-dependent protein kinase, expressed on the host cell membrane [15]. This interaction promotes a cascade of signalling events, including the Arp2/3 complex [16], Cdc42, cofilin, c-Cbl, clathrin, and caveolin 2 [17], that induce the necessary cytoskeletal rearrangements that lead to a zipper-like entry mechanism. However, OmpB appears to account for only a 50% of rickettsial entry, thus involvement of other ligands such as sca2 [18] and adr2 [19] has been proposed. Once inside the host cell, rickettisae escape into the cytosol is mediated by phospholipase D and haemolysin C [20], thereby avoiding destruction within the phagolysosome. *In vitro*, Fc receptor-mediated entrance of opsonized rickettsiae to macrophages has also been observed. Interestingly, this entry pathway inhibits phagosomal escape resulting in intraphagolysosomal killing of rickettsiae [21].

A major difference between SFG and typhus group rickettsiae is the absence of the rickettsial outer membrane protein OmpA (Sca0) in the typhus group, which has been linked to adherence to host cells in the SPG rickettsiae [22]. Other differences are associated with growth and actin polymerization. Typhus group rickettsia grow until the host cell ruptures allowing released rickettsiae to infect adjacent cells [23], while SFG rickettsiae spread from cell to cell [24] by exploiting its actin-polymerization machinery, which facilitates intracellular and intercellular movement [25]. In contrast, typhus group

rickettsiae either does not induce actin polymerization (*R. prowazekii*), or produce short tails that result in non-directional movement (*R. typhi*).

Pathogenesis of Rickettsial Diseases and Immune Response

Humans develop rickettsemia and disseminated infection of the vascular endothelium after rickettsial infection. Replication of rickettsiae inside endothelial cells stimulate oxidative stress and cause injury to the endothelial cells; the brain and the lungs are the most affected organs by this endothelial dysfunction which leads to meningoencephalitis, interstitial pneumonitis, noncardiogenic pulmonary edema and, in severe cases, hypotensive shock [3, 14, 26]. Disseminated rickettsial infection of the vascular endothelium is promoted by inhibition of apoptosis by a mechanism involving nuclear factor-κB (NF-κB) activation [27, 28]. Rickettsial infection of endothelial cells results in increased vascular permeability, generalized vascular inflammation, edema, increased leukocyte-endothelium interactions, release of vasoactive mediators that induce coagulation, expression of chemokines (CXCL9, CXCL10), pro-inflammatory cytokines (IL-1α, IL-6 and IL-8), and adhesion molecules (E-selectin, VCAM-1, ICAM-1) [29–34].

The anti-rickettsial immune response has been rarely investigated in humans. Thus, most of the protective immune mechanisms have being elucidated using relevant murine models that reproduce the vascular pathology observed in human typhus and spotted fevers. These animal models use intravenous inoculation of *R. conorii* and *R. typhi* into susceptible mice (C3H/HeN) [35, 36]. Although the murine model does not support infection by highly pathogenic *R. rickettsii and R. prowazekii*, the clinical and

pathological findings of mice infected with *R. conorii* and *R. typhi* mimic those produced by *R. rickettsii and R. prowazekii* in humans.

In the murine model, early resistance to infection is mediated by IFN-γ secreted by NK cells, which in turn activates infected target cells, mainly endothelial cells and macrophages [3]; clearance of rickettsiae is mediated by $CD8^+$ T cells which promote elimination of infected cells by a perforin-dependent mechanism and IFN-γ production [37, 38]. The relevance of $CD8^+$ T cells in resistance to rickettsial infections has been experimentally demonstrated. Depletion of $CD8^+$ T cells has a tremendous impact on susceptibility to infection, inducing increased mortality rates (~71%) and overwhelming rickettsial infection after a sublethal challenge; in contrast $CD4^+$ depleted mice are able to clear the infection and successfully recover [38]. The critical role of $CD8^+$ over $CD4^+$ T cells has been further confirmed by studies involving MHC class I gene knockout mice which, compared to wild-type C57BL/6 mice, turn out to be extremely susceptible (50,000-fold higher), having a lethal outcome after a challenge with theoretical 0.5 PFU of *R. australis*. Furthermore, $CD8^+$ T cells can provide protective immunity against rickettsiae even in the absence of IFN-γ as demonstrated by the reduction of the *Rickettsia* load after adoptive transfer of immune $CD8^+$ T cells from IFN-γ gene knockout mice into *R. australis*-infected IFN-γ gene knockout mice [37]. Nonetheless, $CD4^+$ T cells also contribute to protective immunity mainly through the production of IFN-γ and TNF-α, which activate microbicidal activities of infected target cells, and by providing help for the induction of protective antibodies as well as cytotoxic and, likely, memory $CD8^+$ T cells [3]. Although, antibodies do not play a role in recovery from a primary infection [39], as they only appear once rickettsial infection has been controlled, anti-

Rickettsia antibodies have a prominent role in protection against reinfection [40]. Cytokine-activated target cells, namely endothelial cells and macrophages, also have a pivotal role in killing rickettsiae; the mechanisms that contribute to bacteria clearance include production of nitric oxide and hydrogen peroxide, oxidative burst, and/or tryptophan starvation via indoleamine-2, 3-dioxygenase (IDO) induction. The relevance of these rickettsicidal mechanisms is further supported by studies performed on skin lesions of patients with Mediterranean spotted fever [3, 41].

Many *Rickettsia* spp. are transmitted through the bite of ticks and mites, implying that resident skin cells, particularly dendritic cells (DC), might have a role in initiating the immune response against invading rickettsiae; *in vitro,* it has been demonstrated that rickettsial infection of bone marrow DCs results in maturation (upregulation of CD40, CD80, CD86 and MHC-II), presentation of rickettsial antigens to T cells, and production of Th1-promoting cytokines (IL-2, IL-12p40 and IL-23), which in turn can effectively activate $CD4^+$ and $CD8^+$ T cells [42, 43].

As previously discussed, there is a large genetic similarity between genomes of rickettsiae of different groups; it is suspected that these similarities also exist at the antigenic level as supported by the cross-protection between SFG and typhus group rickettsiae that has been observed in animal models. Recovery from a rickettisial infection induces long-lasting protective immunity against homologous or heterologous rickettsial challenges. This protection is mediated by T cells that recognize cross-reacting antigens of the two rickettsial groups; more importantly, cross-reaction occurs in humans as well: T lymphocytes specific for SFG rickettsial antigens recognize and become activated by typhus group rickettsial antigens [44]. However, thus far, cross-

reactive T cell protective-antigens have not been identified. In contrast, antibodies do not exhibit cross-protective capability among distantly related rickettsiae [40], suggesting that long-lasting cross-protective immunity is a T cell-mediated mechanism.

Epidemiology

The epidemiology of rickettsioses is complex and is dependent on interactions between the arthropod vector and the mammalian hosts. In the case of SFG rickettsiae, since tick species have distinctive ecologic features and feeding preferences among animal hosts, human exposure is dependent on changes introduced to the ecological niche where the arthropod vector and the mammalian hosts co-exist [45]. For *R. prowazekii* infections, poverty and poor hygiene conditions combined with social and political instability pose a major risk for epidemic typhus outbreaks as recently observed in African countries. Moreover, latency and Brill-Zinsser disease adds an extra element of complexity to the epidemic typhus epidemiology since the number of survivors to the primary infection is generally unknown and individuals developing relapsing illness under these conditions can become the source of new epidemics if louse infestation is also present [46].

At first glance, rickettsial infections seem to be sporadic, with only a small proportion of vectors infected, leading to the assumption that the disease is not a significant threat to human health [45]. Nevertheless, rickettsiae include some of the most pathogenic bacteria known to humans and rickettsial diseases are prevalent in nature, as supported by the emergence and re-emergence of rickettsioses worldwide [45, 47, 48]. A rise in the cases of RMSF in the Americas has been documented in the past years; in

2002, a significant increase in the average annual incidence of RMSF in the United States was observed, changing from a low 1.4 cases per million persons in 1998 to a high incidence of 3.8 cases per million [49]. RMSF has also been reported in several provinces of Canada, several states in Mexico, and in Panama, Costa Rica, Colombia, Brazil, and Argentina [50–59]. Although RMSF occurs only in the Americas, increased occurrence of other rickettsioses caused by agents in the spotted fever group have been reported in Europe, Asia, Africa, and Australia [45, 47, 48, 60]. Moreover, new SFG rickettsioses have been described, such as the mild spotted fever caused by *R. parkeri* infection, which was considered a non-pathogenic *Rickettsia* for a very long time [61]. In the case of epidemic typhus, the most recent cases have occurred in the rural highlands of Africa and Central and South America, as well as in refugee camps in Rwanda, Burundi, and Zaire, particularly when poor conditions of hygiene are observed. In 1997, a large outbreak of epidemic typhus was reported in Burundi during the civil war; 100,000 people were estimated to be infected, and the case fatality rate was 15% [46]. This re-emergence has been evident despite the fact that the initial presentation (fever, headache, myalgia and rash) of rickettsial diseases is non specific and the lack of timely diagnostic tests, which makes diagnosis difficult; these factors lead to underestimation of morbidity, mortality and case-fatality rate. For instance, the most widely applied diagnostic tool, serologic analysis, is not useful during active infection since most patients with RMSF will develop diagnostic IFA titers (i.e., >64) only after the second week of disease, while at least half of all deaths will occur within the first 7-9 days [62].

Vaccines for *Rickettsia*

It is believed that *R. prowazekii*, *R. rickettsii*, *R.conorii*, and *R. typhi* can cause symptomatic disease in 100% of infected individuals; in the absence of timely and proper antibiotic treatment, case fatality rate for the etiological agents of epidemic typhus (*R. prowazekii*) and RMSF (*R. rickettsii*) can be as high as 60% [6]. Besides its high mortality rate, rickettsial agents pose a serious bioterrorist threat due to its high infectivity at low dose aerosols and its potential to be intentionally aerosolized [6, 7]; nevertheless, there are no prophylactic vaccines available for preventing any rickettsial disease at the present time. Moreover, the lack of diagnostic tests for establishing an opportune diagnostic and the non-specific initial clinical presentation of rickettsioses might compromise the effectiveness of antibiotic treatment. Therefore, the development of a safe and effective anti-rickettsia vaccine would be the best strategy to reduce the high case fatality associated with rickettsial infections.

Previous attempts to develop vaccines for *Rickettsia* had difficulties in consistently meeting the standards for acceptable vaccines with respect to safety and induction of protective immunity. Early vaccines were highly reactogenic and conferred incomplete protection, and most of them did not prevent infection, although they did reduce the case-fatality ratio. Moreover, due to *Rickettsia* growth requirements, these initial attempts also encountered difficulties in obtaining large amounts of purified bacteria for high scale production of vaccine batches with reliable potency and antigenic content. The first vaccines consisted of whole killed or live attenuated rickettsiae, arthropod vectors, cell lines, embryonated chicken eggs as well as infected tissues from laboratory animals were used as source of bacteria [6].

For the typhus group, initial vaccine development attempts in the 1930's used dried flea feces containing *R. typhi*. However, only individuals that developed murine typhus became immune to epidemic typhus, evidence of cross-protection among rickettsiae of the same group [63]. Later, in the 1970's, the production of an inactivated epidemic typhus vaccine proved to be cumbersome due to its great variability in antigenicity and potency [64]. Finally, the reversion of *R. prowazekii* Madrid E, an attenuated strain and promising vaccine candidate [65], to a virulent phenotype *in vivo* precluded its further use and prevented additional attempts at developing a *Rickettsia* vaccine using conventional approaches. In the case of the SFG, inactivated vaccines offered partial protection by prolonging the illness incubation period, abating symptoms or improving the response to antibiotic treatment; solid immunity was only granted by RMSF illness [66–69].

Subsequent experiments allowed the identification, for the first time, of potential rickettsial protective antigens, OmpA and OmpB, and described the induction of antibodies against conformational epitopes of these outer membrane proteins as the first protective mechanism and correlate of protection identified in rickettsial infections [70, 71].

Thus far, antigens that provide long-lasting and cross-protective immunity to rickettsial infections remain unidentified and uncharacterized. Some efforts have been made to further characterize the immunogenic potential of OmpA and OmpB [39, 72–77]. Also, recent studies identified immunodominant antigens for the humoral response in *R. parkeri* (translation initiation factor IF-2, cell division protein FrsZ, and cysteinyl-

tRNA synthase) and *R. heilongjiangensis* (periplasmic protein YbgF and extra-cellular chaperone PrsA) [78, 79].

T CELL VACCINES

Vaccines are the best single instrument of prophylaxis against infectious diseases, the impact of vaccination is highlighted by studies like the one in 2001 that followed a single US birth cohort and showed that 7 of the 12 vaccines administered during routine childhood immunization prevented 33,000 deaths and 14 million cases of disease [80].

In general, vaccines can be classified to two main groups. Firstly, live attenuated vaccines, which confer a type of protection that resembles the one achieved upon recovery from an active infection and elicit strong and long-lasting protective antibody and cellular immune responses. This group includes invariant pathogens such as smallpox, yellow fever, measles, mumps, rubella, and varicella. Secondly, subunit vaccines (hepatitis B), toxoid vaccines (diphtheria and tetanus), carbohydrate vaccines (pneumococcus) and conjugate vaccines (*Haemophilus influenzae* type B and meningococcus). These types of vaccines are generally weak activators of the immune system and require adjuvants to enhance their immunogenicity [81].

Since the abrogation of T cell help in different scenarios correlates with diminished immunogenicity and lack of generation of memory, it has been proposed that the new generation of vaccines must, at a minimum, contain two types of antigenic epitopes: one to induce specific B-cell or cytotoxic T cell responses and another to induce specific “helper” T cells [82–84]. Most currently licensed vaccines mediate protection

through a mechanism that involves the induction of serum IgG antibodies, yet the protective mechanisms of remaining targets for vaccine development, mostly intracellular pathogens and cancer, require T cell responses for protection [82, 85].

Immune Response Induced by T cell-Based Vaccines

Despite the prominent role of antibodies, there is growing evidence that supports a pivotal role for T cells in developing protective immunity after vaccination. Among currently licensed vaccines, BCG was the first vaccine for which it was demonstrated that T cells, specifically $CD4^+$ cells, were the main effectors [86]. A protective mechanism that involves both antibody production and $CD8^+$ T cell activation has been demonstrated for intranasal influenza and measles vaccines, while a role for $CD4^+$ T cells is suspected for acellular pertussiss and varicella vaccines [85]. In the case of influenza, it has been shown that antibody titers after vaccination fail to predict the risk of influenza in the elderly; in contrast, the extent of influenza-specific T cells is inversely correlated to the risk of acquiring influenza [87]. For varicella, T cell induction has shown to correlate with protection against infection and reactivation (shingles) in children and the elderly [88, 89].

The goal of T cell-based vaccines is to induce long-lived antigen-specific T cells that can mediate efficient protection averting either morbidity and/or mortality upon re-encounter with the same antigen [90]. Much effort has been devoted to the design of vaccines that can induce adaptive cellular immunity, with particular emphasis on $CD8^+$ T cells which have a central role in the host response to infections caused by intracellular microorganisms and cancer.

The quality and persistence of $CD8^+$ T cell responses depends on the frequency of epitope-specific naïve $CD8^+$ T cell precursors, the competence of the antigen presenting cells (APCs), as well as the initial priming conditions such as the presence of pathogen-associated molecular patterns (PAMPS), or the availability in the tissue microenvironment of danger-associated molecular patterns (DAMPS) [81, 90]. Thus, targeting the appropriate receptors on APCs, mainly DCs, could significantly improve the quality of $CD8^+$ T cell memory induced after vaccination: Toll-like receptors (TLR), nucleotide-binding oligomerization domain receptors (NLR), and retinoic-acid-inducible protein 1-like receptors (RLR) are among the innate immunity receptor systems susceptible to be targeted since they can mediate the induction of inflammatory cytokines at the T cell priming stage [91].

Upon encounter with APCs bearing cognate peptides, antigen-specific $CD8^+$ T cells rapidly expand and differentiate into effector cells. During this transition, naïve $CD8^+$ T cells lose the expression of costimulatory molecules such as CD27 and CD28, as well as IL-7 receptor α chain (IL-7Rα, CD127); simultaneously, they start to express effector mediators such as, perforin, Granzyme B and IFN-γ as well as effector markers such as KLRG1 (Killer cell lectin-like receptor subfamily G member 1) and the activated isoform of CD43 (1B11), which allows the differentiation between activated and quiescent T cells [92, 93]. After pathogen clearance, most effectors (around 90 to 95%) will die during the contraction phase, with a small proportion of pathogen-specific $CD8^+$ T cells surviving as part of the memory pool [84, 93].

Besides TCR engagement by cognate-peptide MHC complex on APCs (signal 1) and the presence of inflammatory cytokines such as type I IFNs and IL-12 (signal 3),

costimulatory signals (signal 2) are pivotal for enhancing activation signals delivered via TCR engagement and preventing the induction of anergy or deletion [84]. Although the main costimulatory signal is provided by the interaction between CD28, which is constitutively expressed on naïve T cells, and its ligands CD80 and CD86 expressed on APCs, other molecules, especially members of the TNFR superfamily, can provide signals that promote not only $CD8^+$ T cell effector function but also memory differentiation. Among them, CD27, CD137, and OX-40 and their respective ligands expressed on competent APCs (CD70, CD137L, and OX-40L) have been proposed as potential targets for optimizing vaccine-induced T-cell memory [84, 94].

DCs are important inducers of $CD8^+$ T cell responses; thus, the generation of DCs fully competent for antigen presentation is pivotal for the generation of protective long-lasting immune responses; help provided by $CD4^+$ T cells is among the critical factors that modulate DC activation. Cognate $CD4^+$ T cell help occurs when both $CD8^+$ and $CD4^+$ T cells concomitantly recognize an antigen presented by the same DC [95]; $CD4^+$ help in this context operates through the activation of DCs via interaction of CD40 with its ligand CD40L, which is upregulated on activated $CD4^+$ T cells. This interaction renders DCs fully competent (enhanced expression of CD80, CD86, CD70, IL-12) for activating $CD8^+$ T cells, a process known as "licensing" [84, 96]. Transient upregulation of CD40L directly on DCs induced by viral infections or some TLR ligands can circumvent the need for $CD4^+$ help and allow DCs to prime $CD8^+$ T cells in a CD4-independent manner [97]. The induction of CD70 on DC, the ligand for CD27, is another prominent result of DC "licensing"; in fact, blocking CD70-CD27 interactions can compromise memory development [98, 99]. Thus, for $CD8^+$ T-cell based vaccines,

mimicking $CD4^+$ help via CD40-CD40L interactions, or by including epitopes that can concomitantly activate $CD4^+$ T cells, represent one of the main strategies being implemented in modern vaccinology aimed towards improving $CD8^+$ T cell memory induction [94]. In addition, $CD4^+$ T cells can also help $CD8^+$ T cells by direct interaction (via CD40 and IL-2) or indirectly by secreting chemokines that subsequently will recruit antigen-specific naïve $CD8^+$ T cells to secondary lymphoid organs or sites of infection where APCs bearing cognate antigens are present [100–102].

Antigen-specific memory $CD8^+$ T cells are present at higher frequencies and can recognize antigen concentrations >50-fold lower than their naïve counterparts, which facilitates their efficient and rapid activation upon antigen reencounter [103]. Although maintenance of long-lived memory cells is a complex process, it is generally accepted that memory cells do not require persisting antigen to survive and that common-γ-chain receptor cytokines, specifically IL-7 and IL-15, play a prominent role in supporting the homeostatic maintenance of memory T cells [84, 94]. This dependence is in agreement with the high levels of expression of receptors for these cytokines observed on memory-type cells, CD127 and CD122, respectively [94]. However, the requirement for $CD4^+$ T cell help for maintenance of functional memory $CD8^+$ T cells is not well understood.

Memory T cells can be divided in two main subpopulations based on the expression of CD62L and CCR7: T central (T_{CM}; $CD62L^{high}CCR7^{high}$) or T effector ($T_{EM;}$ $CD62L^{low}CCR7^{low}$) memory cells. While T_{CM} have superior proliferation capabilities and are mainly located in secondary lymphoid tissues, T_{EM} can rapidly exert effector functions and are located in non-lymphoid tissues and mucosal sites where reencounter with invading pathogens is more likely to occur [84]. Although there is no consensus

about the mechanisms operating towards memory transition, it is currently accepted that a large proportion of T cells in the memory-pools passed through a time effector phase [84, 93, 104]. Moreover, it has been reported that even under restricted inflammatory conditions as the ones observed following immunization with peptide-coated mature DCs, which favor transition to memory within 4-7 days after immunization, memory $CD8^+$ T cells also pass through a condensed effector phase, suggesting that inflammation favors the generation of effector cells at the expense of memory formation [105].

T-cell based vaccines are being designed to meet strict safety standards following the subunit-based approach. However, compared to live attenuated vaccines, they are poor immunogens, as they lack the PAMPS and DAMPS that shape the induction of protective and long-lasting immunity after natural infections or immunization with live attenuated pathogens. Overcoming this weakness without compromising vaccine safety is one of the challenges of modern vaccinology; different strategies have been proposed to address this need:

1. Combination of vaccine targets with adjuvants that can boost immunogenicity, specifically aimed towards TLR, NLR and RLR systems [91, 94].
2. Inclusion of immomodulatory cytokines such as IL-12, IL-7, and IL-15 [94].
3. Provision of costimulation with CD137L, OX40L, and CD70 [94, 84].
4. Optimization of prime and boost. This immunization strategy is based on the repeated administration of the same antigen, some of the improvements include: a) heterologous prime and boost, which consist of priming and repeated boosting with different vaccine vectors carrying the same antigen to improve memory generation (its main drawback is that repeated boosting can also deplete T_{CM}, an

issue that needs to be addressed); b) rapid prime and boost, a strategy that can use peptide pulsed or transfected mature DCs to induce rapid generation of memory-type $CD8^+$ T cells that can be boosted 5-7 days after priming, compared to 2-3 months which is the appropriate time for optimal boosting with the usual approach (the major drawback of this approach for human vaccination is that it needs to be highly individualized, which renders it time-consuming and expensive); c) cross-priming and boost, an approach that circumvents some of the issues observed for the rapid prime and boost regime because it takes advantage of the immune system's ability to cross-present antigens to $CD8^+$ T cells by using antigen coated microspheres instead of pulsed DCs for priming with the same accelerated induction of memory $CD8^+$ T cells [106, 107].

5. Provision of efficient $CD4^+$ T cell "help" through inclusion of epitopes that enhance $CD4^+$ help as well as addition of CD40L and/or agonist CD27 antibody [94].
6. Use of live vector viruses as antigen carriers for immunization, which appears to efficiently induce strong antibody and T cell responses. Among them, although some biosafety issues still need to be addressed, modified vaccinia Ankara virus (MVA) is a promising candidate [108].

Correlates of Cellular Immunity

Vaccines represent the most cost-effective method to avert mortality and morbidity associated with infectious diseases; however, most current vaccines were developed empirically without having insight on how protection was achieved [81]. The

failure to develop new efficient vaccines that counteract current human pathogen threats such as HIV, *Plasmodium falciparum*, *Mycobacterium tuberculosis*, dengue virus and hepatitis C virus, which are suspected to require the induction of strong T cell responses to achieve protection, has stressed the need to understand and elucidate the mechanisms that contribute to the induction of vaccine-mediated cellular protective immunity [81, 90].

Thus far, the development of effective T cell vaccines remains elusive. This is due, in part, to the lack of reliable correlates of protection that can predict the induction of protective T cell immunity upon vaccination [90]. Correlates of protection are specific to the vaccine formulation being developed and tested; in general, they represent measurable immunological readouts that have a statistically significant correlation with protection, ideally survival, in appropriate animal models that mimic human infection. Thus, given the strong connection of a given immune correlate with protection, the same immunological readout can be applied to predict the protective efficacy of a candidate vaccine [109, 110]. These measurements include some of the following: vaccine-specific antibody titer and functionality (e.g., toxin neutralization, plaque reduction or bactericidal/bacteriostatic activity), cytokine secretion patterns, the induction of cell-mediated immunity with display of activation markers on immune effector cells, proliferation or cytotoxic T-cell responses towards the vaccine antigen(s) or infected eukaryotic cells, or protection after adoptive transfer of immune-T cells [109, 110].

Recent publications have indicated that T cells that produce multiple factors simultaneously, multifunctional T cells (MFT), provide protection against disease progression in HIV-1 infection and vaccine induced immunity with the anti-TB vaccine,

AERAS- 402 [111, 112]. Furthermore, the degree of protection against *Leishmania major* infection in mice is predicted by the frequency of MFT $CD4^+$ T cells simultaneously producing IFN-γ, IL-2, and TNF-α. Multifunctional effector cells generated by candidate vaccines demonstrated to be unique in their capacity to produce high amounts of IFN-γ, indicating that the quality of $CD4^+$ T cell cytokine responses can be a crucial determinant of whether a vaccine is protective or not, and may provide a new and useful prospective immune correlate of protection for T cell-based vaccines [113, 114].

Since, together with the induction of protective immunity, generation of memory is one of the goals of vaccination, instead of focusing only on the induction of effector molecules as has been done for $CD4^+$ T cells [112, 114] definition of potential correlates of protection for $CD8^+$ T cells also has included the assessment of a set of activation markers that could be useful for predicting the potential of antigen-specific $CD8^+$ T cells to become memory cells after vaccination, as well as the capability of these vaccine-induced memory cells to mediate strong recall responses upon re-encounter with the same antigen. These markers have been selected based on experimental data obtained from diverse relevant mouse models including lymphocytic choriomeningitis virus (LCMV), *Listeria monocytogenes*, vesicular stomatitis virus (VSV), Sendai virus, influenza and vaccinia [92, 94, 115–117]. These markers include CD62L, CCR7, CD127 (IL-7Rα), KLRG1, CD27, CD43 (1B11), CD122 (IL-2/ IL-15Rβ), CXCR3 and Bcl-2 (Table 1.2); it has been proposed that the relative proportion $CD8^+$ T cells expressing different combinations of these markers could be a useful predictor of vaccine efficacy [92, 94, 116, 117]. Particular attention has been given to CD127, KLRG1, CD27, and CD43 (1B11), since different combinations of these markers allow the early detection of

memory precursors at the peak of the effector phase and enhance the predictability of the efficacy of recall responses, circumventing some of the limitations observed when only T central (T_{CM}) or T effector (T_{EM}) memory cells markers are used (i.e. CD62L and CCR7 homing markers). These new approaches include the early identification of memory precursors as well as the actual capability of memory cells to mediate recall responses as opposed to only their ability to localize in lymphoid (T_{CM}) or peripheral (T_{EM}) tissues [92, 94].

From the pool of $CD8^+$ T cells expanding upon immunization, two populations with potential implications for the assessment of vaccine efficacy emerge at the peak of the effector phase: 1) $CD8^+$ T cells expressing low levels of CD127 and high levels of KLRG1 (termed short-lived effector cells [SLECs]) [93, 118], representing terminally differentiated effector cells with limited expansion and long-term survival capabilities [116]; and 2) $CD8^+$ T cells that express high levels of CD127 and low levels of KLRG1 (termed memory precursor effector cells [MPECs]) [93, 118, 119], which have greater capacity for self-renewal and differentiation towards memory; over time, the latter subset becomes the dominant memory population able to regenerate, upon rechallenge, all effector and memory subsets defined by this marker combination, suggesting that this subset has "stem cell "-like properties and that the induction of large numbers of MPECs should be one of the goals of $CD8^+$ T cell targeting vaccines [116].

It is suspected that different subpopulations of memory $CD8^+$ T cells co-exist and that these subsets might have a specialized distribution and organization based on their effector functions and activation status [94, 117]. The classical T_{CM} and T_{EM} subsets are known to mediate optimal protection in different models [120–122]; however it is not

well understood what marker combination is the most appropriate for assessing the efficacy of protective recall responses against diverse pathogens since only limited insights about the activation status of the memory $CD8^+$ T cells responding upon rechallenge can be inferred from the T_{CM} and T_{EM} status [92, 117]. Thus, an alternative classification for memory $CD8^+$ T cells based on the expression of the activation markers CD27 and CD43 was proposed by Hikono *et al* [92]. This marker combination allowed the detection of distinct memory subpopulations; upon recall, an inverse correlation between the activation status and the proliferative potential of these subsets was observed. In general, cells with the most "rested" phenotype, $CD27^{high}CD43^{low}$, mediate the strongest recall responses and eventually become the dominant subset of the memory pool; in fact, both the classical T_{CM} and T_{EM} subsets appear to be encompassed in the $CD27^{high}$ subset [117]. In contrast, $CD8^+$ T cells expressing a $CD27^{high}CD43^{high}$ or $CD27^{low}CD43^{low}$ phenotype showed an intermediate or weak proliferative response after rechallenge, and a progressive loss of these memory subpopulations was observed [92]. Nonetheless, it was recently demonstrated, using a heterologous protection model and adoptive transfer experiments, that $CD27^{low}CD43^{low}$ cells can provide optimal protective immunity against *L. monocytogenes* and vaccinia despite their weak proliferative recall responses. This $CD27^{low}CD43^{low}$ subset was named "effector-like memory cells" as it bears a phenotype associated with effector cells ($CD27^{low}$, $KLRG1^{high}$, $Eomes^{low}$, T-bet^{high}); furthermore, it was suggested that cells with effector-like memory traits persist until the memory phase can provide immediate protection against reinfection and that their protective potential upon vaccination should be addressed [117, 123].

Alternatively, CD127 together with CD43 also can be used to identify memory-type ($CD127^{high}CD43^{low}$) and effector-type ($CD127^{low}CD43^{high}$) $CD8^{+}$ T cells [106]; moreover, these marker combination follows a similar expression and homeostatic proliferation pattern to the one reported for CD27 and CD43 [92].

Although the role of these activation markers (CD27, CD43, KLRG1) on memory T cells is still not well understood, it is suspected that they represent surrogate markers of imprinted activation states among memory subsets that can be related to memory potential and/or recall efficiency [92, 124].

T cell Protective Antigens and Immunodominance

Vaccine antigens clearly determine the type of immune effectors that will mediate protection, thus the first step in the development of T cell-based vaccines is the successful identification of antigens than can mediate protective cellular immune responses which remains a gap in the field. Protective T cell antigens are able to stimulate complex interactions between APCs and T cells; however, there is not a "rule of thumb" for T cell antigen identification and little is known about the features of these antigens [125].

Immunogenicity is not randomly distributed, instead antigenic proteins encompass T-cell epitope clusters ranging from 9 to 25 amino acids which can contain 4 to 40 MHC binding motifs [126]; however, density of MHC-binding epitopes alone does not seem to be the decisive factor for defining a protective T cell antigen, as it has been shown that vaccine antigens tend to contain less predicted MHC-binding epitopes; therefore, it has been suggested that the presence of immunodominant epitopes might be one driving factor accounting for the protective capabilities of T cell antigens [127].

Table 1.2 Phenotypic markers associated with memory potential and vaccine efficacy[b]

Marker	Function
CCR7	Homing to lymph nodes / Expressed by T_{CM} $CD8^+$ but not by T_{EM} $CD8^+$
CD62L	Homing to lymphoid tissue / Expressed by T_{CM} $CD8^+$ but not by T_{EM} $CD8^+$
CD27	Costimulatory molecule / Expressed by memory-type $CD8^+$ T cells
CD43 (1B11)	T cell activation and trafficking / activation-associated glycoform
CD127	IL-7 receptor α chain
CD122	IL-2 receptor β chain / Critical component of IL-2 and IL-15-mediated signaling
Bcl-2	Inhibition of apoptosis
KLRG1	Inhibitory receptor / Senescence-associated marker
CXCR3	Receptor for the interferon-inducible chemokines CXCL9, CXCL10, and CXCL11

Immunodominance is the tendency of T cells to elicit responses directed only towards a small fraction of the epitopes contained within a protein, which limits the breadth of T cells reacting against an invading pathogen, and it has been studied in more detail for $CD4^+$ T cell epitopes [128]. Initially, factors related to antigen-specific T cell precursor frequency and processing of complex antigens, such as the tertiary structure, the presence of peptide signals for protease targeting, and the presence of competing peptides were thought to play a major role in determining immunodominance. However, immunodominance seems to be more complex than initially anticipated. It has been

[b] Adapted from J. D. Ahlers and I. M. Belyakov, "Memories that last forever: strategies for optimizing vaccine T-cell memory.," Blood, vol. 115, no. 9, pp. 1678–89, Mar. 2010.

demonstrated that MHC class II interactions with dominant peptides are highly stable with a half life of 100-200 hours; in contrast, the off-rate for cryptic or subdominant peptides is 2-10 hours [128, 129], which is consistent with the observation that optimal T cell activation requires 2-4 days of antigenic stimulation and that proliferation is terminated if the encounter with the antigen is less than 20 hours [84]. Moreover, HLA-DM seems to play a role in defining immunodominance by favoring export and cell surface presentation of high stability peptide-MHC complexes [128]. Surprisingly, peptide immunization, a scenario that does not require antigen processing or HLA-DM editing, was not sufficient to overcome immunodominance; in fact, it seems that averting immunodominance, for both $CD8^+$ and $CD4^+$ T cells, requires subdominant or cryptic epitopes to be allowed, during vaccination, to target different DCs and dominate the immune response spatially or temporarily in order to avoid the suppressive microenvironment provided by IDO induction and T regulatory cells (Tregs) that accompany T cell responses to immunodominant peptides [128, 130]. The latter is an important observation for vaccine development since immonodominance hierarchies do not always correlate with protection, and several models have shown that subdominant epitopes can also mediate protective T cell responses [131–134].

REVERSE VACCINOLOGY

Infectious diseases represent the greatest cause of mortality and morbidity around the world and it has been estimated that pathogenic bacteria are responsible for about 50% of all infections [135]. Vaccines represent probably the most cost-effective strategy to avert morbidity and mortality associated with infectious diseases; however, the approaches followed to develop many of the currently licensed vaccines may not be suitable for many of the current pathogen threats. Some of these pathogens cannot be cultivated outside of the host (which is the case of *Rickettsia*), and many proteins are only expressed transiently during the course of infection or not easily expressed *in vitro* in sufficient quantities; thus, many potential vaccine candidates might be missed. Moreover, new vaccines are required to meet higher standards of safety and physico-chemical characterization underscoring the need to explore new approaches for vaccine discovery [135–137]. Recent advancements in high-throughput "omics" technologies and the accessibility to complete genome sequences for diverse pathogens have changed the time frame and scope for the discovery of novel vaccine candidates. Reverse vaccinology is a genomics-based *in silico* predictive tool with early success in the identification of protective antigens against animal and human pathogens. This approach allows whole ORFeome (collection of all open reading frames from an organism) analysis and identification of potential vaccine targets independently of their abundance, phase of expression and immunogenicity; thus, in principle, protective antigens would not be missed and advances toward the most effective vaccine antigen formulation can be attained by using animal models for direct *in vivo* testing of protection or indirectly by

measuring correlates/surrogates of protection in serum or cells from patients or immune animals [135, 136, 138].

Two main *in silico* strategies have been used for the identification of potential vaccine targets: the prediction of MHC class-I and class-II binding peptides for the discovery of T cell targets or, alternatively, the identification of cell surface or secreted proteins, subcellular locations that have been associated with immunogenicity, as potential targets for the humoral immunity or, in the case of intracellular pathogens, as targets for the MHC class I processing pathway [139, 125].

The reverse vaccinology approach was validated for the first time on the Gram-negative bacteria *Neisseria meningitidis* serogroup B (MenB) [140]. The genome-based approach has been applied to other pathogens like *Streptococcus pneumoniae*[141], *Bacillus anthracis* [142], *Helicobacter pylori*[143], *Porphyromonas gingivalis* [144], *Pasteurella multocida* [145], *Chlamydia pneumoniae* [146], *Streptococcus agalactiae* [147], and *Leishmania major* [148].

Reverse Vaccinology and Cellular Immunity

As discussed above, one major impediment for the development of T cell-based vaccines is the lack of reliable parameters for defining T cell protective antigens or an efficient strategy to identify them [125]. Reverse vaccinology combines genomic and immunological information to identify antigen targets for diagnostics or vaccine development; thus, the prediction of epitopes recognized by $CD4^+$ or $CD8^+$ T cells could serve as a ‘‘reverse’’ approach for identifying protective T cell antigens [149–152].

The first step towards an effective T-cell response is the successful processing of microbial proteins into peptides (epitopes) that can be loaded on MHC molecules to be presented to T cells. Two separate pathways mediate this process [153]:

1. MHC class-I pathway: microbial proteins in the cytosol or the nuclear compartment of infected cells are cleaved by the proteasome, the resulting peptides are transported to the ER (endoplasmic reticulum) by TAP (transporter associated with antigen processing) and then loaded on MHC class I molecules with the resulting MHC class-I-peptide complexes being presented on the surface of APCs for possible interaction with the TCR of $CD8^+$ T cells for activation of their effector functions such as cytotoxicity and cytokine secretion. Extracellular endocytosed antigens transported to the cytoplasm, can also be presented via this pathway, a phenomenon known as cross-presentation.
2. MHC class II pathway: target pathogens or their proteins enter to the endocytic pathway and are cleaved into peptide fragments by lysosome proteases, some of these fragments bind to MHC class II molecules to form complexes that are recognized by $CD4^+$ T cells, which facilitate an adaptive immune response to the pathogen by providing help to $CD8^+$ T cells and B cells.

T cell epitope prediction by *in silico* analysis of protein sequences has been proposed as an alternative for rational vaccine development; however, since only a small fraction of peptides in a given pathogen proteome are able to bind MHC molecules, the accurate and reliable prediction of peptide-MHC binding is pivotal for the robust identification of T-

cell epitopes and for the successful design of peptide- and protein-based vaccines (i.e., subunit vaccines) [82, 154, 155].

Algorithms for predicting T-cell epitopes have notably improved since first described in the 1980s [156]. Peptides (epitopes) that bind to MHC alleles have residues with similar properties at different positions of their primary sequences that allow them to fit into polymorphic grooves or "pockets" by interacting with complementary residues of specific MHC alleles, the "anchor" residues. An increasing number of bioinformatic tools for T cell epitope prediction have been developed in recent years; methods that predict peptide binding to MHC molecules can be divided in two main groups: sequence-based and structure-based; the more widespread methods use the sequence based approach and are based on experimentally determined MHC–peptide affinity binding data [157, 158]. The most common methods are the ones using binding matrices or artificial neural networks (ANNs). The binding matrices approach correlates residue positions in a given peptide to binding; then, consensus scores are generated by summing, multiplying or averaging the matrix coefficients and comparing them against a predetermined threshold to predict peptide binders to an array of MHC class I and class II molecules. ANNs are connectionist models trained to perform classification and complex pattern recognition tasks; using peptide features, such as amino acid composition, hydrophobicity, volume and charge, ANNs classify peptides into binders and nonbinders and with increasing peptide data can gradually outperform the binding matrices approach [157].

Although the accuracy of computer algorithms for prediction of T cell epitopes has notably improved in recent years, some drawbacks persist. In general, $CD8^+$ T cell

epitope predictions outperform those for $CD4^+$ T cells; it has been estimated that current algorithms can provide over 75% and 50% of correct predictions for MHC class-I and class-II binding, respectively [82, 154, 155]. These differences are explained in part by the nature of the binding groove, which is closed in MHC class-I, allowing only 8-10 amino acids, and open at both ends in MHC class-II, allowing peptides ranging from ~9-22 residues for which the 9 amino acids that represent the binding core are frequently unknown; moreover, there are also difficulties in predicting antigen processing and peptide loading in the MHC class-II pathway due to the participation of several proteases with no well defined specificities for protein cleavage [138, 158, 159]. In addition, underestimation of the epitope breadth has been observed for $CD8^+$ T cell epitopes [160]. Despite these drawbacks, the current algorithms can still assist and facilitate T cell epitope discovery in a cost-effective manner, compared to traditional approaches such as proteolytic fragmentation, derivation of genetic constructs, MHC-peptide complex elution or epitope mapping which are expensive and labor-intensive [159]. It is expected that adjustments in the parameters on how the algorithms are "trained" could improve epitope predictions, especially for $CD4^+$ T cells [125, 158, 159]. However, antigen discovery across entire proteomes still is a challenge for complex pathogens which have large genomes and express hundreds of proteins, since only about 2% of all epitopes generated will have the right amino acid conformation for successful MHC-binding, and from those only a small fraction will elicit protective cellular immune responses [125, 161]. Thus, to address specific pathogen-related challenges, it has been proposed that *in silico* approaches should be combined and adapted to meet pathogen- and study-specific requirements [162], and for large-genome organisms, protein-based approaches, instead

of overlapping peptides, have been suggested as a cost-effective strategy for T cell antigen discovery [125].

Computational approaches that combine prediction of antigen processing with MHC-peptide binding activity and presentation have been used to identify T cell-specific epitopes from vaccinia, which turned out to be highly conserved across the poxvirus family, including variola, the causative agent of smallpox; such data suggest that this strategy might be useful for developing a new generation of smallpox vaccines [163]. T cell epitope prediction tools have also been successful in identifying epitopes from Dengue virus [164], *L. major* [148], and *Plasmodium falciparum* [165].

Methods for Measuring Protective Cellular Immunity

There is an increasing interest in vaccine research to elucidate the mechanisms of protection induced by licensed vaccines and new vaccine candidates [166]; early identification of immune activity could represent a way to prioritize vaccine targets for further characterization and potential clinical evaluation [167]. Screening of vaccine candidate-induced cellular immune responses can be performed using T cells from exposed individuals (human or mouse), and the time point at which T cells are obtained is important in order to define the potential challenges and limitations of the screening process [125]. If cells are collected at the peak of the primary encounter with the pathogen or vaccine antigens, robust responses can be observed and immune profiles will correspond to primary T cells; however, exceptions should be considered when special immunization protocols that can accelerate memory development are used, i.e. rapid prime and boost [106], in which case memory-type T cells can be detected at the peak of

the primary encounter with the antigen. Nevertheless, interrogation of memory T cells causes concerns about having sufficient numbers of antigen-specific cells; thus, frequently, T cells must be expanded either in a non-specific manner using anti-CD3 antibodies and cytokines such as IL-2, IL-7 and IL-15 or in an antigen-specific manner using APCs that have been pulsed with an specific antigen or pathogen [125]. Both methods have drawbacks; the former will expand a large number of cells that will not react to the antigen of interest, while the latter might not reflect accurately the epitope breadth generated in *vivo*. Another important aspect is that the memory approach is biased by immunodominance, thus revealing only a narrow range of antigen-specific responses. Alternatively, for MHC class I screening, APCs can be transfected to express candidate antigens in the cytosol and target them for proteasome processing; however, not all pathogen antigens can be successfully expressed by mammalian cells and codon optimization might be required for efficient expression [125].

Detection of relevant T cell responses recognizing vaccine antigens can be performed using three types of validated assays: peptide-MHC tetramer staining, the enzyme-linked immunospot (ELISpot), and intracellular cytokine staining (ICS) [167]. Peptide-MHC tetramer staining allows direct enumeration of circulating epitope-specific T cells by binding fluorescent tetrameric peptide-MHC complexes to their respective TCR [168]; however, well characterized T cell epitopes are not always available, especially at the first stages of antigen discovery. ELISpot is highly sensitive and reliable; it offers an alternative for enumerating T cells secreting cytokines, such as IFN-γ, upon antigen encounter, but it has limitations related to the number of cytokines that can be detected simultaneously. In contrast, ICS allows simultaneous detection of

cytokines and cell markers which can provide information about distinctive patterns of T cell subsets that correlate with protection; moreover, it can be combined with peptide-MHC tetramer staining offering a highly specific tool for tracking T cell responses. This aspect can be particularly informative when monitoring possible epitope loss or escape, which is important in vaccination against highly variable pathogens [138, 166, 167]. These assays, together with direct *in vivo* readouts such as survival or pathogen load, are expected to offer insights about the quality and quantity of the protective immune responses induced by T cell-based vaccines, and assist in the selection of the best vaccine formulations and immunization protocols [167].

CHAPTER 2: Validation of a Reverse Vaccinology Approach for the Discovery of Protective *Rickettsia prowazekii* Antigens Recognized by T cells[c]

ABSTRACT

R. prowazekii has been tested for biological warfare due to the high mortality that it produces after aerosol transmission of very low numbers of rickettsiae. A vaccine to prevent epidemic typhus would constitute an effective deterrent to the weaponization of *R. prowazekii*; however, an effective and safe vaccine is not currently available. Due to the cytoplasmic niche of *Rickettsia*, $CD8^+$ T cells are critical effectors of immunity; however, the identification of antigens recognized by these cells has not been systematically addressed. To help close this gap, I used empirical antigen discovery data to formulate a reverse vaccinology strategy to improve correlations with empirical data. The resulting method highlights the importance of combining proteasome-processing as well as MHC class-I-binding predictions.

[c]A significant portion of this chapter has been previously published in the journal PloS ONE. PloS ONE does not require copyright permission as long as proper citation is given. The citation for this article is: Gazi M, Caro-Gomez E, Goez Y, Cespedes MA, Hidalgo M, Correa P, Valbuena G. 2013. Discovery of a Protective *Rickettsia prowazekii* Antigen Recognized by $CD8^+$ T Cells, RP884, Using an In Vivo Screening Platform. PLoS ONE 8(10): e76253.

INTRODUCTION

Epidemic typhus is one of the most lethal infections known to humans; mortality can be as high as 60% without antibiotic treatment [169]. The etiologic agent, *R. prowazekii*, is an obligately intracellular bacterium transmitted by the human body louse in nature, but it also has the potential for intentional aerosol transmission; indeed, *R. prowazekii* remains on CDC's list of biothreat select agents because of its high mortality, history of development as a bioweapon, transmissibility by aerosol, prolonged infectious stability in louse feces, and ID_{50} of fewer than 10 organisms [6, 7]. Prophylactic vaccines are not currently available to prevent this lethal disease or any of the other rickettsioses. This is a public health priority because clinical diagnosis of rickettsioses is very difficult due to the non-specific initial clinical presentation and the lack of commercially available diagnostic tests that can be used during the acute stage when antibiotic intervention is helpful. To address this need, it will be more cost-effective to produce a cross-reactive vaccine that can also protect against at least the other member of the typhus group rickettsiae, including *R. typhi*, the agent of flea-borne murine typhus. This is a prevalent and underdiagnosed infectious disease that is more frequent in rat-infested locations [5]. Although it is clinically milder than epidemic typhus, it causes considerable morbidity.

Until recently, antigen identification for vaccine development was almost exclusively biased towards the humoral immune response. This bias was partly due to the effectiveness of antibodies in protection against almost all of the currently approved vaccines for human use, the relative technical simplicity of working with serum and antibodies, and the methodological challenges of working with T cells. Presently, the barriers to identify potent vaccine antigens recognized by T cells need to be addressed

because most of the vaccines that remain to be produced require a strong T cell component to afford significant protection. In particular, there is an urgent need to develop appropriate techniques to identify antigens recognized by T lymphocytes because antigen discovery is the most important aspect of any vaccine development project; without appropriate antigens, a vaccine is unlikely to succeed.

Given the evidence that $CD4^+$ T cells and $CD8^+$ T cells target different antigens [170, 171], antibody-based screening methods are not always suitable to identify antigens recognized by $CD4^+$ T cells or, particularly, $CD8^+$ T cells. Several approaches to more directly identify antigens recognized by T-cells have been used; many of them rely on reverse vaccinology [138], a branch of systems biology that analyses entire microbial genomes to predict immunogenic proteins based on predefined rules derived from the analysis of large empirical datasets. This predictive *in silico* tool allows the identification of antigens with defined immunogenic, structural or functional criteria; this approach has had early success in the identification of protective antigens against animal and human pathogens. On the other hand, empirical methods for identification of antigens recognized by T cells rely on cells from animals or individuals that are immune to the pathogen. Those memory T cells had been selected during the physiological immune response to persistent infection and recognize a limited number of antigens (i.e., immunodominant antigens). Thus, methods that use memory T cells for antigen identification are more likely to miss potentially protective subdominant antigens. One strategy for T-cell antigen identification that is not biased towards immunodominant antigens is genomic immunization or Expression Library Immunization (ELI) [172]. Although ELI has been successfully used [173], it has its own problems as it relies on a

DNA immunization strategy; thus, antigen expression is not guaranteed in all cases. Accordingly, it is not possible to know which pathogen genes were not screened validly; a negative response can be due to lack of an immunological response or to failed expression of the microbial gene.

Herein, I describe the use of empirical antigen discovery data in the formulation of an *in silico* analysis strategy for the discovery of antigens with immunogenicity potential towards $CD8^+$ T cells; this novel *in silico* analysis strategy is based on the identification of proteins that contain predicted high-affinity proteasome-derived MHC class I-binding peptides [174].

MATERIALS AND METHODS

Bacteria

R. typhi (Wilmington strain) is a clinical reference strain with an unknown number of passages. *R. typhi* working stock was produced in a CDC-certified biosafety level 3 (BSL3) laboratory by cultivation in specific pathogen free embryonated chicken eggs. Yolk sacs were pooled and homogenized in a Waring blender, diluted to a 10% suspension in sucrose-phosphate-glutamate buffer (SPG; 0.218 M sucrose, 3.8 mM KH2PO4, 7.2 mM K2HPO4, 4.9 mM monosodium L-glutamic acid, pH 7.0) and centrifuged at low speed (200 × g, 10 minutes). The supernatant was aliquoted and stored at -80°C. *Rickettsia* present in the stock was quantified by plaque assay [175], and the LD_{50} was determined experimentally in C3H/HeN mice.

Animal Model

The mouse model of endothelial-target typhus group rickettsioses consisting of C3H/HeN mice infected intravenously through the tail vein (i.v.) with *R. typhi*, which is phylogenetically closely related to *R. prowazekii*, the other member of typhus group rickettsiae, has been previously described in detail [35]. Briefly, C3H/HeN mice (Charles River Laboratories, stock 025) were housed in an animal biosafety level-3 (ABSL3) facility and infected i.v. with 3 or 6 LD_{50} of *R. typhi* in a volume of 300 µl of phosphate-buffered saline (PBS). We followed the recommendations in the Guide for the Care and Use of Laboratory Animals of the National Institutes of Health. Our experimental protocol was approved by the Institutional Animal Care and Use Committee (IACUC) of the University of Texas Medical Branch (protocol number: 0903026).

Antigen Discovery Platform

Thirty-six ramdomly selected *R. prowazekii* antigens were empirically tested using the discovery platform illustrated in figure 2.1. Importantly, this methodology is not biased by immunodominance because T-cells from immune animals are not used to select antigens; an aspect potentially important for discovery of vaccine targets because subdominant or cryptic antigens have been shown to elicit protective immune responses in other systems [130, 132, 176]. The idea behind this platform is to produce APCs expressing individual open reading frames (ORFs) from a sequenced pathogen and use them for immunization of naïve mice. Immunization with pooled APCs containing 3 to 5 pathogen's ORFs is followed by challenge with live virulent *R. typhi* and measurement of an indicator of protection such as decreased bacterial load. Once protective pools are

identified, each member of the pool is tested individually (deconvolution) to identify ORF(s) responsible for a protective immune response. This platform, which verifies pathogen ORF expression, can potentially screen a pathogen's entire ORFeome; it also allows testing for cross-protective responses by immunizing with the ORFs of one pathogen (*R. prowazekii* in this case) and challenging with a related agent (i.e., *R. typhi*).

Immunoinformatic Analysis

For the computational analysis, protein sequences from *R. prowazekii* strain Madrid E (Gene Bank ID AJ235269.1) were analyzed for the prediction of 9 mer peptides binding the MHC class-I mouse allele H-2K^k using the following publicly available servers: NetMHCpan (http://www.cbs.dtu.dk/services/NetMHCpan/), IEBD-ANN http://tools.immuneepitope.org/main/html/tcell_tools.html), and SYFPEITHI (http://www.syfpeithi.de/). NetMHCpan and IEBD-ANN use artificial neural networks and have been reported to outperform other servers in the prediction of known MHC class-I binding epitopes and in predicting MHC binding [177–179]. Only proteins containing peptides predicted to be strong binders (IC_{50} values ≤ 50) were considered for further analysis. SYFPEITHI uses the binding matrix approach for generating the S-score, which indicates how well a peptide sequence matches the canonical MHC class-I binding motifs [180]. Only peptides with an S-score of 21 and higher were further analyzed. This score was arbitrarily chosen; it represents 70% of the S-score for the influenza A matrix protein epitope GILGFVFTL. RANKPEP (http://imed.med.ucm.es/Tools/rankpep.html) a predictive algorithm that allows performing protein sequence analysis using a proteasome filter that combines MHC

class-I binding affinity and proteasome processing for mouse alleles was also used [181]. This server uses position-specific scoring matrices (PSSM) for epitope prediction; for assessment of rickettsial proteins only the percentage of the optimal score value (%OPT) was considered, this value is calculated by dividing the individual peptide score by the optimal score value of a consensus sequence, for H-2K^k binding the consensus sequences is PENRWEHGI and its optimal score value is 52.472. RANKPEP was used to analyze peptides predicted by NetMHCpan, IEBD-ANN and SYFPEITHI for their likelihood to be derived from the proteasome.

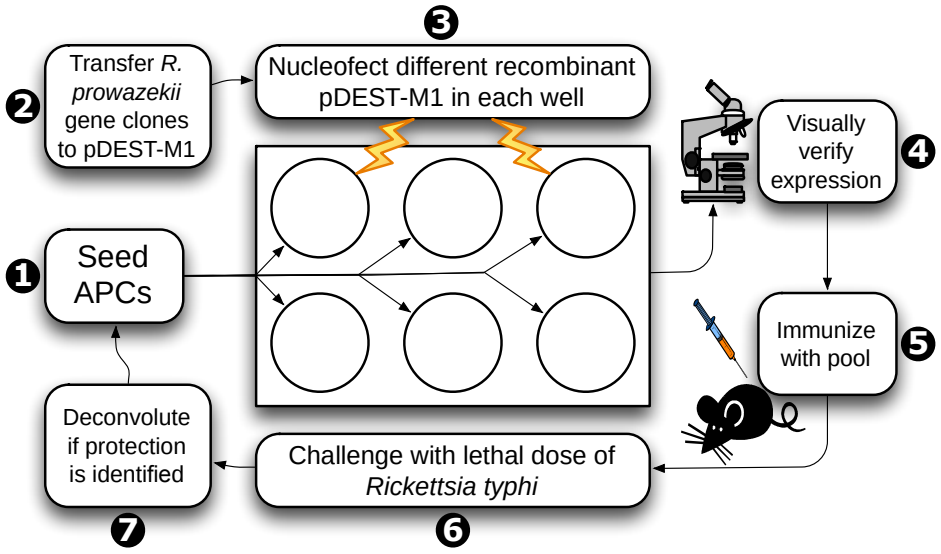

Figure 2.1 Diagram of the methodology to discover antigens recognized by T-cells. The steps involved are numbered as follows: 1) selection of appropriate antigen presenting cells (APCs) based on MHC class-I expression, 2) transfer of *R. prowazekii* gene clones to an eukaryotic expression vector, 3) expression vector transfer to APCs, 4) visual screening to verify expression of rickettsial gene, 5) APC-based immunization of naive mice using pools of 3-5 different APCs expressing rickettsial genes, 6) challenge with *R. typhi* and determination of bacterial load as indicator of protection, and 7) identification of protective rickettsial genes by deconvolution of protective pools.

Subcellular Localization Prediction

Subcellular localization prediction of selected proteins was performed using PSORTb 3.0.2 (http://www.psort.org/psortb/), a multicomponent approach that generates likelihood scores for the localization of proteins in each of the five Gram-negative localization sites (cytoplasm, cytoplasmic membrane, periplasm, outer membrane and extracellular space). In order to generate a final prediction, the results of each module are combined and assessed; a probabilistic method and 5-fold cross validation are used to assess the likelihood of a protein being at a specific localization given the prediction of a certain module. If one of the sites has a score of 7.5 or greater, this site and its score are returned as the final prediction [182].

Immunization Protocol

Selected *Rickettsia* genes were cloned into the eukaryotic expression vector pDEST-M1 as recently described [174]. Briefly, pDEST-M1 was assembled in four cloning steps. The ptdTomato-N1 plasmid (Clontech Laboratories) was used as a backbone. First, the Destabilization Domain (DD) from the pDD-tdTomato plasmid (Clontech Laboratories) was cloned into ptdTomato-N1 linearized with NheI and BglII. The second component, Ubiquitous Chromatin Opening Element (UCOE), a generous gift from Dr. Michael Antoniou, was added upstream of the CMV promoter using the AseI site. The third component was the ampicillin resistance gene, which replaced the kanamycin-neomycin resistance gene originally present in the ptdTomato-N1 backbone; it was cloned into the expression vector using BspHI for linearization which also removed the original kanamycin-neomycin resistance gene. The fourth step was to insert the Gateway system (Invitrogen) cassette using HindIII.

This plasmid vector directs the expressed protein towards presentation through the MHC class-I pathway because the DD sequence expressed on the N-terminus of the cloned rickettsial gene leads to rapid proteasomal degradation [183]. Naïve C3H/HeN mice were immunized with APCs expressing rickettsial proteins as follows, SVEC4-10 cells were used as antigen presenting cells; this is an endothelial cell line derived from C3H mice, obtained from the American Type Culture Collection (ATCC), that expresses high levels of MHC class-I and that was further modified in our laboratory to express the costimulatory molecules CD80 and CD137L through lentiviral transduction. Rickettsial proteins were nucleofected into these cells using the Amaxa SE Cell Line 96-well Nuclefector kit (Lonza). The success of the nucleofection procedure was corroborated by assessing the expression of the tdTomato fluorescent protein using an inverted fluorescence microscope (Olympus IS71) equipped with a TRITC filter. Cells expressing RP884 were detached with Accumax™ (Millipore) and washed twice with PBS; each mouse received 300 μl of cell suspension i.v. ($4x10^5$ cells). Four days later, mice received the same dose of cells intraperitoneally (i.p.); 10 days after the second immunization, mice were infected i.v with 3 or 6 LD_{50} of *R. typhi* and euthanized 7 days post-infection.

Flow Cytometry

Spleens were collected and disaggregated in HBSS containing 2%BGS, 3mM HEPES, Golgi Plug™ and Golgi Stop™ (BD Biosciences), at the concentrations specified by the manufacturer. Mononuclear cells were purified by density gradient centrifugation (Lympholyte™-M, Cedarlane Laboratories) and stained with Live/Dead

Fixable Blue (Life Technologies), APC-Alexa Fluor 750-conjugated anti-CD8 (clone 5H10), FITC-conjugated anti-CD3 (clone YCD3-1), BD Horizon V500-conjugated anti-CD44 (clone IM7), PE-Cy5 anti-CD127 (clone A7R34), PE-Cy7-conjugated anti-IFN-γ (clone XMG1.2) and Alexa Fluor 647-conjugated anti-Granzyme B (clone 16G6). CountBright™ Absolute Counting Beads (Life Technologies) were added to each sample prior to acquisition. All samples were acquired on a LSRII Fortessa cytometer (BD Biosciences); 500,000 events were captured and data were analyzed using FlowJo 9.5.3 software (Tree-Star Inc.). All analyses were performed on live $CD3^{+}CD8^{+}$ cells. Thresholds for positivity were determined with fluorescence-minus-one (FMO) control stains. Gating stratregy is shown in the appendix as Figure A1.

Measurement of Rickettsiae by Quantitative Real-Time PCR (Q-PCR)

Approximately 10 mg from each collected organ were placed into 2 ml microcentrifuge tubes (Eppendorf) together with one stainless steel grinding ball (5/32", Fisher Scientific). Samples were homogenized in a TissueLyser II, and the homogenate was processed for DNA isolation using DNeasy Blood & Tissue Kit (QIAGEN). Primers and probes were designed using Visual OMP and ThermoBLAST software (DNAsoftware). The DNA sequences of mouse L-lactate dehydrogenase A-like 6B (ldhal6b) gene and rickettsial citrate synthase (glt-A) genes were obtained from GenBank database (http://www.ncbi.nlm.nih.gov/genbank/). For rickettsial glt-A gene quantification, a 97-bp fragment was amplified using forward primer gltA-F (5'-GCTATGGGTATACCGTCGCA-3'), reverse primer gltA-R (5'-CAGGATCTTCGTGCATTTCTTTCC-3'), and TaqMan MGB (minor groove binder)

glt-A-probe labeled with 5'-FAM (5'FAM- GCCATCCAACCTACGGTTCTTGC-3'). For quantification of the mouse ldhal6b gene, a 102-bp fragment was amplified using forward primer M-ldhal6b-F (5'-TCGGGCAGAGGCTTGGGATC-3'), reverse primer M-ldhal6b-R (5'-CGGCGATGTTCACACCACTC-3'), and TaqMan MGB M-ldhal6b-probe labeled with 5'-VIC (5'VIC-CCACCCGTGGCAGCTTTCAGAGT). Primers were obtained from Integrated DNA Technologies and probes from Applied Biosystems (Life Technologies). Real-time PCR reactions were run using a 7900HT Fast Real-Time PCR device (Applied Biosystems).

Statistics

The proportion of surviving animals was analyzed with the Log-rank (Mantel-Cox) test. Mean absolute counts of T-cell subpopulations were compared using unpaired t-tests (GraphPad Prism, version 6).

RESULTS

Validation of a New Platform for the Discovery of Rickettsial Protective Antigens

Previous work with *Rickettsia* has focused on surface proteins for the discovery of epitopes recognized by $CD8^+$ T-cells [73–76]. However, there is evidence that the antigens recognized by antibodies (e.g., surface antigens), which are similar to the ones recognized by $CD4^+$ T cells, tend to be different from the ones mediating $CD8^+$ T cell responses [170, 171, 184, 185]. Also, any protein encoded by a microbial genome, independently of its physical location in the microbial cell, can theoretically be processed

for presentation through the class I pathway. Thus, as a proof-of-principle, 36 rickettsial genes available in our collection of *R. prowazekii* genes were randomly selected to test this platform (Fig. 2.1).

APCs expressing high levels of rickettsial proteins encoded by the 36 randomly selected rickettsial gene clones were combined into 8 random pools (Table 2.1). Eight groups of C3H/HeN mice ($H2\text{-}K^k$) were immunized with the pools of MHC-haploidentical APCs expressing *R. prowazekii* proteins and challenged as described in the methods section. Control groups included one group that was immunized with APCs expressing a control gene from *Arabidopsis thaliana* and one group that did not receive any immunization treatment (naïve control). Fourteen days after initial immunization, all animals were terminated, and rickettsial load in liver and lungs, two critical target organs, was determined using Q-PCR. One group of mice with a significantly lower load of *Rickettsia* was identified (Figure 2.2A).

To identify the individual rickettsial component(s) that were triggering protection, separate groups of naïve mice were immunized with nucleofected APCs expressing each individual rickettsial gene from the positive pool (RP884, RP703, RP778, and RP655) and repeated the challenge procedure as above. The new bacterial load analysis showed that RP884 was the rickettsial gene triggering the protective immune response of the original pool as assessed by a significant decrease in rickettsial load and increased survival; 60% of the RP884-immunized animals survived while 100% of control animals succumbed to the rickettsial infection (Fig. 2.2B and C). RP884 is annotated in the *R. prowazekii* genome as a ferrochelatase (hemH), an enzyme that participates in protoheme biosynthesis. This protein is highly conserved among the *Rickettsiaceae* and it is 95%

identical to that of *R. typhi*. Outside the Rickettsiales, the maximum protein sequence identity using BLASTp was 44%.

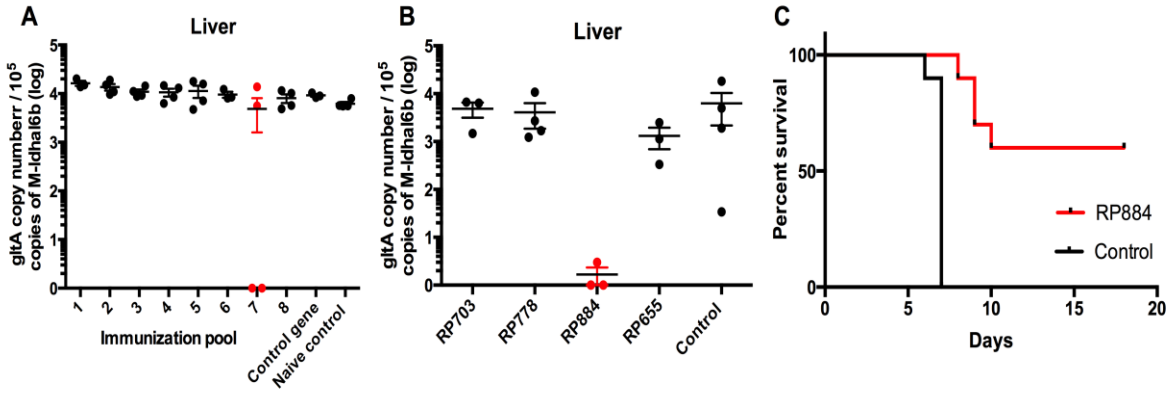

Figure 2.2 ***In vivo*** **identification of rickettsial antigens.** (A) Thirty-six APC lines expressing high levels of individual *R. prowazekii* ORFs were randomly combined into 8 pools. Eight groups of mice (4 mice per group) were immunized with pools of APCs expressing 4 or 5 different *R. prowazekii* proteins (see table 2.1). As a control, one group of mice was immunized with APCs expressing a gene from *A. thaliana*. One group without any manipulation (blank control) was also included. Fourteen days after immunization, all mice were challenged with 3 × LD_{50} of *R. typhi*. At day 7 post-infection, all animals were terminated, and rickettsial load in liver and lungs (not shown) was determined using quantitative real-time PCR targeting the rickettsial gene *gltA* and the mouse gene *ldhal6b*. One group of mice showed a significantly lower load of *Rickettsia*. (B) This group was deconvoluted by immunizing mice with the individual constructs following a similar strategy as the one above. One protective rickettsial antigen was found in this group, RP884. (C) Naïve mice immunized with APCs expressing either RP884 or an *A. thaliana* gene (control) were challenged with 3× LD_{50} of *R. typhi* and followed in time to determine survival; 60% of RP884-immune animals survived while none of the control animals did ($p<0.0001$). Individual data points, mean, and standard error of the mean (SEM) are shown.

Table 2.1 Pool assignment of *Rickettsia prowazekii* proteins used for antigen screening and predicted characteristics according to PSORTb 3.0*.

Rickettsial protein	Annotated function	Subcellular localization prediction	PSORTb score	Pool number
RP042	cell cycle protein MESJ (mesJ)	Cytoplasmic	9.97	1
RP058	SOJ protein (soj)	Cytoplasmic	8.96	1
RP189	DNA polymerase III subunit delta	Cytoplasmic	8.96	1
RP199	Adrenodoxin	Cytoplasmic	8.96	1
RP221	threonyl-tRNA synthetase	Cytoplasmic	10.00	1
RP410	UDP-N-acetylmuramoyl-L-alanyl-D-glutamate synthetase	Cytoplasmic	9.97	2
RP531	translation initiation factor IF-3	Cytoplasmic	10.00	2
RP585	preprotein translocase subunit YajC	Cytoplasmic Membrane	9.82	2
RP688	hypothetical protein	Cytoplasmic	8.96	2
RP718	lipid A biosynthesis lauroyl acyltransferase	Cytoplasmic	8.96	2
RP045	hypothetical protein	Cytoplasmic	8.96	3
RP168	16S ribosomal RNA methyltransferase RsmE	Cytoplasmic	8.96	3
RP192	hypothetical protein	Cytoplasmic Membrane	9.82	3
RP226	hypothetical protein	Unknown	-	3
RP875	hypothetical protein	Cytoplasmic Membrane	9.82	3
RP227	DNA topoisomerase IV subunit B	Cytoplasmic	9.97	4
RP336	hypothetical protein	Cytoplasmic	8.96	4
RP403	hypothetical protein	Cytoplasmic	8.96	4
RP485	scaffold protein	Cytoplasmic	9.26	4
RP511	hypothetical protein	Cytoplasmic	8.96	4
RP482	hypothetical protein	Cytoplasmic	9.97	5
RP530	branched-chain alpha-keto acid dehydrogenase subunit E2	Cytoplasmic	9.97	5
RP548m	DNA repair protein RecO	Cytoplasmic	8.96	5
RP572	excinuclease ABC subunit C	Cytoplasmic	9.97	5
RP627	co-chaperonin GroES	Cytoplasmic	9.26	6
RP803	F0F1 ATP synthase subunit alpha	Cytoplasmic	9.97	6
RP839	hypothetical protein	Unknown	-	6
RP848	hypothetical protein	Cytoplasmic	8.96	6
RP655	30S ribosomal protein S19	Cytoplasmic	9.26	7
RP703	cytochrome C-type biogenesis protein CCMF (ccmF)	Cytoplasmic Membrane	10.00	7
RP778	DNA polymerase III subunit alpha	Cytoplasmic	9.97	7
RP884	Ferrochelatase	Cytoplasmic	9.97	7
RP374	protein transport protein SEC7 (sec7)	Cytoplasmic	8.96	8
RP498	cell surface antigen (sca4)	Cytoplasmic	8.96	8

Predictive Power of Immunoinformatic Tools

Since our strategy for antigen discovery was entirely empirical, I wanted to compare our results to those generated with publicly available bioinformatic systems that predict the immunogenicity of proteins toward $CD8^+$ T-cells. The algorithms supporting each system are different; thus, each one produces a different ranking. I used the individual scores generated by each server and also ranked *R. prowazekii* proteins using two different scoring systems that I developed: a) Single peptide score (SpS) and b) overall protein score (OpS). For SpS, rickettsial proteins were ranked according to the inverse IC_{50} value of the predicted peptide with highest affinity in each protein so that the rickettsial protein containing the peptide with the lowest IC_{50} value was ranked first; only NetMHCpan and IEBD-ANN were used since both servers can generate IC_{50} values. The SpS score resulted from averaging the rank generated with each one of the two servers. This score only included proteins with high-affinity MHC class-I-binding peptides regardless of the number of potential binding peptides predicted in each protein.

The purpose of the OpS score was to rank rickettsial proteins according to the number of MHC class-I binding peptides that can potentially be generated from each one. First I produced a protein score (pS) for each server from the inverse of the average of the IC_{50} values (for NetMHCpan or IEBD-ANN) and the S-Score (for SYFPEITHI) of all peptides predicted to bind to $H\text{-}2K^k$ from each rickettsial protein divided by the number of predicted binding-peptides in the same protein. The OpS score was calculated from the average of the three pS ranks.

As shown in table 2.2, RP884 ranked rather low with all systems used, suggesting that individual scores from these servers or the calculated SpS and OpS scores were not

optimal predictors. To overcome this problem, I redefined our analysis strategy as follows: First, we used NetMHCpan, IEBD-ANN, and SYFPEITHI to generate a database of high-affinity MHC class-I binding peptides for each protein. Then, I used RANKPEP to query the top 5 proteasome-derived peptides among all the MHC class-I binding peptides predicted for each protein. With this information, I generated a manually curated database that included only proteasome-derived peptides with their respective RANKPEP scores (calculated by dividing the individual peptide scores by the optimal score value, expressed as %OPT). With this information, a new rickettsial protein score was obtained by multiplying the number of proteasome predicted peptides found among all the predicted MHC class-I peptide-binders in each protein by the average of the RANKPEP scores for each protein. After performing these modifications to the *in silico* analysis strategy, RP884 emerged as a top-ranked *in silico*-defined vaccine candidate (New modified score, Table 2.2). These results highlight the importance of combining proteasome-processing as well as MHC class-I binding predictions for *in silico* approaches aimed at discovering $CD8^+$ T cell antigens.

T Cell Priming

The immunization strategy for antigen discovery was designed to be biased towards MHC class-I presentation because the antigens are rapidly delivered to the proteasome as a consequence of the fusion of the rickettsial protein to a destabilization domain. To explore the role of class I presentation, the effector functions in T-cell subpopulations from immunized animals were analyzed. I used an *ex vivo* method that

Table 2.2 Immunoinformatic analysis and immunogenicity ranking of *R. prowazekii* proteins

Predictors	Rank of positive pool genes among all *R. prowazekii* proteins (834)				Rank of positive pool genes among those tested in this study (36)			
	RP655	**RP703**	**RP778**	**RP884**	**RP655**	**RP703**	**RP778**	**RP884**
NetMHCpan	790	185	11	650	34	16	2	32
IEBD-ANN	795	135	35	197	35	16	6	18
SYFPEITHI	624	308	15	311	33	26	2	24
SpS score	807	48	173	358	35	3	16	18
OpS score	781	169	10	392	35	20	1	26
New score	518	129	38	4	35	10	8	3

provides direct information about the response of T cells *in vivo* because T cells are stained and analyzed immediately after their extraction without further *in vitro* stimulation [186, 187]. Mice were injected with brefeldin A and monensin, two substances that stop secretory processes, four hours before retrieval of the spleen in order to detect cytokines that were being secreted by T cells at the time of the injection. *Ex vivo* analysis of $CD3^+CD8^+$ cells from animals immunized with SVEC4-10 cells expressing RP884 showed increased numbers of $CD44^{high}$ cells among $CD8^+$ T-cells. Since CD44 is a surface marker expressed by antigen-experienced T-cells, its increased expression suggested that RP884 immunization efficiently primed $CD8^+$ T cells ($CD3^+CD8^+CD44^{high}$cells, figure 2.3A). Furthermore, this subset also produced increased levels of IFN-γ after rickettsial challenge compared to control animals immunized with SVEC4-10 cells expressing an irrelevant antigen (control gene, figure 2.3B) increased production of Granzyme B was also observed in RP884 immune animals, although it was not statistically significant (data not shown, $p = 0.058$). Effector-type $CD8^+$ T-cells ($CD44^{high}CD127^{low}$) and memory-type $CD8^+$ T cells ($CD44^{high}CD127^{high}$) were also

increased in RP884-immune animals (Fig. 2.4A and B), and significantly larger numbers of IFN-γ producing cells were observed among these subpopulations (Fig 2.4C and D).

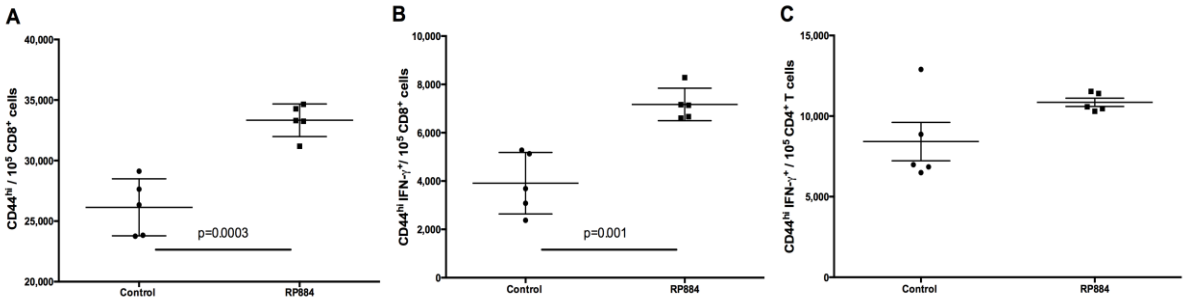

Figure 2.3 RP884 immunization induced increased expression of IFN-γ in antigen experienced CD8$^+$ T cells. RP884-immune animals and mice immunized with the *A. thaliana* control gene were challenged with 6 × LD_{50} of *R. typhi* and sacrificed 7 days later (4 hours after i.p. injection of brefeldin A and monensin) to obtain splenocytes for flow cytometric analysis. (A) Number of antigen-experienced CD8$^+$ T-cells ($CD3^+CD8^+CD44^{high}$). (B) IFN-γ expression in $CD3^+CD8^+CD44^{high}$ cells. (C) IFN-γ expression in $CD3^+CD4^+CD44^{high}$ cells. Differences were statistically significant (p=0.0003 for panel A and p=0.001 for panel B). Individual data points and mean ±SEM are shown.

On the other hand, the IFN-γ response of antigen-experienced CD4$^+$ T cells ($CD3^+CD4^+CD44^{high}$) was not significantly different (Fig 2.3C). These data indicate the development of an anti-RP884 CD8$^+$ T-cell response in immunized animals, and supports the concept that our antigen discovery strategy functions through stimulation of CD8$^+$ T-cell responses as expected.

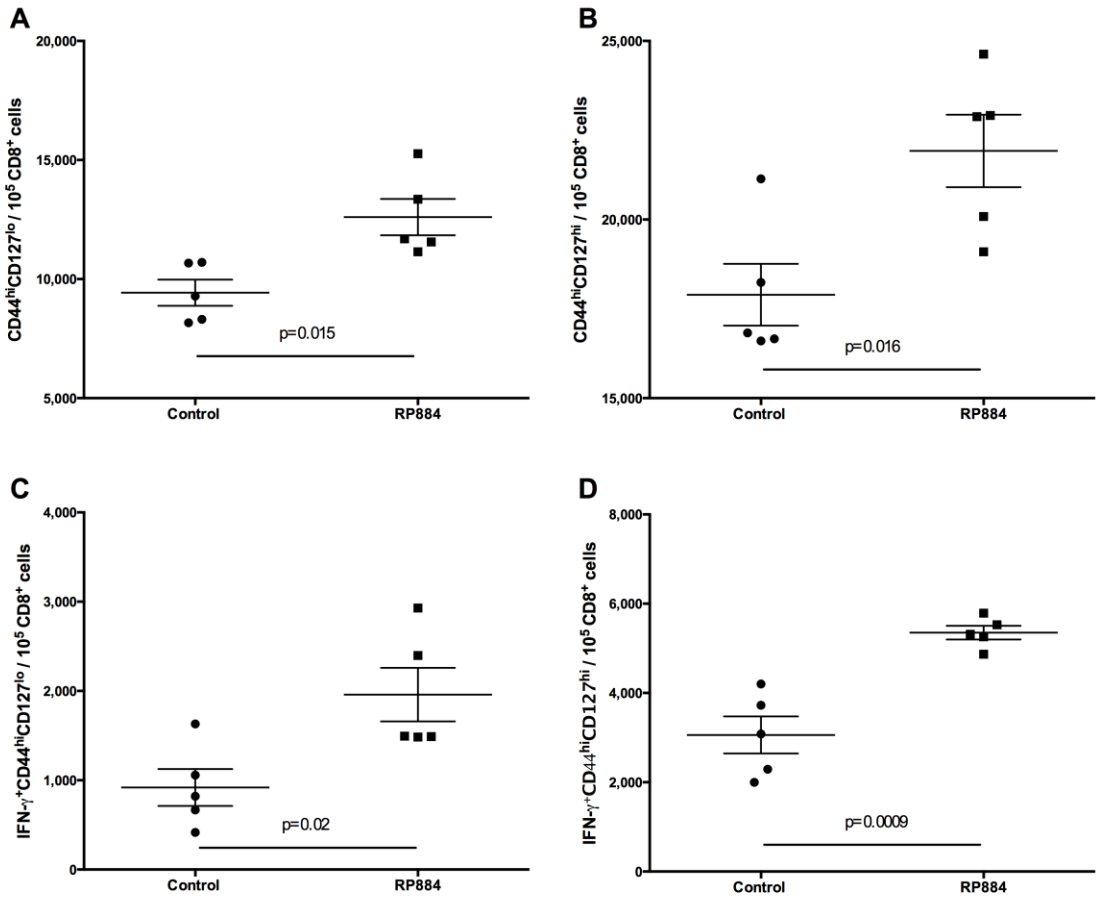

Figure 2.4 Increased effector and memory CD8$^+$ T-cells in mice immunized with RP884. RP884-immune animals and mice immunized with the *A. thaliana* control gene were challenged with 6 × LD_{50} of *R. typhi* and sacrificed 7 days later to obtain splenocytes for flow cytometric analysis. The proportion of antigen-experienced CD8$^+$ T-cells with an effector (A) or memory (B) phenotype was determined based on the expression of CD127. IFN-γ expression among effector-type (C) and memory-type (D) cells was also determined. Individual data points and mean ±SEM are shown.

DISCUSSION

Despite the many efforts to develop a vaccine against *R. prowazekii* [63], an effective vaccine has not been produced; the production of the most recent vaccine was stopped due to its significant variability in antigenicity and potency [64]. More recent work was aimed at the development of a subunit vaccine using the rickettsial surface proteins OmpA [73, 74] and OmpB [75, 76] as potential targets for $CD8^+$ T-cells.

In this proof-of-principle study, a new platform with the potential to discover relevant antigens for vaccine development independently of their ranking in the natural hierarchy of immunodominance, which expands the universe of possible antigens, is described. This platform also has the capability of identifying multiple antigens from a pathogen, which can then be used as components of a cross-protective subunit vaccine. Indeed, these results demonstrate that a single antigen from *R. prowazekii*, the product of the RP884 gene, can stimulate $CD8^+$ T-cells and immunize mice against a challenge with *R. typhi* (Fig. 2.2 and 2.3). The resulting effector- and memory-type $CD8^+$ T-cells (Fig. 2.4) produced IFN-γ, a known critical effector of the anti-rickettsial immune response [35, 41, 188].

The fact that the empirically-discovered protective antigen RP884 was not ranked highly by several different immunoinformatic programs (Table 2.2) is not necessarily surprising since the predicting power of those immunoinformatic strategies has not been directly compared against an empirical approach testing all ORFs (the ORFeome) of a pathogen. Moreover, at least for bacterial proteins, known protective antigens actually have less predicted epitopes than randomly selected bacterial protein sets used as a

control [139] . Thus, empirical approaches could contribute to the refinement of the *in silico* strategies for antigen discovery. Here, I used empirical antigen discovery data to formulate a reverse vaccinology strategy that better matched the empirical findings. The present results highlight the importance of combining proteasome-processing as well as MHC class-I binding predictions for *in silico* approaches aimed at discovering $CD8^+$ T cell antigens.

The discovered antigen, RP884, is highly conserved among members of the family Rickettsiaceae and it is 95% identical to that of *R. typhi*, which is consistent with the finding of cross-protection. The feasibility of a subunit vaccine that triggers T cell-mediated cross-protection against typhus group *Rickettsia* is further supported by the following: 1) T cell cross-reactivity is favored by the T cells themselves since the T cell receptor is multispecific due to structural flexibility and interactions with only a few residues within the presented peptides [103, 189]; 2) T cell-mediated cross protection has been demonstrated between organisms as genetically distant as *Aspergillus* and *Candida* [190] or as diverse as influenza virus [191]; 3) T cells are critical for effective immune responses against all *Rickettsia*, which is congruent with their intracellular cytoplasmic niche [37, 38]; 4) the anti-rickettsial T cell response is sufficient for protection as demonstrated through T cell transfer studies [37, 38]; and 5) these T cell responses are naturally cross-protective within the two major rickettsial groups (typhus and spotted fever groups) [40] and, even between those major groups [44].

Together these results represent a step forward toward the development of a subunit vaccine against typhus group *Rickettsia*, and suggest that by combining the

reverse vaccinology and *in vivo* screening approach described here, relevant protective antigens could be identified in the future.

CHAPTER 3: Discovery of Novel Cross-Protective *Rickettsia prowazekii* T cell Antigens Using a Combined Reverse Vaccinology and *In Vivo* Screening Approach[d]

ABSTRACT

T cells can mediate cross-protective immunity between typhus and spotted fever group *Rickettsia*, a finding consistent with the remarkable similarity among rickettsial genomes. However, protective *Rickettsia* T cell antigens remain unidentified. In the present study, I report the use of an *in silico* algorithm that allowed me to identify and validate four novel *R. prowazekii* vaccine antigen candidates recognized by $CD8^+$ T cells. The novel rickettsial vaccine candidate antigens, RP778, RP739, RP598, and RP403, protected mice against a lethal challenge with *R. typhi* and *R. conorii*, which is indicative of cross-protective immunity within the two major groups of pathogenic *Rickettsia*, typhus and spotted fever group *Rickettsia*. Together, these findings validate a reverse vaccinology approach as a viable strategy to identify protective rickettsial antigens and highlight the feasibility of a subunit vaccine that triggers T cell-mediated cross-protection between phylogenetically distant *Rickettsia*.

[d]A significant portion of this chapter has been accepted for publication in the journal Vaccine. Vaccine does not require copyright permission as long as proper citation is given. The citation for this article is: Caro-Gomez E, Gazi M, Goez Y, Valbuena G. Discovery of novel cross-protective *Rickettsia prowazekii* T-cell antigens using a combined reverse vaccinology and *in vivo* screening approach. Vaccine. 2014 Jul 7. pii: S0264-410X(14)00901-3.

INTRODUCTION

R. prowazekii, a louse-borne obligate intracellular bacterium, is the agent of epidemic typhus, which is one of the most lethal pathogens known to humans [6]. Due to lethality as high as 60% and its prior use as a bioweapon [6, 7, 169], it is classified as a category B priority pathogen and a CDC select agent. Unfortunately, an effective vaccine, a deterrent to its weaponization, is not currently available for this or any of the other rickettsial diseases. In addition, the potential impact of vaccines against these pathogens is highlighted by two facts: 1) there are no commercial methods for the acute diagnosis of rickettsioses, and 2) all rickettsial diseases present with non-specific initial clinical symptoms.

In appropriate animal models, $CD8^+$ T cells are critical effectors of protective anti-*Rickettsia* immunity [35, 37, 38]; moreover the critical role of $CD8^+$ T cells over $CD4^+$ T cells in resistance to rickettsial infections has been demonstrated in depletion and adoptive-transfer experiments [3, 35, 38]. Nevertheless the activation of a Th1 cytokine profile in anti-*Rickettsia* $CD4^+$ T cells is thought to contribute to $CD8^+$ T cell memory development, as well as to the generation of protective antibodies [3]. Therefore, the presence of antigens able to induce $CD4^+$ T cell-help in an anti-*Rickettsia* vaccine is desirable.

Previous work explored rickettsial surface proteins OmpA and OmpB as potential targets for $CD8^+$ or $CD4^+$ T cells [72–76]; however, the selection of these proteins for testing was based on the fact that they are immunodominant for the humoral immune response, which now is known is not a good predictor of antigens recognized by $CD8^+$ T

cells [170, 171]. No other antigens that trigger T cell-mediated protective immunity have been identified since. To address this gap, our laboratory developed an *in vivo* screening approach to identify antigens recognized by $CD8^+$ T cells as published [174] and described in chapter 2. Herein, I extended this work through refinement of our screening platform and the identification of novel *R. prowazekii* T cell antigens that stimulate a cross-protective response against the closely related *R. typhi*, the agent of flea-borne murine typhus, which is the most prevalent and neglected of the rickettsioses [5]. The entire *R. prowazekii* ORFeome (834 proteins) was analyzed *in silico* in order to identify and prioritize potential targets for $CD8^+$ T cells. From a set of twenty-two top-ranked T-cell antigenic targets, we identified and validated four novel cross-protective vaccine candidates.

MATERIALS AND METHODS

Bacteria

R. typhi (Wilmington strain) and *R. conorii* (Malish 7 strain) working stocks were produced in a CDC-certified BSL3 laboratory by cultivation in specific pathogen free embryonated chicken eggs. *Rickettsia* present in the stock was quantified by plaque assay [175], and the LD_{50} was determined experimentally in C3H/HeN mice.

***In silico* Prediction of *R. prowazekii* Proteins Encompassing Peptides Recognized by CD8$^+$ T cells.**

834 protein sequences from *R. prowazekii* strain Madrid E (Gene Bank ID AJ235269.1) were analyzed for the prediction of 9-mer peptides restricted to MHC class-I mouse allele H-2K^k using the following servers: NetMHCpan (http://www.cbs.dtu.dk/services/NetMHCpan/), IEBD-ANN (http://tools.immuneepitope.org/main/html/tcell_tools.html), and SYFPEITHI (http://www.syfpeithi.de/) [177–180]. Only proteins containing peptides predicted to be strong binders were considered for further analysis. For predictions performed using NetMHCpan and IEBD-ANN, only peptides with IC_{50} values $\leq$ 50 nM were considered; for SYFPEITHI, only peptides with an S-score of 21 and higher were included; this score was arbitrarily chosen and it represents 70% of the influenza A matrix protein epitope GILGFVFTL S-score. Rickettsial proteins were further analyzed using RANKPEP (http://imed.med.ucm.es/Tools/rankpep.html), which combines MHC class-I-binding affinity and proteasome processing [181]. We used RANKPEP to evaluate the likelihood of peptides predicted by NetMHCpan, IEBD-ANN and SYFPEITHI to be generated via proteasome-processing as we previously described [174]. Servers used for the *in silico* analysis are summarized in table 3.1.

***In silico* Prediction of *R. prowazekii* Proteins Encompassing Peptides Recognized by CD4$^+$ T cells.**

834 protein sequences from *R. prowazekii* strain Madrid E (Gene Bank ID AJ235269.1) were analyzed for the prediction of 9 mer peptides binding the mouse MHC

class-II allele I-A^k. Predictions were performed using RANKPEP (http://imed.med.ucm.es/Tools/rankpep.html) and SYPEITHI (http://www.syfpeithi.de/); which allowed the prediction of T cell epitopes restricted to the I-A^k allele. Only proteins encompassing peptides predicted to be strong binders were considered for further analysis. For RANKPEP, only peptides with a %OPT value ≥ 30% were included (binding to the I-A^k consensus sequence DFWCWECCC has an optimal score value of 39.9). In the case SYFPEITHI only proteins encompassing peptides with an S-score ≥ 20 were considered for further analysis. Additionally, with the aim of enhancing the probability of selecting proteins with protective potential, the immunodominance filter from RANKPEP was also used [181]. *R. prowazekii* proteins were ranked according to a score obtained by multiplying the number of peptides predicted by the averaged score of all predicted MHC class-II binding peptides for each protein; this step was performed independently for each server. Only the top 100 proteins from each server were further analyzed. Instead of using a single combined RANKPEP-SYPEITHI score for defining the top vaccine targets, the following criteria were used: The first set of selected proteins included only those predicted by both algorithms. Next, proteins ranked among the top 30 and predicted by only one server were added to the vaccine target list. Finally, in order to include a higher number of potential vaccine targets, a new score was calculated and applied only to RANKPEP predictions as described above; however, this time, only peptides predicted as after applying the immunodominance filter (%OPT value > 35.5%) were considered. New proteins ranked among the top 30 after applying the RANKPEP immunodominance score were also included in the final target list.

Table 3.1 Servers used for the *in silico* prediction of *R. prowazekii* MHC class-I and MHC class-II binding peptides.

Parameter	NetMHCpan	IEBD-ANN	SYFPEITHI	RANKPEP
Prediction method	ANNs	ANNs	Binding matrix	Binding matrix
Training dataset	Immuneepitope	Immuneepitope	SYFPEITHI	MHCPEP
Output	IC_{50}	IC_{50}	S-score	% of optimal score value from consensus peptide
Justification	Performance	Performance	High quality database	Proteasome filter Immunodominance filter

Generation of Antigen Presenting Cells (APCs) for Immunization

For immunization with the selected targets, we used a recently described platform with some modifications [174]. Briefly, SVEC4-10 cells modified to express the costimulatory molecules CD80 and CD137L were used as APCs. For this study, the original pDEST-M1 vector was modified as follows: the expression cassette was flanked by PiggyBac inverted terminal repeats and the tdTomato gene was replaced by a fused hygromycin/GFP gene preceded by a 2A peptide (it allows dissociation into component proteins on translation so that the rickettsial gene is not fused) and an HA tag (which is fused to the rickettsial protein to aid in identification). The new vector, pDEST-M2 was

nucleofected, together with an expression plasmid encoding the PiggyBac transposase, into APCs using the Amaxa SE Cell Line 96-well Nucleofector kit (Lonza). With this new vector system, cell lines stably expressing selected ORFs from *R. prowazekii* through transposition were generated. Success of nucleofection was corroborated by assessment of EGFP expression and hygromycin selection.

Screening and Validation of *In Silico* Vaccine Targets

We used an established mouse model of typhus [35] consisting of C3H/HeN mice infected i.v. with *R. typhi*, which is phylogenetically closely related to *R. prowazekii*, the other member of the typhus group rickettsiae. C3H/HeN mice were housed in an ABSL3 facility. For immunization, we followed a short immunization protocol that enhances $CD8^+$ T cell responses [106]. Changes to the immunization scheme described in the previous chapter were performed after a set of imaging experiments designed to track SVEC4-10 cells that were transduced to express the luciferase gene (Luc2); these experiments showed that, although after i.v. inoculation the signal rapidly declined (probably because it was not concentrated in a single anatomical site), it persisted for up to 6 days after i.p. or intramuscular (i.m.) inoculation [174]. Consequently, each mouse received 4.5×10^5 cells of cell suspension i.v. and i.m.; 5 days later, mice received the same dose of cells i.m. and i.p. Seven days after the second immunization, mice were infected i.v. with 5 or 6 LD_{50} of *R. typhi*. Animals were monitored for clinical symptoms and mortality for 21 days or euthanized after 7 days for rickettsial load assessment in the lungs. Rickettsiae were measured by quantitative real-time PCR using a validated assay previously described [174]. We followed the recommendations in the Guide for the Care

and Use of Laboratory Animals of the National Institutes of Health. Our experimental protocol was approved by the Institutional Animal Care and Use Committee (IACUC) of the University of Texas Medical Branch (protocol number: 0903026).

Flow Cytometry

We used an *ex vivo* approach that provides direct information about the response of T-cells *in vivo* since staining and analysis are performed after their extraction without further *in vitro* stimulation[186, 187]. Four hours prior to sacrifice, mice were injected i.p. with brefeldin A (250 µg/mouse) and monensin (500 µg/mouse). Mononuclear cells from spleens were purified by density gradient centrifugation (Lympholyte™-M, Cedarlane Laboratories) and stained with Live/Dead Fixable Blue (Life Technologies), APC-Alexa Fluor 750-conjugated anti-CD8 (5H10), FITC-conjugated anti-CD3 (17A2), BD Horizon V500-conjugated anti-CD44 (IM7), PE-Cy5 anti-CD127 (clone A7R34), and PE-Cy7-conjugated anti-IFN-γ (XMG1.2). CountBright™ Absolute Counting Beads (Life Technologies) were added to each sample prior to acquisition. All samples were acquired on a LSRII Fortessa cytometer (BD Biosciences); ~400.000 events were captured and data were analyzed using FlowJo 9.5.3 software (Tree-Star Inc). All analyses were performed on live $CD3^{+}CD8^{+}$ cells. Thresholds for positivity were determined with fluorescence-minus-one (FMO) control stains. Gating strategy is shown in the appendix as Figure A1.

Statistics

The proportion of surviving animals was analyzed with the Log-rank (Mantel-Cox) test. Mean absolute counts of $CD8^+$ T-cell subpopulations were compared using one-way analysis of variance (ANOVA) followed by Dunnett's correction for multiple comparisons (GraphPad Prism, version 6).

RESULTS

Rank of Proteins Encompassing MHC Class-I-Binding Peptides.

In chapter 2 and a recent publication, we described an *in silico* analysis strategy for the discovery of antigens with immunogenicity potential towards $CD8^+$ T-cells based on the identification of proteins encompassing predicted high-affinity proteasome-derived MHC class I-binding peptides [174]. In the present study, this *in silico* approach was extended to the entire *R. prowazekii* ORFeome (Fig. 3.1). A total of 834 *R. prowazekii* protein sequences were analyzed, and rickettsial proteins were ranked according to the described algorithm, which includes information about the number of predicted peptides per protein, their likelihood of being generated by the proteasome, and their predicted affinity for MHC class-I ($H\text{-}2K^k$). Analysis of the relative frequency of high-affinity proteasome-derived MHC class I-binding peptides among rickettsial proteins showed the following: 21.5% (179/834) of all *R. prowazekii* proteins did not include any peptide that fulfilled our inclusion criteria; 30% (250/834) contained one; 25% (209/834) contained two; 14.9% (124/834) contained three; 6.8% (57/834) contained four; and 1.9% (16/834) contained five proteasome-derived peptides.

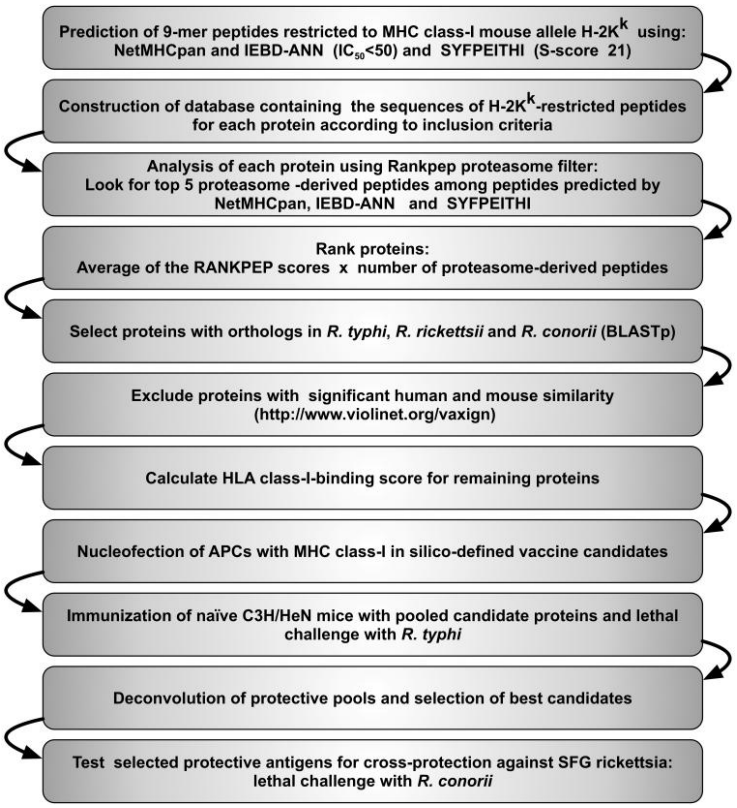

Figure 3.1 Flow diagram of the discovery process for antigens recognized by CD8$^+$ T cells.

Rank of Proteins Encompassing MHC Class-II-Binding Peptides.

CD4$^+$ T cell epitopes are suspected to play an important role in the induction of protective immune responses, given that the help provided by CD4$^+$ T cells is crucial for the generation of strong and long lasting humoral and cytotoxic CD8$^+$ T cell responses [184, 192]. Thus, one could speculate that proteins encompassing peptides that have a significant chance to bind MHC class-II molecules, i.e. proteins containing high-affinity CD4$^+$ T cell epitopes, might contribute to elicit significant immune responses.

R. prowazekii protein sequences were analyzed and ranked according to the described algorithm; 86% of all *R. prowazekii* proteins were found to encompass high-affinity I-A^k allele-binding peptides. After analyzing the top 100 ranked proteins for each server, a final list of 85 top ranked vaccine targets was generated as follows: 54 proteins were predicted by both servers SYFPEITHI and RANKPEP; among them, 68.5% (37/54) were predicted to encompass immunodominant epitopes, 22 proteins were predicted only by one algorithm, and 9 additional proteins become top-ranked after applying the RANKPEP immunodominace-based score.

Selection of *In Silico*-Defined Antigen Candidates

Further *in silico* analysis was restricted to the top 100 and top 85 rickettsial proteins predicted to encompass MCH class-I or MHC class-II high-affinity binding-peptides, respectively. Protein length among predicted vaccine targets was variable; overall, proteins predicted to encompass MHC class-II binding peptides were longer (mean length MHC class-I candidates=488.1 aminoacids vs. mean length MHC class-II candidates=769.7 aminoacids). Interestingly, 41% of rickettsial proteins ranked among the top 100 proteins for MHC class I had only 2 or 3 proteasome-derived peptides, indicating that both number of peptides and binding affinity contributed to the position in the final ranking (**Fig. 3.2**).

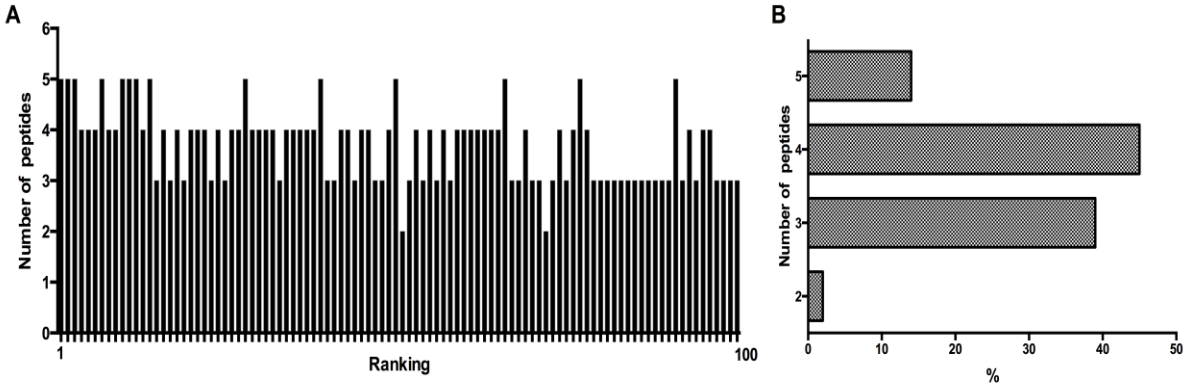

Figure 3.2 Number of proteasome-derived peptides. (A) Number of proteasome-derived peptides and rank position. (B) Relative frequency of proteasome-derived peptides among top 100 *in silico*- defined MHC class-I antigen candidates.

To limit the number of proteins to be tested as vaccine candidates with potential for cross-protection, I first used BLASTp (http://blast.ncbi.nlm.nih.gov/Blast.cgi) to search for the presence of orthologs in other pathogenic *Rickettsia* species: *R. typhi* strain Wilmington, *R. conorii* strain Malish 7 and *R. rickettsii* strain 'Sheila Smith'. Proteins with a query coverage ≥ 60% and sequence identity ≥ 60% were considered orthologs to *R. prowazekii* proteins. In the case of MHC class-I targets, four proteins were excluded, one protein did not meet these inclusion criteria, and three others were absent in spotted fever group (SFG) *Rickettsia*. From the MHC class-II group, five proteins were excluded because they were absent in the SFG *Rickettsia*.

Subsequently, the subcellular localization of the remaining *R. prowazekii* proteins was predicted using PSORTb 3.0.2 (http://www.psort.org/psortb/) [182]. Although subcellular localization is not critical for T cell mediated responses, this analysis revealed that *Rickettsia* proteins encompassing high-affinity MHC calss-I binding-peptides were

preferentially predicted as cytoplasmic: 68.8 % (66/96) vs. 55% (44/80) for MHC class-II. In contrast, proteins located in the cytoplasmic membrane, outer membrane or extracellular proteins were mainly predicted to contain MHC class-II binding-peptides: 31.25% (25/80) vs. 19.79% (19/96) for MHC class-I (**Fig. 3.3A**). In terms of potential function, most of the proteins were annotated as hypothetical or metabolism related, followed by proteins involved in DNA synthesis, repair, transcription, and replication (**Fig. 3.3B**).

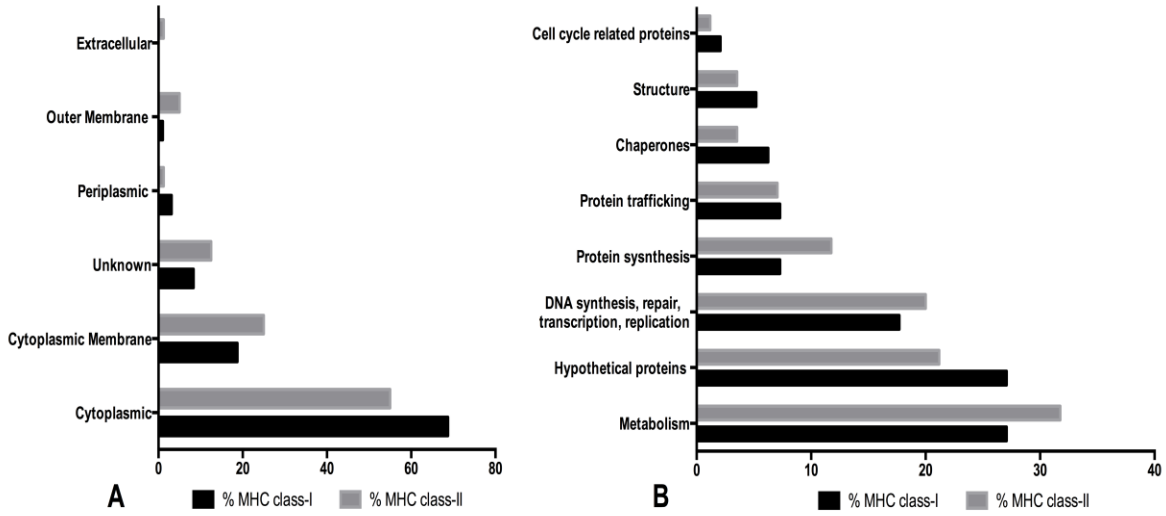

Figure 3.3 Subcellular localization and annotated function. (A) Subcellular localization predicted by PSORTb 3.0.2, and (B) Annotated function of *in silico*-predicted MHC class-I and MHC class-II vaccine targets with orthologs in the SFG *Rickettsia*.

Next, proteins with similarities to human and mouse proteins were excluded. This component of the analysis was performed using Vaxign, available through the Vaccine Investigation and Online Information Network (VIOLIN, http://www.violinet.org/). Forty-five and thirty proteins with homology to mouse or human were found among

MHC class-I and MHC class-II predicted targets, respectively; since the area of homology for some of these proteins (MHC class-I n=8 and MHC class-II n=11) was of only 16 amino acids or less (with 4 or fewer regions like this per protein), these proteins were also included in our final testing list; the rationale was that, if they are protective, the epitopes conferring protection might be outside the regions of homology, and it would not preclude their further use as part of a subunit vaccine.

Until this point of the analysis, *in silico* vaccine targets were defined based on: 1) the presence of proteasome-derive peptides that are also strong binders to the MHC class-I mouse allele H-2K^{k}, and 2) the presence of high-affinity MHC class-II I-A^{k} allele binding peptides. In a final step, a corresponding HLA class-I or HLA class-II binding score was assigned to the 63 MHC class-I or 61 MHC class-II *in silico*-defined vaccine targets. This new score incorporated the capability of peptides derived from the selected proteins to bind HLA alleles; the score resulted from dividing the number of HLA class-I or HLA class-II epitopes predicted by Vaxitope from VIOLIN, regardless of the allele or binding affinity, by the number of amino acids in the rickettsial protein (length adjustment). For MHC class-I predictions, compared to the original ranking, which was only mouse-based, several proteins had striking changes in their ranking positions when binding to HLA class-I alleles was incorporated (Table 3.2)**.** When RANKPEP immunodominance-based score was applied to MHC class-II binding predictions performed by this server, for some proteins, the new position in the ranking was not so distant compared to the original RANKPEP rank; however, some others showed significant differences indicating that these proteins contained a large number of peptides either below or above the immunodominance binding affinity threshold (Table 3.3).

Also, it was interesting to note that after applying the HLA class-II binding score, 43.3% of the top 30 proteins (13/30) were not predicted by SYFPEITHI compared to 6.6% (2/30) that were not predicted by RANKPEP.

Table 3.2 Antigens from *R. prowazekii* predicted *in silico* to encompass MHC class-I-binding peptides.

Rickettsial protein	Annotated function	Predicted subcellular localization*	HLA class I-binding score	Proteasome / $H2K^k$ binding score	Number of proteasome - peptides
RP216	cytochrome D ubiquinol oxidase subunit I (cydA)	Cytoplasmic Membrane	1	45	3
RP739[1]	**ADP,ATP carrier protein**	**Cytoplasmic Membrane**	**2**	**21**	**4**
RP047	hypothetical protein RP047	Cytoplasmic Membrane	3	51	4
RP403[1]	**hypothetical protein RP403**	**Cytoplasmic**	**4**	**2**	**5**
RP884	Ferrochelatase	Cytoplasmic	5	1	4
RP718	lipid A biosynthesis lauroyl acyltransferase	Cytoplasmic	6	58	3
RP876	Lipoyltransferase	Cytoplasmic	7	42	5
RP734[1]	**ATP-dependent nuclease subunit A (addA)**	**Cytoplasmic**	**8**	**55**	**3**
RP329	hypothetical protein RP329	Cytoplasmic Membrane	9	27	4
RP027	hypothetical protein RP027	Cytoplasmic	10	47	2
RP042[5]	**cell cycle protein MESJ (mesJ)**	**Cytoplasmic**	**11**	**7**	**4**
RP339	minor teichoic acids biosynthesis protein ggab (ggab)	Cytoplasmic Membrane	12	31	3
RP864	hypothetical protein RP864	Cytoplasmic	13	39	4
RP540[2]	**primosome assembly protein PriA**	**Cytoplasmic**	**14**	**28**	**4**
RP006[2]	**hypothetical protein RP006**	**Cytoplasmic**	**15**	**16**	**4**
RP512	ribonucleotide-diphosphate reductase subunit beta	Cytoplasmic	16	60	3
RP120	hypothetical protein RP120	Unknown	17	56	3
RP804	F0F1 ATP synthase subunit delta	Cytoplasmic	18	62	3
RP246[2]	**hypothetical protein RP246**	**Cytoplasmic Membrane**	**19**	**41**	**4**
RP731	dephospho-CoA kinase	Cytoplasmic	20	4	5

RP048	putative inner membrane protein translocase component YidC	Cytoplasmic Membrane	21	24	3
RP598[3]	**transcription-repair coupling factor**	**Cytoplasmic**	**22**	**12**	**4**
RP778[3]	**DNA polymerase III subunit alpha**	**Cytoplasmic**	**23**	**23**	**4**
RP849	glycyl-tRNA synthetase subunit beta	Cytoplasmic	24	38	3
RP029	recombination protein F	Cytoplasmic	25	14	3
RP431[5]	**hypothetical protein RP431**	**Cytoplasmic**	**26**	**17**	**4**
RP572[5]	**excinuclease ABC subunit C**	**Cytoplasmic**	**27**	**34**	**3**
RP758	hypothetical protein RP758	Cytoplasmic	28	37	3
RP367	hypothetical protein RP367	Cytoplasmic Membrane	29	29	4
RP559[3]	**hypothetical protein RP559**	**Unknown**	**30**	**40**	**3**
RP622	3-demethylubiquinone-9 3-methyltransferase	Cytoplasmic	31	49	3
RP071	transcriptional activator protein CZCR (czcR)	Cytoplasmic	32	44	4
RP170	acriflavin resistance protein D	Cytoplasmic Membrane	33	18	3
RP531[5]	**translation initiation factor IF-3**	**Cytoplasmic**	**34**	**57**	**3**
RP441	hypothetical protein RP441	Cytoplasmic	35	54	4
RP014	hypothetical protein RP014	Periplasmic	36	11	5
RP822	hypothetical protein RP822	Cytoplasmic Membrane	37	5	4
RP203	excinuclease ABC subunit B	Cytoplasmic	38	9	3
RP635	DNA-directed RNA polymerase subunit alpha	Cytoplasmic	39	20	4
RP492	pyruvate phosphate dikinase	Cytoplasmic	40	10	4
RP146[4]	**hypothetical protein RP146**	**Cytoplasmic**	**41**	**30**	**2**
RP505	arabinose-5-phosphate isomerase	Cytoplasmic	42	8	5
RP753	aspartate kinase	Unknown	43	61	3
RP404	hypothetical protein RP404	Cytoplasmic	44	43	3
RP589	inorganic pyrophosphatase	Cytoplasmic	45	22	4
RP306	tRNA (5-methylaminomethyl-2-thiouridylate)-methyltransferase	Cytoplasmic	46	26	4
RP320	ATP-dependent protease ATP-binding subunit	Cytoplasmic	47	32	3
RP030	hypothetical protein RP030	Cytoplasmic	48	53	3

RP314[5]	**alkaline protease secretion protein AprE**	**Cytoplasmic Membrane**	**49**	**52**	**3**
RP848[6]	**hypothetical protein RP848**	**Cytoplasmic**	**50**	**33**	**4**
RP341	hypothetical protein RP341	Cytoplasmic Membrane	51	19	3
RP347	outer membrane assembly protein (asmA)	Unknown	52	48	3
RP858[4]	**RNA polymerase sigma factor RpoD**	**Cytoplasmic**	**53**	**13**	**3**
RP627[6]	**co-chaperonin GroES**	**Cytoplasmic**	**54**	**6**	**5**
RP522	cytidylate kinase	Cytoplasmic	55	46	3
RP300	outer membrane antigenic lipoprotein B precursor (nlpD)	Unknown	56	63	3
RP391	hypothetical protein RP391	Periplasmic	57	35	4
RP228	tail-specific protease precursor (CTP)	Unknown	58	36	3
RP226[4]	**hypothetical protein RP226**	**Unknown**	**59**	**50**	**4**
RP498[6]	**cell surface antigen (sca4)**	**Cytoplasmic**	**60**	**25**	**3**
RP704	cell surface antigen (sca5)	Outer Membrane	61	3	4
RP585[6]	**preprotein translocase subunit YajC**	**Cytoplasmic Membrane**	**62**	**15**	**4**
RP763[6]	**acyl carrier protein**	**Cytoplasmic**	**63**	**59**	**5**

* Subcellular localization was predicted using PSORTb 3.0.2 (http://www.psort.org/psortb/); [1] *R. prowazekii* proteins in pool #1; [2] *R. prowazekii* proteins in pool #2; [3] *R. prowazekii* proteins in pool #3; [4] *R. prowazekii* proteins in pool #4; [5] *R. prowazekii* proteins in pool #5; [6] *R. prowazekii* proteins in pool #6

Table 3.3 Antigens from *R. prowazekii* predicted *in silico* to encompass MHC class-II-binding peptides.

Rickettsial protein	Annotated function	Predicted subcellular localization*	HLA class II-binding score	SYPEITHI binding score §	RANKPEP binding score §	RANKPEP Immuno-dominance score §
☯RP246	**hypothetical protein RP246**	**Cytoplasmic Membrane**	**1**	**45**	**NP**	**NP**
☯RP739	**ADP,ATP carrier protein**	**Cytoplasmic Membrane**	**2**	**NP**	**64**	**88**
RP346	protoheme IX farnesyltransferase	Cytoplasmic Membrane	3	15	NP	NP
☯RP403	**hypothetical protein RP403**	**Cytoplasmic**	**4**	**36**	**79**	**44**
RP465	alkaline phosphatase synthesis sensor protein PhoR	Cytoplasmic Membrane	5	NP	22	10
RP620	acylglycerophosphoethanolamine acyltransferase	Cytoplasmic Membrane	6	40	17	93
RP093	VACJ lipoprotein precursor	Unknown	7	NP	12	67
RP281	protease II	Unknown	8	70	7	8
☯RP042	**cell cycle protein MESJ (mesJ)**	**Cytoplasmic**	**9**	**NP**	**16**	**7**
RP535	uperoxide dismutase (sodB)	Periplasmic	10	NP	6	6
RP107	hypothetical protein RP107	Cytoplasmic Membrane	11	5	4	3
RP106	hypothetical protein RP106	Cytoplasmic Membrane	12	NP	5	4
RP478	hypothetical protein RP478	Unknown	13	NP	45	14
RP678	hypothetical protein RP678	Cytoplasmic Membrane	14	NP	18	25
RP593	ATP-dependent DNA helicase RECG (recG)	Cytoplasmic	15	78	51	83
RP784	VIRB4 protein precursor (virB4)	Cytoplasmic Membrane	16	18	29	22
RP859	DNA primase	Cytoplasmic	17	20	60	55
☯RP006	**hypothetical protein RP006**	**Cytoplasmic**	**18**	**NP**	**41**	**37**
RP239	extragenic suppressor protein SUHB (suhB)	Cytoplasmic	19	NP	97	18
RP780	hypothetical protein RP780	Cytoplasmic	20	24	38	77

RP674	hypothetical protein RP674	Outer Membrane	21	44	8	26
RP558	hypothetical protein RP558	Unknown	22	90	30	100
☯RP540	**primosome assembly protein PriA**	**Cytoplasmic**	**23**	**NP**	**72**	**24**
RP565	penicillin-binding protein (pbpA1)	Cytoplasmic Membrane	24	NP	23	23
☯RP512	**ribonucleotide-diphosphate reductase subunit beta**	**Cytoplasmic**	**25**	**14**	**69**	**95**
☯RP734	**ATP-dependent nuclease subunit A (addA)**	**Cytoplasmic**	**26**	**30**	**24**	**28**
☯RP849	**glycyl-tRNA synthetase subunit beta**	**Cytoplasmic**	**27**	**76**	**61**	**60**
RP785	hypothetical protein RP785	Outer Membrane	28	21	3	5
☯RP758	**hypothetical protein RP758**	**Cytoplasmic**	**29**	**8**	**11**	**96**
RP293	type IV secretion system component VirD4	Cytoplasmic Membrane	30	NP	86	17
☯ RP598	**transcription-repair coupling factor**	**Cytoplasmic**	**31**	**4**	**21**	**31**
RP807	penicillin-binding protein 1A (mrcA)	Cytoplasmic Membrane	32	54	53	73
RP108	hypothetical protein RP108	Cytoplasmic Membrane	33	7	63	92
RP349	hypothetical protein RP349	Unknown	34	NP	27	68
RP720	NAD-dependent DNA ligase LigA	Cytoplasmic	35	60	25	29
RP513	ribonucleotide-diphosphate reductase subunit alpha	Cytoplasmic	36	58	65	94
☯RP559	**hypothetical protein RP559**	**Unknown**	**37**	**25**	**10**	**59**
RP326	DNA topoisomerase I	Cytoplasmic	38	57	85	76
☯RP146	**hypothetical protein RP146**	**Cytoplasmic**	**39**	**67**	**50**	**98**
☯RP778	**DNA polymerase III subunit alpha**	**Cytoplasmic**	**40**	**27**	**13**	**48**
RP840	heat shock protein 90	Cytoplasmic	41	48	56	33
RP575	preprotein translocase subunit SecA	Cytoplasmic	42	26	NP	NP
RP822	hypothetical protein RP822	Cytoplasmic Membrane	43	75	NP	NP
RP614	nitrogen regulation protein NTRY (ntrY)	Cytoplasmic Membrane	44	53	NP	NP
RP511	hypothetical protein RP511	Cytoplasmic	45	6	34	45

RP104	hypothetical protein RP104	Cytoplasmic Membrane	46	14	NP	NP
☯RP492	**pyruvate phosphate dikinase**	**Cytoplasmic**	**47**	**77**	**37**	**75**
RP602	patatin B1 precursor (pat1)	Cytoplasmic	48	43	9	9
RP835	excinuclease ABC subunit A	Cytoplasmic	49	19	70	86
RP373	malic enzyme	Cytoplasmic	50	52	47	40
RP103	type IV secretion system ATPase VirB4	Cytoplasmic Membrane	51	12	NP	NP
☯RP347	**outer membrane assembly protein (asmA)**	**Unknown**	**52**	**NP**	**15**	**34**
RP760	hypothetical protein RP760	Unknown	53	NP	32	13
☯RP203	**excinuclease ABC subunit B**	**Cytoplasmic**	**54**	**28**	**33**	**27**
RP451	cell surface antigen (sca3)	Outer Membrane	55	1	1	1
☯RP858	**RNA polymerase sigma factor RpoD**	**Cytoplasmic**	**56**	**66**	**NP**	**NP**
RP563	hypothetical protein RP563	Extracellular	57	22	19	84
☯RP704	**cell surface antigen (sca5)**	**Outer Membrane**	**58**	**2**	**2**	**2**
☯RP226	**hypothetical protein RP226**	**Unknown**	**59**	**61**	**43**	**20**
☯RP498	**cell surface antigen (sca4)**	**Cytoplasmic**	**60**	**9**	**NP**	**NP**
RP017	hypothetical protein RP017	Unknown	61	17	87	32

*Subcellular localization was predicted using PSORTb 3.0.2 (http://www.psort.org/psortb/); § Ranking among initial 85 top proteins; NP not predicted; ☯ *R. prowazekii* proteins predicted as *in silico* vaccine targets for both MHC class-I and MHC class-II.

Identification of Novel Protective Antigens

Although it has been proposed that $CD4^+$ and $CD8^+$ T cells target a different set of antigens[170, 171], it was interesting to observe that among all *R. prowazekii* T cell predicted vaccine targets, 21 rickettsial proteins were predicted to contain both MHC class-I and MHC class-II binding-peptides (Table 3.3). Twelve out of 21 proteins from this set of vaccine targets were tested *in vivo*. The rationale behind first testing rickettsial proteins predicted as vaccine targets for both MHC class-I and MHC class-II systems was that the presence of $CD4^+$ and $CD8^+$ T cell epitopes in the same protein could provide enhanced protection. These proteins were selected to represent the range of immunogenic potential predicted after applying the HLA class-I-binding score. Thus, six proteins were ranked among the top 20 and the rest were ranked at position 22 or below; tested *R. prowazekii* ORFs are shown in Table 3.2. For the identification of protective antigens, proteins were tested in a context biased towards $CD8^+$ T cell recognition as recently published and also described in chapter 2 [174]. Mice were immunized with APCs expressing individual ORFs (1.5×10^5 APCs per ORF/mouse), pooled in sets of three. Reduction of *Rickettsia* load at 7dpi was used as surrogate measure of protection (Fig. 3.4A); although no statistically significant differences between control and immunized groups were observed, two potentially protective pools were suspected based on the mean value of the *Rickettsia* load in lungs (pool #1 and pool #3). These pools were deconvoluted in order to identify ORF(s) responsible for this potential protective effect. Mice were immunized with 4.5×10^5 APCs individually expressing RP739, RP403, RP734, RP598, RP778 or RP559, and challenged as described. None of the tested ORFs induced significant reduction of *Rickettsia* load; yet, remarkable differences in the

clinical status of mice in different immunization groups at the time of sacrifice to procure samples for bacterial load determination at 7 dpi were observed: some animals were found dead, some others were moribund (unresponsive to stimuli), while others were active. In figure 3.4B, individual mice were labeled accordingly to show that the rickettsial load was not a predictor of clinical behavior. For example, some moribund control mice had rickettsial loads as low or lower than the loads of immunized mice that were active, and some active mice had rickettsial loads that were higher than the load of any control mice; indeed, 6 out of 7 mice from the RP739 vaccinated group were active and clinically healthy. These observations made us reconsider the effectiveness of *Rickettsia* load reduction as readout for screening vaccine targets; thus, we tested whether survival would be more informative. We performed a survival analysis of those vaccine targets shown in figure 3.4B with more active mice and lower mean values of *Rickettsia* load among mice classified as moribund (RP739, RP403, RP734, RP598); RP778, a vaccine target that did not meet these criteria, was also included.

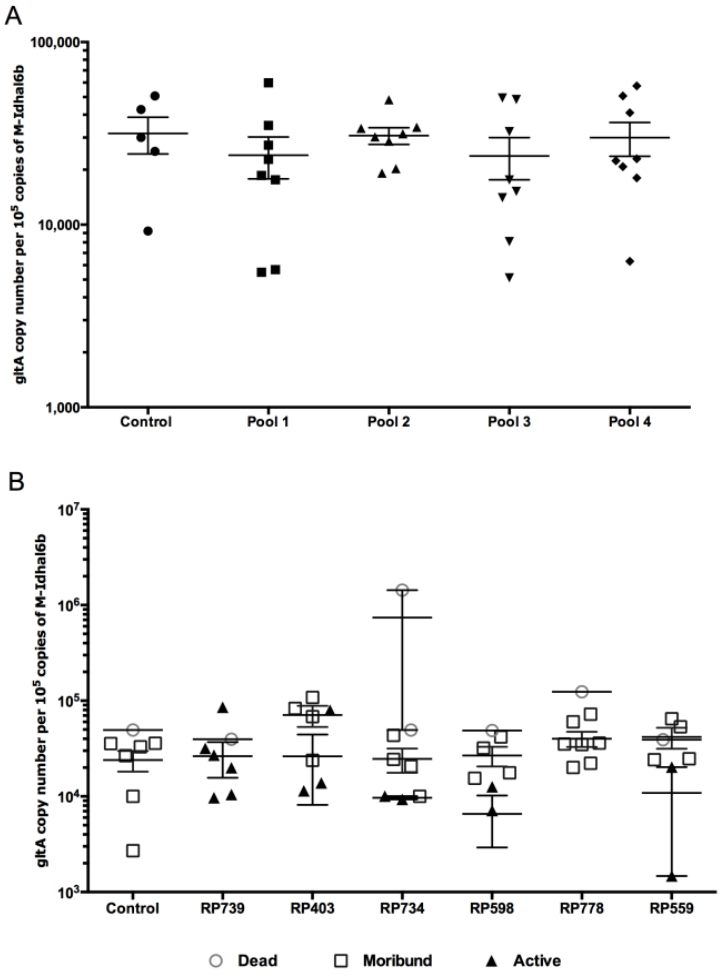

Figure 3.4 ***In vivo*** **testing of** ***in silico*****-defined vaccine targets**. (A) APCs individually expressing selected *R. prowazekii* ORFs were combined in 4 pools as follows: Pool 1 (RP739, RP403, RP734), Pool 2 (RP540, RP006, RP246), Pool 3 (RP598, RP778, RP559), and Pool 4 (RP146, RP858, RP226). Mice were immunized with pooled APCs expressing *R. prowazekii* proteins (8 mice per group) or an irrelevant protein (luciferase, 5 mice per group). Seven days after immunization, mice were challenged with 6 × LD_{50} of *R. typhi*. At 7 dpi, animals were terminated and rickettsial load in the lungs was measured using quantitative real time PCR (Q-PCR) targeting the mouse gene *Idhal6b* and the rickettsial gene *gltA.* Although no significant reduction of *Rickettsia* load was observed, pools 1 and 3 showed lower mean values. (B) *R. prowazekii* ORFs in pool 1 and 3 were individually tested as described above. No significant differences in the rickettsia load were detected after the deconvolution step; however, differences in clinical findings were observed among groups; they were active, moribund, or dead. We show individual data points with mean ± SEM.

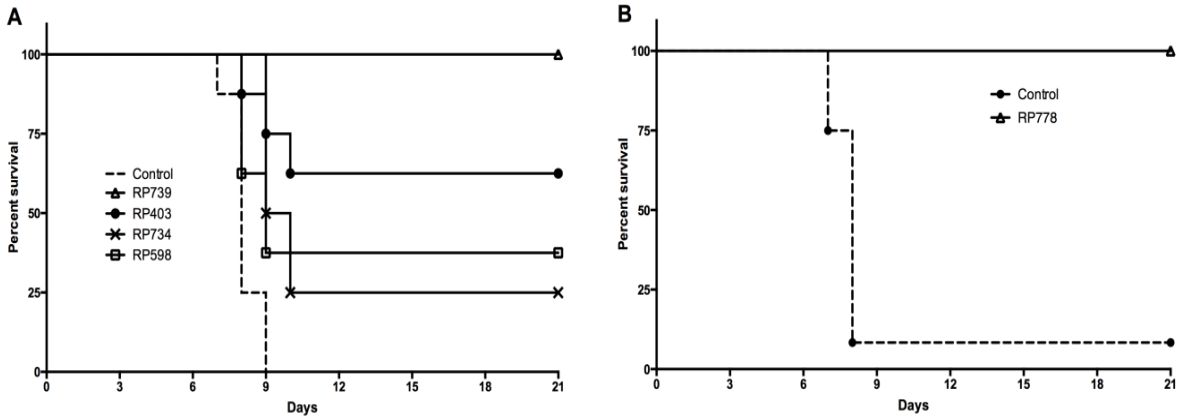

Figure 3.5 Survival analysis allowed the identification of novel *R. prowazekii* protective antigens. (A) Mice immunized with APCs expressing luciferase (control, n=8) or selected rickettsial proteins (n=8) were challenged with 5 × LD_{50} of *R. typhi* and followed for 21 days to determine survival. 100% of RP739-immune mice ($p<0.0001$); 62.5% of RP403-immune mice ($p=0.0014$); 37.5% of RP598-immune mice ($p=0.0413$); and 25% of RP734-immune mice ($p=0.0015$) survived the lethal challenge while none of the control animals did. (B) RP778 was separately tested (because it did not meet our initial criteria for selection from analysis of the pools) as in (A) (12 mice per group); 100% of RP778-immune mice survived while only 8.3% of control animals did ($p<0.0001$).

In silico-Defined Vaccine Candidates Confer Protection Against a Lethal Challenge and Stimulate $CD8^+$ T Cell Responses

Mice were immunized with RP739, RP403, RP734, RP598 or RP778 and challenged with 5LD_{50} of *R. typhi*. Animals were monitored for signs of illness (lethargy, hunchback posture, ruffled hair and paralysis) and death for 21 days. As shown in figure 3.5A and 3.5B, 92% to 100% of control mice succumbed to the rickettsial infection by day 9; in contrast, all tested ORFs decreased mortality and provided significant protection against a *R. typhi* lethal challenge. RP778 and RP739 provided 100% protection while RP403 protected 62.5% of mice; immunization with RP598 or RP734 resulted in 37.5%

and 25% survival, respectively, which is still significant. Thus, it appears that bacterial load at a fixed time point (Fig. 3.4) is not always sufficiently informative as a surrogate for protection.

Since the *in silico* approach used for identification of potential targets and the immunization strategy were designed to be biased towards MHC class-I presentation, I analyzed $CD3^{+}CD8^{+}$ cells from animals immunized with APCs expressing RP739, RP403, RP734, RP598 or RP778 at 7 dpi. Antigen-experienced $CD8^{+}$ T cells ($CD3^{+}CD8^{+}CD44^{high}$) from immunized animals showed increased expression of IFN-γ (Fig. 3.6A), ~ 1.5 fold-increase or higher, after *Rickettsia* challenge compared to control animals immunized with APCs expressing an irrelevant antigen (luciferase); however, this change was only statically significant for RP778 ($p<0.01$) (Fig. 3.6B). Memory-type $CD8^{+}$ T-cells ($CD44^{high}CD127^{high}$) were also increased, particularly in RP778-immune mice (Fig. 3.6C), and significantly larger numbers of IFN-γ-producing cells were observed for this subpopulation (Fig. 3.6D and E). Although tested in a context that favors $CD8^{+}$ T cell responses, RP778 also induced significant IFN-γ expression in antigen-experienced CD4 T cells ($CD3^{+}CD4^{+}CD44^{high}$) (Fig . 3.7).

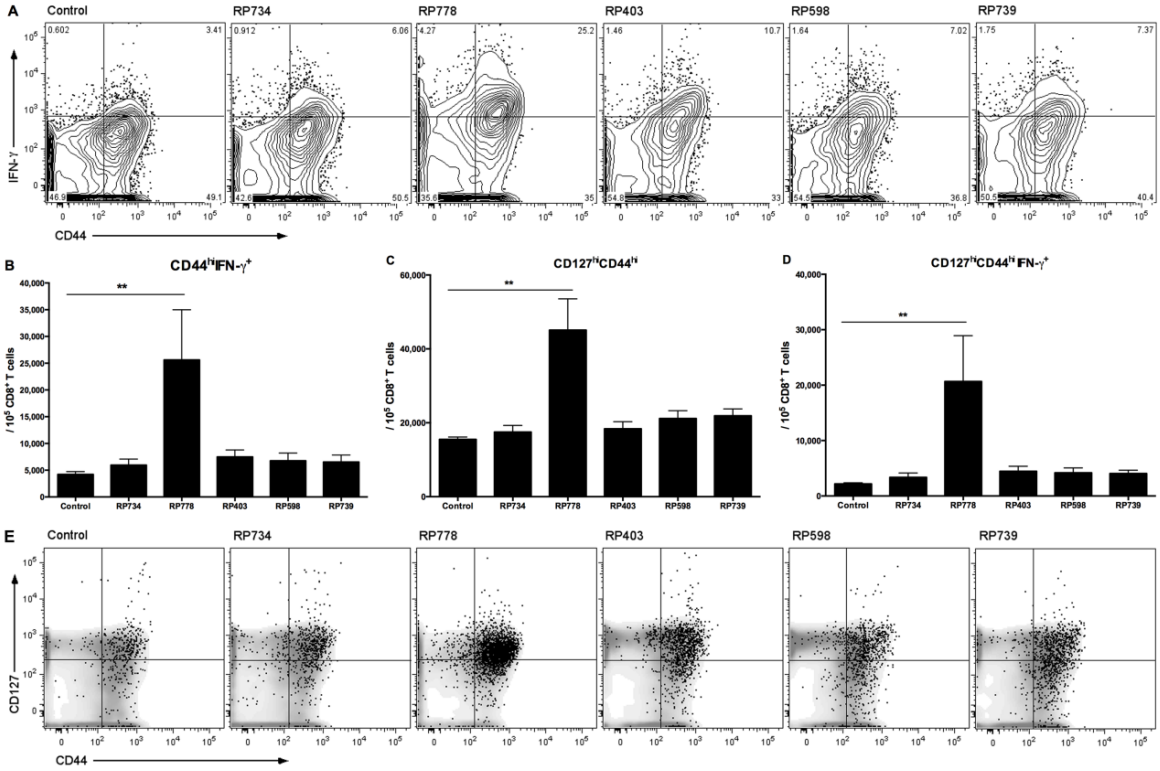

Figure 3.6 Novel rickettsial protective antigens are recognized by CD8$^+$ T cells. Mice immunized with APCs expressing luciferase or *R. prowazekii* proteins were challenged with 5 × LD_{50} of *R. typhi* and sacrificed at 7dpi (4 hours after i.p. injection of brefeldin A and monensin) to obtain splenocytes for flow cytometric analysis. Cells were stained with CD3, CD8, CD44, CD127, and IFN-γ to determine (A) the frequency and (B) the number of antigen experienced CD8$^+$ T cells producing IFN-γ *ex vivo*. (C) Number of memory-type (CD127^{hi}CD44^{hi}) CD8$^+$ T cells. (D) Number of memory-type CD8$^+$ T cells producing IFN-γ. (E) Illustrative density plot of CD127 vs. CD44 expression with IFN-γ expression overlaid on the plot (black dots). Data in (B), (C), and (D) is presented as mean ± SEM from five mice per group. p values for comparisons against control mice are represented as follows: **p<0.01.

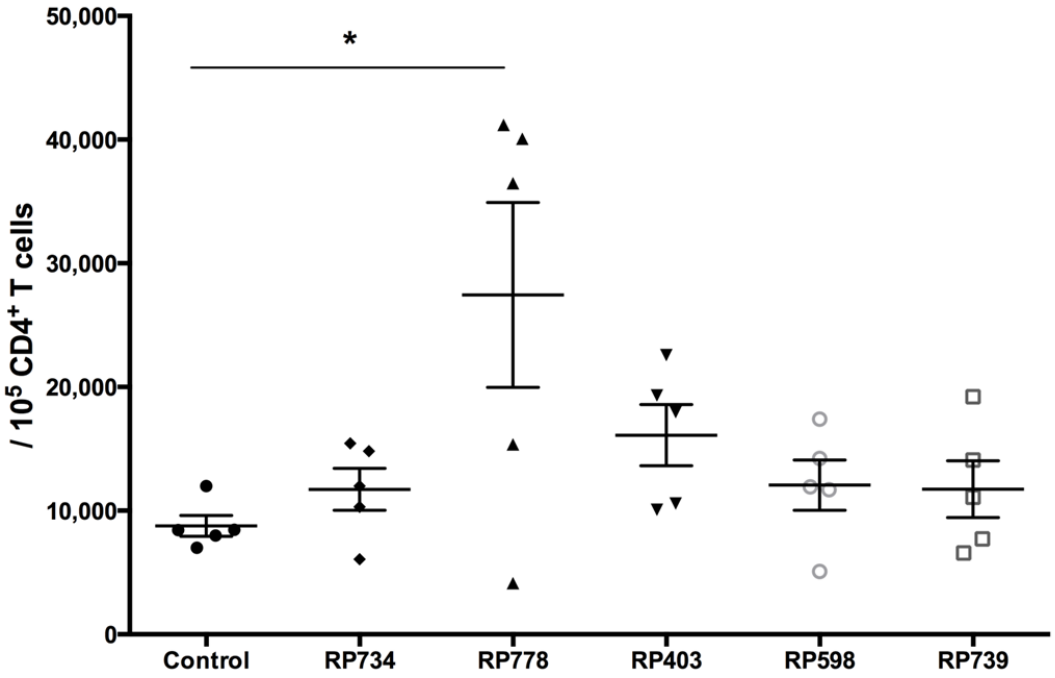

Figure 3.7 Immunization with novel protective antigens induced IFN-γ expression in antigen experienced CD4$^+$ T cells. Mice immunized with APCs expressing luciferase or *R. prowazekii* proteins were challenged with 5 × LD_{50} of *R. typhi* and sacrificed at 7dpi (4 hours after i.p. injection of brefeldin A and monensin) to obtain splenocytes for flow cytometric analysis. Individual data points and mean ±SEM are shown. p values for comparisons against control mice are represented as follows: *p<0.05.

Based on these promising results, a new set of 10 proteins was tested for survival as described; this new set mainly included proteins predicted to encompass MHC class-I-binding peptides (n=8), and only 2 proteins predicted to contain MHC class-I and MCH class-II binding peptides were included (Table 3.2; pools #5 and #6). The idea behind

this experiment was to test if the presence of MHC class-I and MHC class-II epitopes on the same protein correlates with the protective potential of the *in silico*-defined targets. As shown in figure 3.8 none of these pools conferred significant protection against a *R. typhi* lethal challenge.

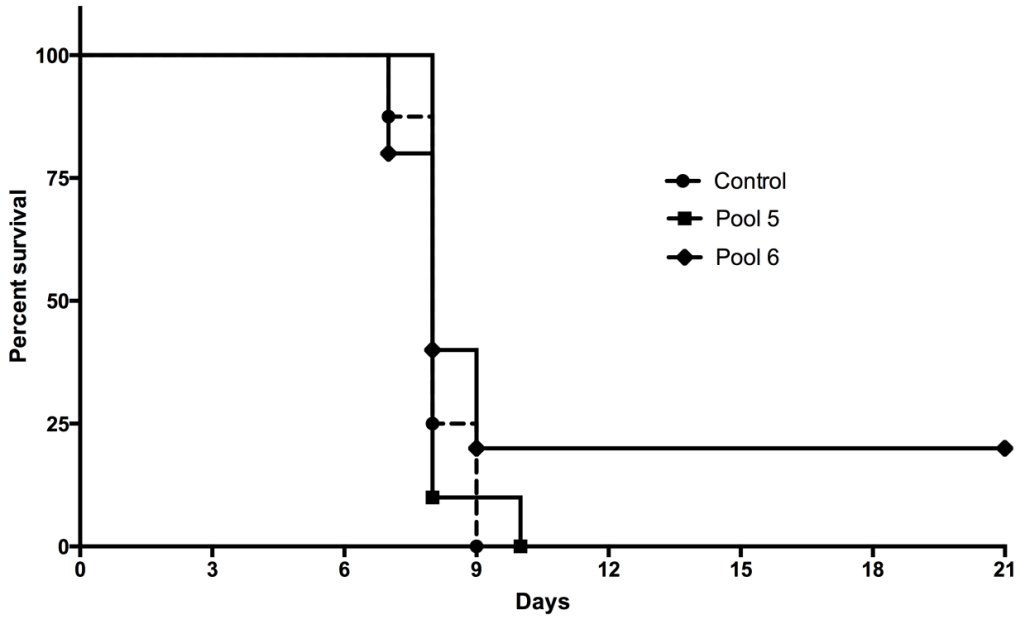

Figure 3.8 Immunization with a new set of *R. prowazekii* antigens did not protect against a lethal challenge. APCs individually expressing selected *R. prowazekii* ORFs were combined in 2 pools as follows: Pool 5 (RP042, RP431, RP572, RP531, RP314); Pool 6 (RP848, RP627, RP498, RP585, RP763). Mice were immunized with pooled rickettsial proteins (n=10) or with APCs expressing luciferase (control, n=8), challenged with 5 × LD_{50} of *R. typhi* and followed for 21 days to determine survival. Although 20% of Pool 6-immune mice survived the lethal challenge while none of the control or Pool 5-immune animals did, differences were not statistically significant.

Novel *R. prowazekii* antigens are cross-protective beyond the typhus group.

Intrinsically, the strategy for discovery of protective antigens used here allows for the detection of cross-protective responses since the rickettsial proteins used for immunization are derived from *R. prowazekii* but mice are challenged with *R. typhi*, the other member of the typhus group *Rickettsia*. Next, I asked whether the cross-protection conferred by these novel protective antigens could be extended to the other group of *Rickettsia* that includes pathogenic members, the spotted fever group. Based on the lethal challenge survival results, survival rate , mice were immunized with a pool of the best candidates found in the present study, RP778, RP739, RP403 and RP598, together with RP884, a protective antigen reported in the previous chapter [174]. Animals were then challenged with $5LD_{50}$ of *R. typhi* or $5LD_{50}$ of *R. conorii*, the agent of Mediterranean spotted fever, which produces a disease that models Rocky Mountain spotted fever in mice. After 21 days of observation, 62.5% of mice challenged with *R. conorii* were protected (Fig. 3.9).

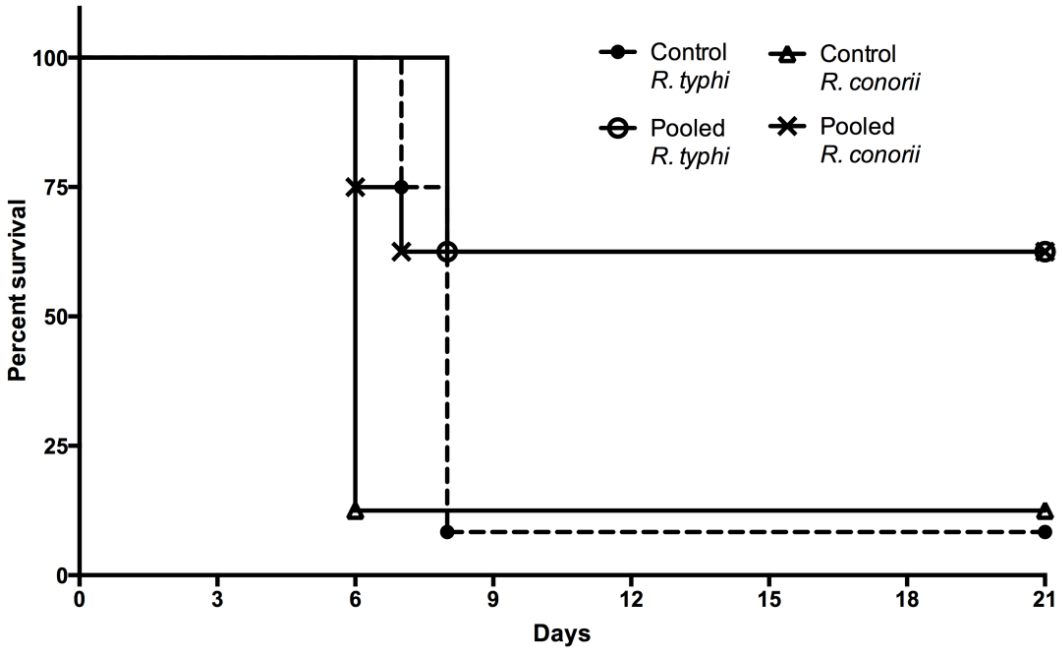

Figure 3.9 Novel *R. prowazekii* vaccine targets are cross-protective against a SFG *Rickettsia* lethal challenge. APCs expressing the novel protective antigens discovered in the present study (RP778, RP739, RP598, and RP403) plus RP884, a protective antigen described in the previous chapter, were pooled (1×10^5 APCs per rickettsial protein) to immunize mice. Control mice received the same total number of cells expressing luciferase. Mice were challenged with $5 \times LD_{50}$ of *R. typhi* or $5 \times LD_{50}$ of *R. conorii*, a clinically-relevant representative of the spotted fever group (SFG) *Rickettsia*. 62.5% of mice immunized with pooled proteins survived either challenge, while only 8.3% of control mice challenged with *R. typhi* (n=12, p=0.009) and 12.5% of control mice challenged with *R. conorii* did (n=8, p=0.0295).

DISCUSSION

This study describes the first application of a reverse vaccinology approach [138] to the discovery of protective *Rickettsia* antigens that are recognized by T cells. The entire *R. prowazekii* ORFeome (834 proteins) was analyzed for the identification of proteins encompassing high-affinity MHC class I and MHC class II-binding peptides. From 63 top-ranked proteins with MHC class-I peptides and 61 proteins with MHC class-II peptides (Tables 3.1 and 3.2), 21 rickettsial proteins were predicted to encompass high-affinity binding peptides for both MHC class-I and MHC class-II; a subset of 12 of these proteins were tested in a CD8-biased context as vaccine targets, and four novel protective antigens were identified (RP778, RP739, RP403, RP598). The critical role of $CD8^+$ T cells in the recovery from rickettsial infections has been previously demonstrated in murine models [35, 37, 38]. Since $CD8^+$ T cells play a key role in protective immunity against many intracellular pathogens, including respiratory viruses, CMV, HIV, *Plasmodium* spp., and *M. tuberculosis*, among others [193–199], it has been proposed that the rational design of the next generation of vaccines should include T cell epitopes [200]. However, finding an efficient approach to identify protective T cell antigens remains one major challenge in the development of T cell-based vaccines [125, 200]. In our laboratory we began to address this challenge by combining *in silico* predictions with an *in vivo* screening method recently published in discussed in chapter 2 [174]. To achieve this goal, I used our empirical antigen discovery data to formulate an *in silico* strategy that better matched that empirical data. The resulting method highlights the importance of combining proteasome-processing as well as MHC class-I-binding predictions. In agreement with this concept, 7 out of 16 rickettsial proteins containing all

5 of the top 5 proteasome-derived peptides predicted by RANKPEP were included in the final list of MHC class-I predicted antigen targets (Table 3.2). This observation is also reinforced by the fact that all rickettsial protective antigens identified thus far (RP884, RP778, RP739, RP403, and RP598) have at least 4 predicted proteasome-derived peptides. To further support the potential relevance of the selected antigens for human application, we added another layer of information to our *in silico* analysis by incorporating human MHC (HLA class-I and HLA class-II) binding data. In this regard, RP739, one of our best candidates as assessed by survival (Fig. 3A), provides an interesting scenario as its position in the protein rank changed drastically when the HLA class I-binding score was introduced, moving from position 21 in the mouse-only ranking to position 2 in the mouse-human combined ranking (Table 3.2). This finding suggests that, notwithstanding target vaccine proteins are being tested using a relevant mouse model of rickettsiosis [35], the inclusion of HLA binding data not only seems to help refine the predictive power of the algorithm, but could also contribute to the prioritization of *in silico*-defined vaccine targets that may be more readily applicable to humans.

Although the accuracy of computer algorithms for prediction of T cell epitopes has notably improved in recent years, some drawbacks persist such as the difficulties to predict antigen processing and peptide loading in the MHC class-II pathway [138, 139, 158, 159], underestimation of the epitope breadth which has been demonstrated for $CD8^+$ T cell epitopes [160], and the fact that antigen discovery across entire proteomes using overlapping peptides is not feasible for all pathogens, especially those with large genomes [138]. Whole-protein-based approaches for T cell antigen discovery have been proposed as a cost-effective alternative[125], and the strategy used here is in line with

this proposal. The novelty of this approach lies in the use of *in silico* predictions of MHC class I or MHC classII-binding peptides for the selection of target antigens to be tested as whole proteins using APCs modified to stably express candidate proteins. In the present study, 22 of 63 MHC class-I *in silico* predicted vaccine targets were tested, and 4 novel protective antigens were identified (RP778, RP739, RP403, RP598). The present results suggest that vaccine targets with immunogenicity potential towards $CD8^+$ T cells that encompass both MHC class-I and class-II binding-peptides might offer superior protective capabilities. From 8 *R. prowazekii* tested proteins predicted as MHC class-I targets, none of them offered significant protection; in contrast, from 14 targets encompassing both MHC class-I and class-II binding-peptides 4 protective antigens were identified (RP778, RP739, RP403, RP598). This finding is in agreement with previous studies showing that the presence of $CD4^+$ and $CD8^+$ T-cell epitopes within the same protein might enhance $CD8^+$ T cell responses and protection against infection [201–203].

Even though immunodominance does not necessarily translate to protection, it has been suggested that it might play a role in protective immune responses mediated by $CD4^+$ T cells [128, 158]. High-affinity binding to MHC class-II has been proposed as one on the factors contributing to the immunodominance of $CD4^+$ T cell epitopes, and the *in silico* analysis strategy used here was designed to be biased towards the selection of rickettsial proteins encompassing high-affinity MHC class-II binding peptides; interestingly, all novel protective antigens (RP403, RP598, RP739, RP778) were predicted to include immunodominant epitopes, although none of them was top ranked (Table 3.3). Despite the linkage that has been described between $CD4^+$ T cell help and induction of antibody responses towards the cognate protein [184], antibodies against

protective antigens were not detected when assessed by indirect immunofluorescence (IFA; data not shown). Although, the mechanism by which our immunization strategy results in T-cell priming and protection is yet to be addressed, we hypothesize that our platform is allowing the APC's intrinsic cellular machinery to process and select the antigenic determinants to be presented to T cells, which is in agreement with the concept that the actual array of critical antigenic determinants driving protective T cell responses might be revealed only if antigens are naturally processed [200].

Our strategy also allowed the identification of antigens mediating cross-protective immunity within the two major groups of *Rickettsia*, SFG and typhus group. *R. prowazekii*, *R. typhi*, and *R. conorii* genomes share 775 genes[9, 10]; the similarity of the *R. prowazekii* protective antigens with their orthologs in *R. conorii* is significant: 90% for RP884, 89% for RP778, 93% for RP739, 73% for RP403, and 88% for RP598; outside the Rickettsiales protein similarity is low (maximum protein sequence identity observed using BLASTp was 45%). When tested as a pool, these *R. prowazekii* antigens provided protection against a lethal challenge with *R. conorii* that was similar to that observed when animals were lethally challenged with *R. typhi* (Fig. 3.9). Interestingly, the protection of the pool against *R. typhi* was less than that afforded by RP778 or RP739 by themselves. This difference may be explained by changes in immunodominance of the most protective antigen when other antigens are also present. Still, the present data supports the feasibility of a subunit vaccine that triggers T-cell-mediated cross-protection among phylogenetically distant *Rickettsia*.

CHAPTER 4: Phenotype of the Anti-*Rickettsia* $CD8^+$ T cell Response as a Guide for the Assessment of the Protective Potential of Novel Protective Antigens[e]

ABSTRACT

The identification and validation of correlates of protective cellular immunity against rickettsial infections, an important step towards vaccine validation, remains a gap in this field. Here, I show that after a primary challenge with *Rickettsia typhi* in the C3H mouse model, the peak of anti-*Rickettsia* $CD8^+$ T cell-mediated responses occurs around 7 days post-infection (dpi), which coincides with the beginning of rickettsial clearance. At this time point, both effector-type and memory-type $CD8^+$ T cells are present, suggesting that 7 dpi is a valid time point for the assessment of $CD8^+$ T cell responses of mice previously immunized with protective antigens following a rapid prime and boost protocol. Based on these results, four correlates of protection against *R. typhi* infection in animals immunized with protective rickettsial antigens are suggested: 1) production of IFN-γ by antigen experienced $CD3^+CD8^+CD44^{high}$ cells, 2) production of Granzyme B by $CD27^{low}CD43^{low}$ antigen-experienced $CD8^+$ T cells, 3) generation of memory-type $CD8^+$ T cells [Memory Precursor Effector Cells (MPECs), as well as $CD127^{high}CD43^{low}$, and $CD27^{high}CD43^{low}$ $CD8^+$ T cells], and 4) generation of effector-like memory $CD8^+$ T cells ($CD27^{low}CD43^{low}$). Moreover, I propose that these correlates could be useful for the early assessment and validation of the quality of the $CD8^+$ T cell immune response induced by novel antigens with potential use in a vaccine against *Rickettsia*.

[e]A significant portion of this chapter has been accepted for publication in the journal Vaccine. Vaccine does not require copyright permission as long as proper citation is given. The citation for this article is: Caro-Gomez E, Gazi M, Cespedes MA, Goez Y, Teixeira B, Valbuena G. Phenotype of the anti-*Rickettsia* $CD8^+$ T cell response suggests cellular correlates of protection for the assessment of novel antigens. Vaccine. 2014 Jul 17. pii: S0264-410X(14)00958-X.

INTRODUCTION

Currently, there are no prophylactic vaccines available for preventing any of the rickettsial diseases. Although antibodies were the protective mechanism and correlate of protection identified in prior killed *Rickettsia* vaccines [65, 70], it is also known that, antibodies do not play a role in recovery from a primary infection [39], and they do not exhibit cross-protective capability among phylogenetically distant *Rickettsiae* [40]. On the other hand, T cells can mediate cross-protection between rickettsiae as distantly related as *R.typhi* and *R. conorii* [44], suggesting that a T cell-mediated mechanism is partly responsible for the induction of long lasting cross-protective immunity and that T cell antigens should be included in the next generation of rickettsial vaccines. To achieve this, the identification and validation of correlates of protective cellular immunity against rickettsial infections is a critical step that has yet to be addressed, and a particular focus on $CD8^+$ T cells is necessary since their critical role over $CD4^+$ T cells in resistance to rickettsial infections has been experimentally demonstrated [37, 38].

Recently, it was proposed that memory $CD8^+$ T cells mediating strong recall responses display a "rested" phenotype consisting of $CD127^{high}$, $CD43^{low}$, $CD27^{high}$ and $KLRG1^{low}$; and different combinations of these markers were proposed to be useful for the assessment of vaccine efficacy [92, 94, 116]. It was also proposed that the relative proportion of the CD127/KLRG1 subsets among antigen-specific $CD8^+$ T cells could be a valuable predictor of vaccine efficacy; specifically, the induction of large numbers of memory precursor effector cells (MPECs), defined as $CD127^{high}$ $KLRG1^{low}$, could be pivotal [116].

Although recovery from a natural or experimental rickettsial infection confers long-lasting protective immunity, little is known about the phenotypic changes that

correlate with the transition of the responding $CD8^+$ T cells towards memory. Here, I explored the development of memory $CD8^+$ T cells after a challenge with *R. typhi* by analyzing the expression of activation markers that have been linked to the development of long-lasting protection after vaccination in other models and asked whether these memory-type subsets could serve as potential correlates of T-cell immunity for the validation *Rickettsia* T-cell vaccine antigen candidates.

MATERIALS AND METHODS

Bacteria

R. typhi (Wilmington strain) and *R. conorii* (Malish 7 strain) working stocks were produced in a CDC-certified BSL3 laboratory by cultivation in specific pathogen free embryonated chicken eggs. Yolk sacs were pooled and homogenized in a Waring blender, diluted to a 10% suspension in sucrose-phosphate-glutamate buffer (SPG; 0.218 M sucrose, 3.8 mM KH2PO4, 7.2 mM K2HPO4, 4.9 mM monosodium L-glutamic acid, pH 7.0). Rickettsiae present in the stock were quantified by plaque assay [175], and the LD_{50} was determined experimentally in C3H/HeN mice.

Animal Model

The mouse model of endothelial-target typhus group rickettsioses has been previously described in detail [35]. Briefly, C3H/HeN mice (Charles River Laboratories, stock 025) were housed in an ABSL3 facility and infected i.v. through the tail vein with sublethal (0.3 LD_{50}) or lethal (5 or 10LD_{50}) doses of *R. typhi* in a volume of 300 µl of phosphate-buffered saline (PBS). We followed the recommendations in the Guide for the

Care and Use of Laboratory Animals of the National Institutes of Health. Our experimental protocol was approved by the Institutional Animal Care and Use Committee (IACUC) of the University of Texas Medical Branch (protocol number: 0903026).

Adoptive Transfer Experiments

Mice previously immunized through sublethal infection with *R. typhi* received $3LD_{50}$ to boost the immune response 2-3 weeks before harvesting immune spleens; $CD8^+$ T cells from immune donors were negatively selected (StemSep™ Mouse CD8+ T Cell Enrichment Kit, STEMCELL Technologies), labeled with 5µM CFSE (Life Technologies) and transferred into naïve recipients in the presence or absence of immune serum. $CD8^+$ T cells and serum from naïve donors, or serum alone from immune donors, were transferred into naïve recipients and used as adoptive transfer controls. Each mouse received 8×10^5 $CD8^+$ T cells and/or 300 µl of serum i.v.; 24 hours after transfer, animals were challenged i.v. with 10 LD_{50} of *R. typhi*. Mice were injected i.p. with BFA (250 µg/mouse) and monensin (500 µg/mouse) ~40 hours post infection; 4 hours later, they were euthanized to obtain tissues for assessment of *Rickettsia* load by Q-PCR as described in previous chapters and for assessment of recall responses in transferred $CD8^+$ T cells by multicolor flow cytometry. The gating stratregy is shown in the appendix as Figure A2.

Flow Cytometry

To analyze $CD8^+$ T cell responses after *Rickettsia* challenge, we used an *ex vivo* method as described in previous chapters. On the day of sacrifice, mice were injected intraperitoneally (i.p.) with BFA and monensin, four hours later spleens were collected and homogenized to a single-cell suspension in HBSS containing 2%BGS, 3mM HEPES, and Golgi Plug™ and Golgi Stop™ (BD Biosciences) at concentrations recommended by the manufacturer. Subsequently, mononuclear cells were purified by density gradient centrifugation with Lympholyte™-M (Cedarlane Laboratories). In order to minimize variability introduced by processing and flow cytometry acquisition, all cells were frozen in 90% fetal calf serum with 10% DMSO and subsequently processed and acquired at the same time. For assessment of the $CD8^+$ T cell response, mononuclear cells were stained with Live/Dead Fixable Blue (Life Technologies), APC-Alexa Fluor 750 anti-CD8 (clone 5H10), FITC anti-CD3 (clone17A2), BD Horizon V500 anti-CD44 (clone IM7), PE-Cy7 anti-IFN-γ (clone XMG1.2), Alexa Fluor 647 anti-Granzyme B (clone 16G6), PE-Cy5 anti-CD127 (clone A7R34), PE anti-CD43 (clone 1B11), PerCP-eFluor 710 KLRG1 (clone 2F1), eFluor 450 CD11a (clone M17/4), PE-Cy7 anti-CD62L (clone MEL-14) or BD Horizon V450 anti-CD27 (clone LG.3A10). In addition to these markers, for recall responses, T cells were also stained with PE anti-IL-2 (clone JES6-5H4) or eFluor 450 anti-TNF-γ (clone MP6-XT22), and/or Alexa Fluor 660 anti-Ki67 (clone SolA15). All antibodies and reagents were purchased from BD Biosciences, eBioscience or Biolegend. CountBright™ Absolute Counting Beads (Life Technologies) were added to each sample prior to acquisition. All samples were acquired on a LSRII Fortessa cytometer (BD Biosciences); 500.000 events were captured and data were analyzed using FlowJo 9.5.3

software (Tree-Star Inc). All analyses were performed on live $CD3^+CD8^+$single cells. Thresholds for positivity were determined with fluorescence-minus-one (FMO) control stains. The gating stratregy is shown in the appendix as Figure A1.

Immunization with Protective Antigens

For immunization with the protective antigens (RP884, RP778, RP739, RP403 and RP598), I used our published platform [174] modified as described in chapter 3. Each mouse received 4.5×10^5 cells i.v. and i.m.; 5 days later, mice received the same dose of cells i.m. and i.p.; seven days after the second immunization, mice were infected i.v. with 5 LD_{50} of *R. typhi* and euthanized after 7 days for flow cytometry experiments and assessment of *Rickettsia* load by Q-PCR as described in chapter 2.

Statistics

Statistical significance analysis was performed using GraphPad Prism version 6.00, (GraphPad Software). Groups were compared by unpaired multiple t-tests followed by Holm-Sidak correction for multiple comparisons, or one-way analysis of variance (ANOVA) followed by Sidak's or Dunnett's multiple comparisons test. Pearson's correlation coefficient was used to calculate the correlation between *Rickettsia* load and the number of $CD8^+$ T cells expressing a given activation trait.

RESULTS

$CD8^+$ T Cell Response After a Primary Sublethal Challenge with *R. typhi*.

Informative time points were selected based on the dynamics of the $CD44^{high}CD62L^{low}$ effector subpopulation. The expression pattern of these two markers suggested that sublethal infection with *R. typhi* induces a biphasic effector phase that peaks at 7 and 11 dpi (Fig. 4.1). Subsequently, we analyzed $CD8^+$ T cell responses at 3, 5, 7, 11, and 14 dpi; 60 dpi was also included in order to capture the phenotype of resting memory $CD8^+$ T cells. In agreement with the systemic nature of rickettsial infections, *R. typhi* load showed comparable patterns in liver, lung and spleen, peaking at 5 dpi (Fig 4.2). At 14 dpi, *Rickettsia* became undetectable by qPCR, indicating that C3H/HeN mice had cleared the infection.

Due to the lack of tetramers to follow *Rickettsia*-specific $CD8^+$ T cell responses, I focused on the study of antigen-experienced cells expressing the $CD3^+CD8^+CD44^{high}$ phenotype, CD44 is an adhesion molecule that mediates binding to the extracellular matrix via hyaluronic acid and whose expression is upregulated on naïve T cells after TCR engagement and steadily maintained at high levels on antigen-experienced and memory T cells [204, 205]; all analyses were performed on this population. Since, it has been proposed that both memory precursors and terminally differentiated effector cells are present at the peak of $CD8^+$ T cell-mediated immune responses [104], critical time points of the anti-*Rickettsia* $CD8^+$ T cell response were determined by exploring the expression of the activated isoform of CD43 (1B11), which discriminates quiescent from

activated T cells, and KLRG1, a marker for terminally differentiated effector cells [92, 93].

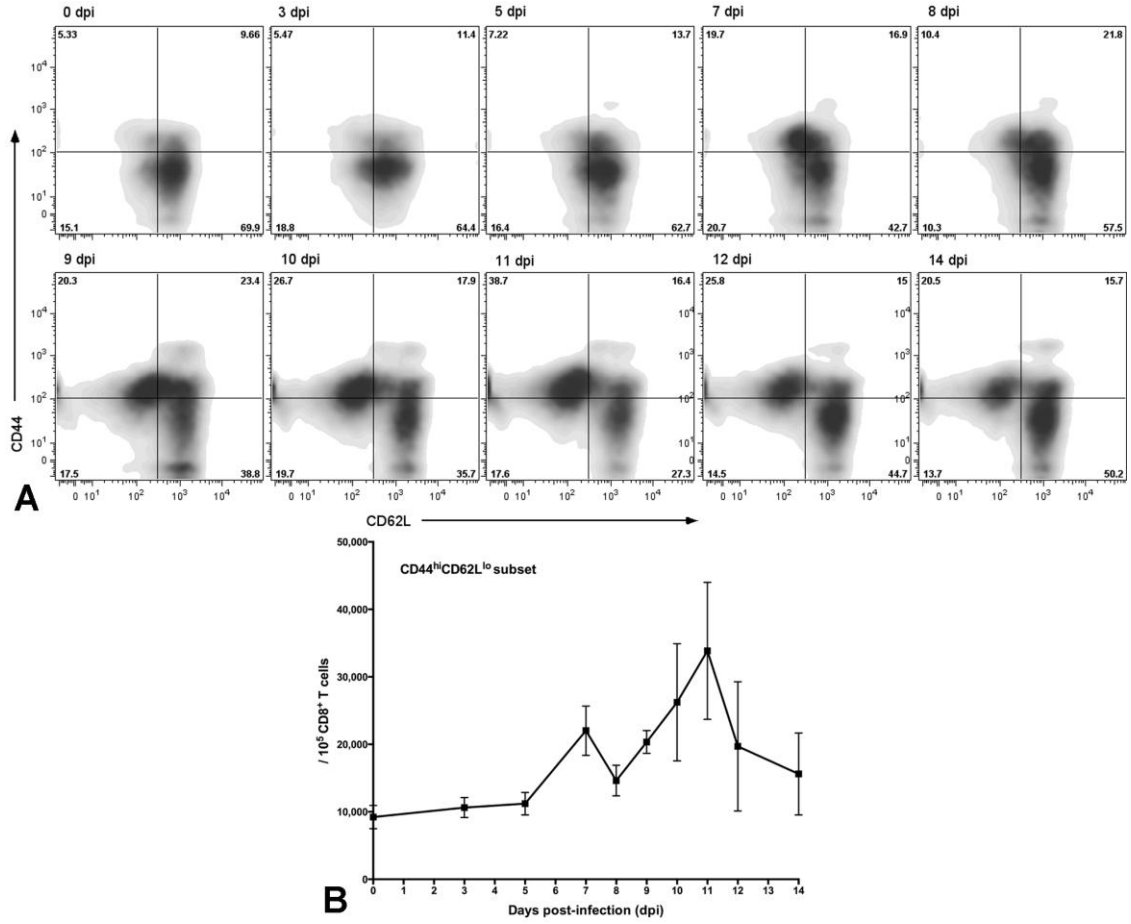

Figure 4.1 Kinetics of effector CD8$^+$ T cells. Naïve mice were infected with 0.3 LD_{50} of *R. typhi* and sacrificed 0, 3, 5, 7, 8, 9, 10, 11, 12 and 14 days post-infection (dpi). Splenocytes for flow cytometric analysis were stained with antibodies against CD3, CD8, CD44 and CD62L. (A) Representative density plots of the frequency of $CD3^+CD8^+$ cells expressing CD44 and CD62L. (B) Number of effector $CD44^{high}CD62^{low}$ $CD8^+$ T cells. Means ± SEM from three mice per time point are shown.

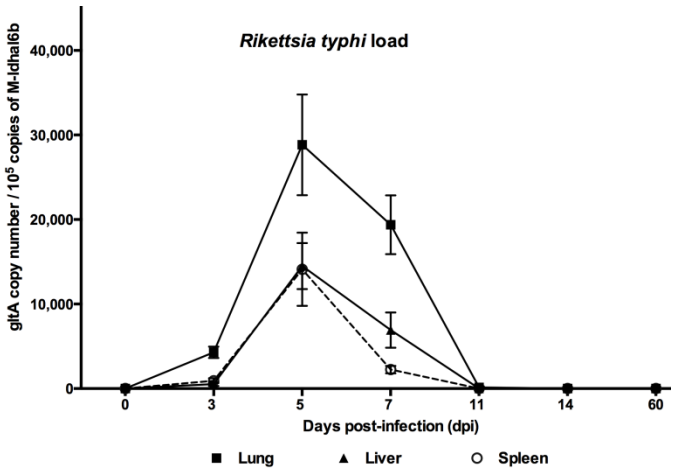

Figure 4.2 Rickettsial load kinetics. Naïve mice were infected with 0.3 LD_{50} of *R. typhi* and sacrificed 0, 3, 5, 7, 11, 14 and 60 dpi. Liver, lung, and spleen tissue fragments were processed to determine the rickettsial load using quantitative real-time PCR targeting the rickettsial gene *gltA* and the mouse gene *Idhal6b*. Means ± SEM from five mice per time point are shown.

After a sublethal challenge with *R. typhi*, effector $CD8^+$ T cells ($CD43^{high}$, $KLRG1^{high}$) were present from 7 to 14 dpi and the peak of expression occurred at 7 dpi (Fig. 4.3 A and B); compared to uninfected controls, both markers remained high until 14 dpi and returned to basal conditions at 60 dpi. This pattern was further confirmed with an approach that relies on the synchronized downregulation of the CD8α chain and upregulation of the integrin CD11a (LFA-1α chain), which is driven by contact with antigens, but not by by-stander inflammation; thus, cells with the $CD8\alpha^{low}CD11a^{high}$ phenotype are considered authentic antigen-experienced $CD8^+$ T cells as opposed to naïve cells which are $CD8\alpha^{high}CD11a^{low}$ [206, 207]. This approach revealed an activation pattern similar to the one described for KLRG1, which is consistent with the concept that

not only inflammation but also TCR signaling are required for the induction of KLRG1 expression on effector $CD8^+$ T cells [208]. The peak of expression for the $CD8\alpha^{low}CD11a^{high}$ subset also included both 7 and 11 dpi (Fig. 4.3C and D). To confirm the effector potential of the highly activated cells identified at 7 and 11 dpi, IFN-γ and Granzyme B expression was measured. Interestingly, compared to uninfected controls, significant expression of IFN-γ was only observed at 7, 11 and 14 dpi (Fig. 4.3E and F); Granzyme B was not detected in the experimental animals but it was detected in positive controls (data not shown). The expression of IFN-γ at 11 dpi could be related to elimination of residual bacteria since low copy numbers of *Rickettsia* were still detectable in some animals at this time point in spleen (mean=17.2; 0-59 gltA copies/10^5 copies of M-Idhal6b) and lung (mean=144.2; 0-640 gltA copies/10^5 copies of M-Idhal6b).

Based on the data above and the elimination of rickettsiae beginning at 7 dpi, I concluded that this time point represents the peak of effector $CD8^+$ T cells responding to a primary *R. typhi* infection. This timepoint is a critical window for the functional assessment, tracking, and potential identification of anti-*Rickettsia* $CD8^+$ T cells induced by infection or vaccination.

Figure 4.3 CD8$^+$ T cell activation after a primary sublethal challenge.

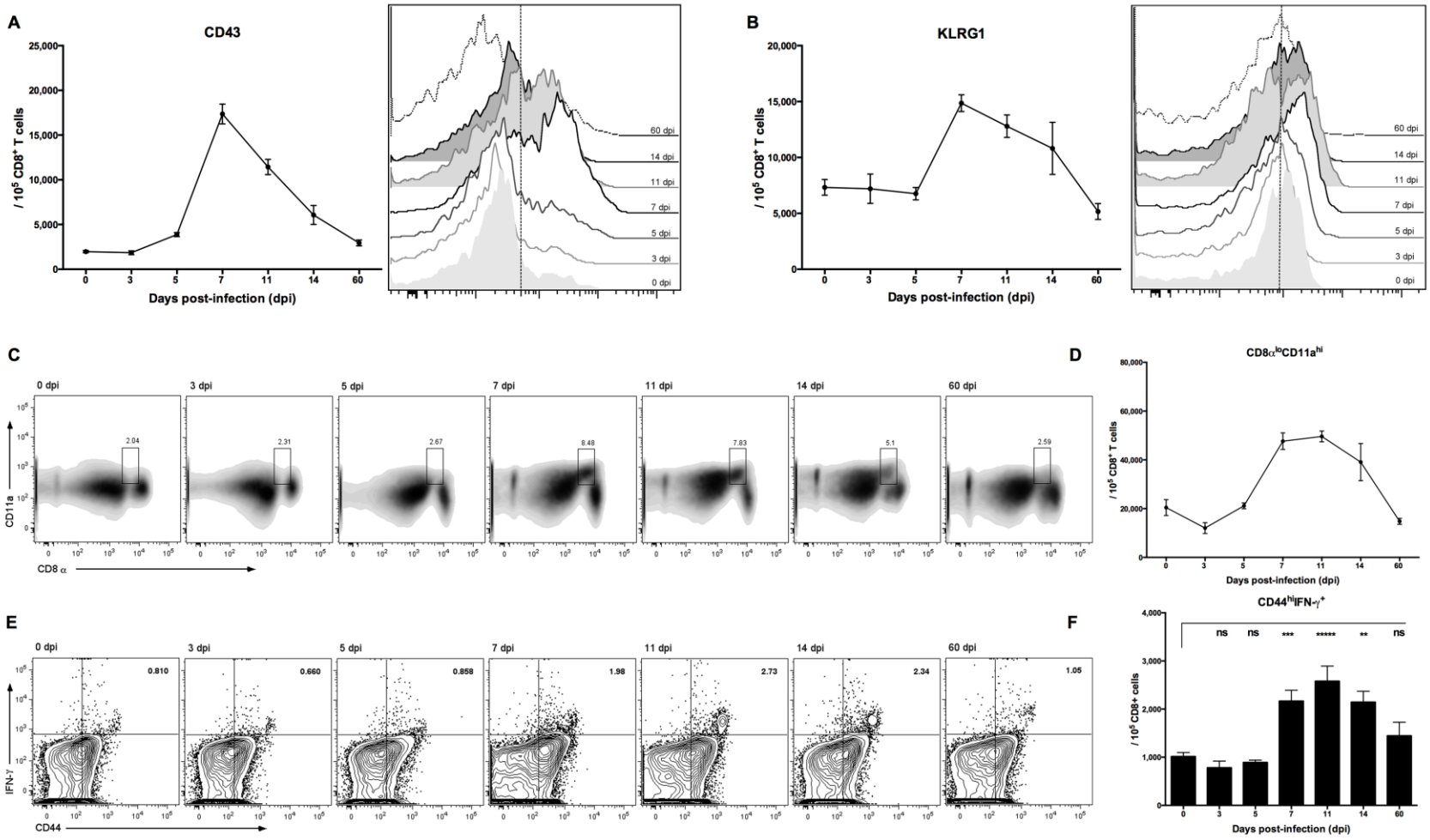

Figure 4.3 $CD8^+$ T cell activation after a primary sublethal challenge. Naïve mice were infected with 0.3 LD_{50} of *R. typhi* and sacrificed at 0, 3, 5, 7, 11, 14 and 60 dpi (4 hours after i.p. injection of BFA and monensin) to obtain splenocytes for flow cytometric analysis. (A) Number of antigen experienced $CD3^+CD8^+CD44^{high}$cells expressing CD43 and representative histograms showing CD43 expression. (B) Number of $CD3^+CD8^+CD44^{high}$cells expressing KLRG1 accompanied by illustrative histograms. (C). Representative density plots showing the kinetics of antigen experienced $CD8^+$ T cells as assessed by the $CD8\alpha^{low}CD11a^{high}$ phenotype. (D) Number of $CD8\alpha^{low}CD11a^{high}$ cells at the indicated time points. (E) Representative density plots of the frequency of $CD3^+CD8^+$cells expressing CD44 and IFN-γ. (F) Number of $CD3^+CD8^+$cells co-expressing CD44 and IFN-γ. Data is presented as the mean ± SEM from five mice per time point; each data point represents the mean value per 10^5 $CD8^+$ T cells. p values for comparisons against 0 dpi are represented as follows: **p<0.01; ***p<0.001; ****p<0.0001, non-significant (ns).

Assessment of $CD8^+$ T Cell Memory Potential Following a Challenge with *R. typhi*

Previous studies showed that the adoptive transfer of memory $CD8^+$ T cells protects against a *Rickettsia* lethal challenge [37, 38]; however, the phenotypic changes associated with transition towards memory or the activation pattern of memory $CD8^+$ T cells upon a secondary *Rickettsia* encounter have not been described. Relevant $CD8^+$ T cell phenotypes studied in this chapter are summarized in table 4.1.

Based on the analysis of CD127 vs. KLRG1 or CD127 vs. CD43 populations, I studied the effector- and memory-type $CD8^+$ T cell subsets generated after a primary *R. typhi* challenge. At early time points, compared to uninfected controls, lower numbers of $CD127^{high}$ cells were observed; this downregulation of CD127 is consistent with the

instauration of the effector phase (Fig. 4.4). The peak of the effector cells, defined by the $CD44^{high}CD127^{low}CD43^{high}$ phenotype, was observed at 7 dpi, returning to basal numbers by the end of the experiment on day 60 (Fig. 4.4A and B). Over time, I was expecting to observe enrichment of the $CD44^{high}CD127^{high}CD43^{low}$ subset, a phenotype representing memory $CD8^{+}$ T cells [106]; however, compared to uninfected controls, lower numbers for this subpopulation in the spleen remained even at 60 dpi. Interestingly, a ~2-fold increase in the $CD44^{high}CD127^{low}CD43^{low}$ subset was observed at 60 dpi. Analysis of CD127 and KLRG1 co-expression (Fig. 4.4C and D) indicated that after an initial decrease following *R. typhi* infection, MPECs ($CD127^{high}KLRG1^{low}$) increased by 7 dpi; similarly, the peak for short-lived effector cells (SLECs), defined as $CD127^{low}KLRG1^{high}$, was observed at 7 and 11 dpi. In fact, equivalent numbers of memory (MPECs) and effector (SLECs) type $CD8^{+}$ T cells were observed at 7 and 11 dpi. In addition, increased numbers of early effector cells (EECs), a subset suspected to have the potential for generating all effector lineages and defined as $CD127^{low}KLRG1^{low}$ [116], were also observed beginning at 7 dpi remaining high until the end of the experiment. Moreover, compared to uninfected controls, significantly higher numbers of SLECs, MPECs and EECs were observed at 60 dpi. The observed enrichment of MPECs, a subset that has been proposed to predict $CD8^{+}$ T cell long-term memory potential, is very significant because the production of these cells has been proposed as one of the goals for vaccines targeting $CD8^{+}$ T cells [116].

Figure 4.4 Kinetics of CD127 vs. CD43 and CD127 vs. KLRG1 subsets among antigen experienced $CD3^{+}CD8^{+}CD44^{high}$ cells.

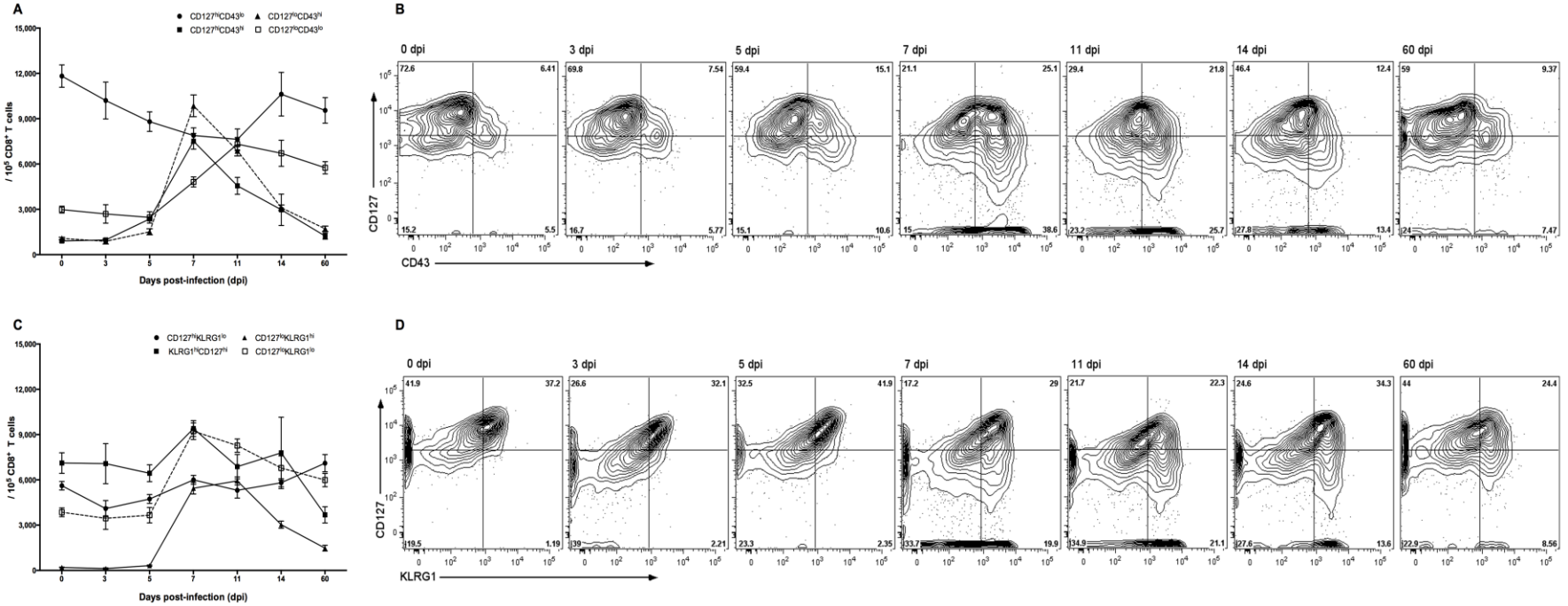

Figure 4.4 Kinetics of CD127 vs. CD43 and CD127 vs. KLRG1 subsets among antigen experienced $CD3^+CD8^+CD44^{high}$ cells. Naïve mice were infected with 0.3 LD_{50} of *R. typhi* and sacrificed at 0, 3, 5, 7, 11, 14 and 60 dpi (4 hours after i.p. injection of BFA and monensin) to obtain splenocytes for flow cytometric analysis. (A) Based on the expression of CD127 and CD43, four different subpopulations were identified: $CD127^{high}$ $CD43^{low}$, $CD127^{high}CD43^{high}$, $CD127^{low}CD43^{high}$, and $CD127^{low}CD43^{low}$; each data point represents the mean value per 10^5 $CD8^+$ T cells from 5 mice per time point with the standard error of the mean. (B) Representative flow cytometry plots showing the frequency of the same subsets. (C) Numbers of cells expressing different combinations of CD127 and KLRG1: $CD127^{high}KLRG1^{low}$, $CD127^{high}KLRG1^{high}$, $CD127^{low}$ $KLRG1^{high}$, and $CD127^{low}KLRG1^{low}$; each data point represents the mean value per 10^5 $CD8^+$ T cells from 5 mice per time point with the standard error of the mean. (D) Illustrative flow cytometry plots of the frequency of cells co-expressing CD127 and KLRG1.

Next, I explored the activation pattern of memory $CD8^+$ T cells upon a secondary *Rickettsia* encounter. *Rickettsia*-immune mice were challenged at ~60 dpi with $10LD_{50}$ of *R. typhi*, and the changes induced on antigen experienced $CD3^+CD8^+CD44^{high}$ cells by a secondary rickettsial infection after 0, 6, 24, 72, and 120 hours postinfection (hpi) were explored. In addition to the memory subsets defined by CD127 vs. CD43 or CD127 vs. KLRG1, the subsets defined by CD27 vs. CD43 were also included because they may be more informative than the classical central (T_{CM}) and effector memory (T_{EM}) phenotypes for the assessment of $CD8^+$ T cell recall responses [92]. Upon a secondary *Rickettsia* encounter, compared to resting immune mice (0 hpi), a rapid decrease of the $CD127^{high}KLRG1^{low}$ and $CD127^{high}CD43^{low}$ memory subpopulations was observed at 6 and 24 hpi (Fig. 4.5A and B). In contrast, a slight increase in the $CD27^{high}CD43^{low}$ subset, about ~1.2-fold, which represents the dominant memory pool, was observed at 24 and 72 hpi (Fig. 4.5C). No major changes in the $KLRG1^{high}$ or $CD43^{high}$ effector subsets were detected and no significant changes in the production of Granzyme B, TNF-α or

IFN-γ were identified; only increased expression of IL-2 was observed at 72 and 120 hpi (Fig 4.6). Unexpectedly, after a secondary *Rickettsia* challenge, increased numbers of the $CD127^{low}CD43^{low}$, $CD127^{low}KLRG1^{low}$ and $CD27^{low}CD43^{low}$ subpopulations (72 hpi), which have been described as having suboptimal recall capabilities [92], were observed; the significance of these findings is unclear given that mice were healthy and *Rickettsia* load was undetectable after a secondary challenge (data not shown). Similar to other models [92, 117], our results suggest that CD27 and CD43 are informative markers for the assessment of anti-*Rickettsia* memory $CD8^+$ T cells.

Table 4.1 Relevant $CD8^+$ T cell phenotypes

Memory –type $CD8^+$ T cells	
"Memory pool"	CD27 / $CD127^{high}CD43^{low}$
MPECs	$CD127^{high}KLRG1^{low}$
Memory-like	$CD44^{high}CD127^{high}$
T_{CM}	$CD44^{high}CD127^{high}$ $CD62L^{high}CD27^{high}$
Effector –type $CD8^+$ T cells	
Effector-like	CD27 / $CD127^{high}CD43^{high}$ CD27 / $CD127^{low}CD43^{high}$ $CD127^{high}KLRG1^{high}$
SLECs	$CD127^{low}KLRG1^{high}$
T_{EM}	$CD44^{high}CD127^{high}$ $CD62L^{low}CD27^{high}$
Effector –like memory $CD8^+$ T cells	
$CD27^{low}CD43^{low}$	

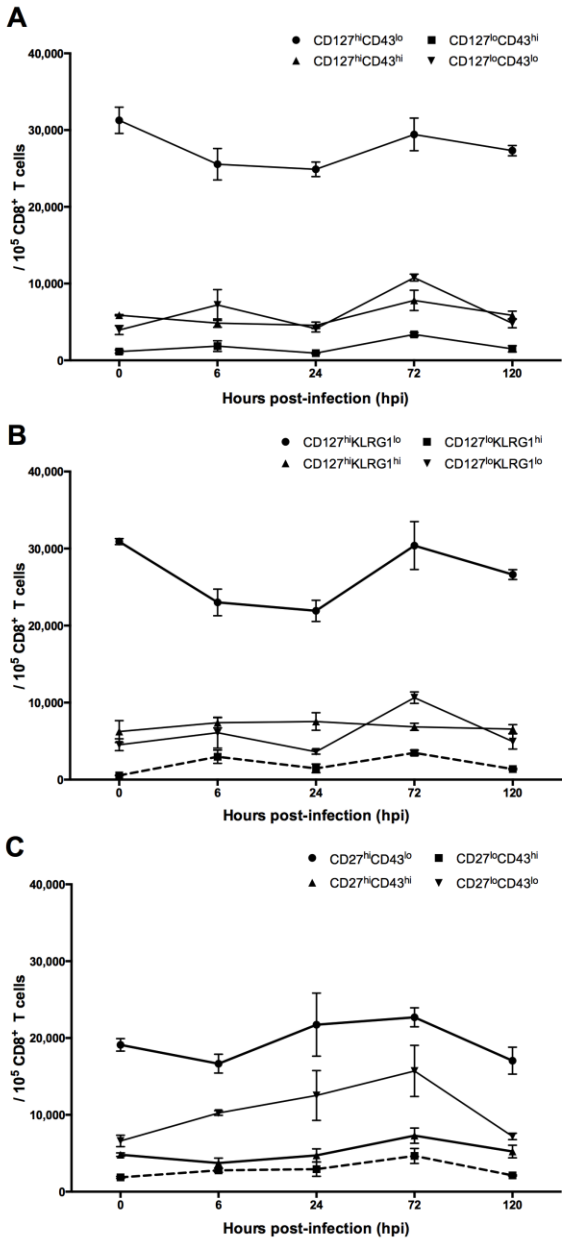

Figure 4.5 Dynamics of CD8$^+$ T cell subpopulations after a secondary challenge with *R. typhi.* *Rickettsia*-immune mice were challenged with 10LD$_{50}$ at ~60 dpi and sacrificed at 6, 24, 72 and 120 hours post-infection (hpi) to obtain splenocytes for flow cytometric analysis; animals were injected with BFA and monensin 4 hours prior to sacrifice. 0 hpi was included as resting immune control mice. Expression of CD127 vs. CD43 (A), CD127 vs.KLRG1 (B), and CD27 vs.CD43 (C) among CD3$^+$CD8$^+$CD44^{high}cells was analyzed. Each data point represents the mean value per 10^5 CD8$^+$ T cells ± SEM from three mice per time point.

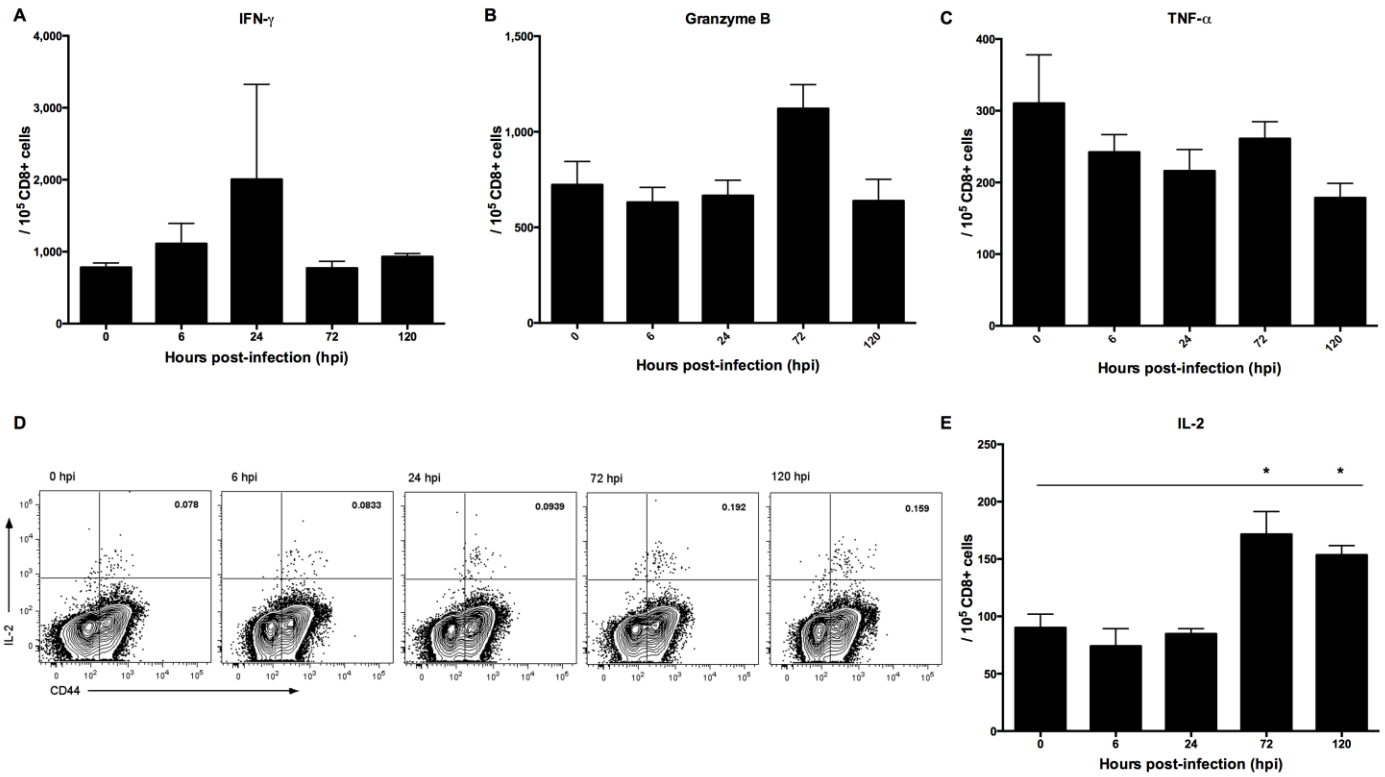

Figure 4.6 Expression of IFN-γ, Granzyme B, TNF-α, and IL-2 after a secondary challenge with *R. typhi*. Splenocytes were obtained as described in figure 4.5. Numbers of $CD3^{+}CD8^{+}CD44^{high}$ cells expressing IFN-γ (A), Granzyme B (B), TNF-α (C) and IL-2 (E). Illustrative flow cytometry plots of the frequency of cells co-expressing CD44 and IL-2 are shown in (D). Each data point represents the mean value per 10^5 $CD8^{+}$ T cells ± SEM from three mice per time point. p value for comparisons against 0 hpi (resting-immune mice) for IL-2 expression at 72 and 120 hpi was * $p<0.05$.

Minimal $CD8^+$ T Cell Activation After a Secondary Lethal Challenge

It has been suggested that prompt generation of effector cells as well as efficient secondary proliferation upon secondary antigen exposure of memory $CD8^+$ T cells would explain, at least in part, their protective capabilities [209]. Since increased numbers of $CD27^{high}CD43^{low}$ $CD8^+$ T cells, which represents memory pool cells, and $CD27^{low}CD43^{low}$ cells, which probably represents effector-like memory cells [117], were observed, I was interested in confirming these changes using more classical markers such as CD44 and CD127. Upon recall, memory-type ($CD127^{high}CD44^{high}$) and effector-type ($CD127^{low}CD44^{high}$) cells followed the same pattern described for the CD27 vs. CD43 subsets (Fig. 4.7A). Next, I focused on the $CD127^{high}CD44^{high}$ subset and explored T_{CM} and T_{EM} status of these cells, and found that they were mainly T_{CM} cells following the same pattern observed with the other marker combinations (CD27 vs. CD43 and CD127 vs. CD44) (Fig. 4.7B).

Although a peak of effector-type T cells was observed at 72 hpi, expression of effector molecules such as Granzyme B, TNF-α, or IFN-γ was not detected (Fig 4.6). Interestingly, IL-2 production was mainly associated with $CD8^+$ T cells expressing the $CD127^{high}CD44^{high}$ memory phenotype (data not shown). Next, I asked whether the increase in T_{CM} cells was related to redistribution of the memory pool after a secondary *Rickettsia* encounter or if these cells were actually proliferating. Hence, I investigated the expression of Ki67, a marker of mitotic activity, and found that at 24 and 72 hpi the expression of this proliferation marker among cells with a central memory-like phenotype ($CD44^{high}CD62L^{high}CD27^{high}$) was not different from resting immune mice (data not shown), suggesting that increased numbers of memory-type cells might be related to

redistribution of the memory pool. Although increased numbers of $CD8^+$ T cells with a central memory phenotype were observed, fully activated cells expressing effector markers (CD43 and KLRG1), effector mediators (Granzyme B, TNF-α or IFN-γ), or markers of cell cycling were not observed, despite the fact that rickettsiae were undetectable in liver and lung at all tested time points (data not shown).

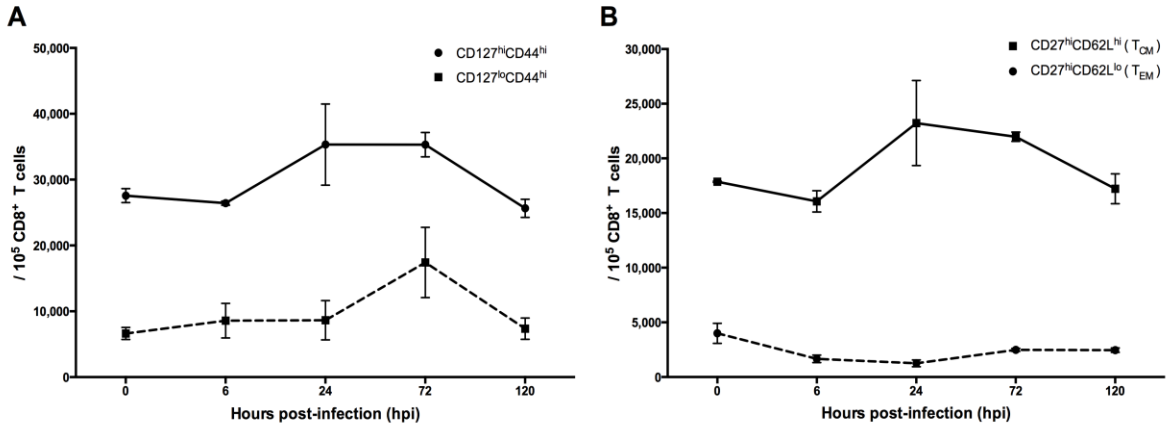

Figure 4.7 Dynamics of memory $CD8^+$ T cell subpopulations after a secondary challenge with *R. typhi.* *Rickettsia*-immune mice were challenged with $10LD_{50}$ at ~60 dpi and sacrificed at 6, 24, 72 and 120 hours post-infection (hpi) to obtain splenocytes for flow cytometric analysis; animals were injected with BFA and monensin 4 hours prior to sacrifice. 0 hpi were included as resting immune control mice. The dynamics of effector-type ($CD127^{low}CD44^{high}$) and memory-type ($CD127^{high}CD44^{high}$) subpopulations (A), and T_{CM} ($CD27^{high}CD62L^{high}$) and T_{EM} ($CD27^{high}CD62L^{low}$) subsets gated on $CD127^{high}CD44^{high}$ $CD8^+$ T cells (B) were studied. Each data point represents the mean value per 10^5 $CD8^+$ T cells ± SEM from three mice per time point.

Interference of Anti-*Rickettsia* Antibodies with $CD8^+$ T Cell Activation Upon a Secondary Challenge.

Since recovering from rickettsial infections induces long lasting and cross-protective immunity [40, 44], a sublethal infection could be considered as the experimental paradigm for developing a vaccine for *Rickettsia*; thus, one could argue that in delineating the protective memory T cell responses is the key towards the discovery and validation of protective antigens; this is the reason why the paucity of $CD8^+$ T cell recall responses was puzzling. Although anti-*Rickettsia* antibodies are unlikely to play a role during primary infection, since protective antibodies appear around 12 dpi, it has been demonstrated that they are protective against reinfection [39] through Fc-dependent and opsonic mechanisms that result in phagolysosomal killing of rickettsiae [21, 77]. On the other hand, to what extent antibodies and $CD8^+$ T cells cooperate to protect against re-infection is unknown. In this study, anti-*R. typhi* antibodies were detected starting at 5 dpi (IFA titer 1:64) and they were still detectable at 60 dpi (IFA titer 1:4,000) (data not shown). Given the minimal phenotypic changes reflecting $CD8^+$ T cell activation after a secondary *Rickettsia* challenge, I hypothesized that antibodies might be interfering with the $CD8^+$ T cell recall responses; hence, I performed adoptive transfer and heterologous challenge experiments in order to determine if $CD8^+$ T cells would exhibit a fully activated phenotype upon *Rickettsia* reencounter in the absence of anti-*R. typhi* antibodies. As expected, mice that received immune serum, either alone or together with immune $CD8^+$ T cells were fully protected against reinfection (Fig. 4.8A). *Rickettsia* were detectable only in the lungs of mice receiving serum and $CD8^+$ T cells from naïve donors or only $CD8^+$ T cells from immune donors; however, when mice received immune

$CD8^+$ T cells, the bacterial loads were much lower than those from mice receiving naive $CD8^+$ T cells. Furthermore, *Rickettsia* was detected in 66.7% of controls compared to 28.6% of mice receiving immune cells, confirming that memory $CD8^+$ T cells are protective against reinfection.

The activation status of the transferred immune $CD8^+$ T cells labeled with CFSE was also assessed through restricted analysis of the $CFSE^+$ population. As expected, higher numbers of memory-type $CD8^+$ T cells, either $CD127^{high}CD44^{high}$ or $CD44^{high}CD27^{high}CD43^{low}$, were observed among mice that received immune cells compared to those that received naïve cells (Fig. 4.8B and C); however, the absence of anti-*Rickettsia* antibodies did not induce further significant changes (including cytokine expression) on the behavior of any of these subpopulations upon *Rickettsia* reencounter in naïve mice that received immune $CD8^+$ T cells. In contrast, significantly increased numbers of effector-type cells defined by the $CD127^{low}CD44^{high}$ phenotype were observed in the absence of anti-*Rickettsia* antibodies, compared to mice that received both $CD8^+$ T cells and serum from immune mice (Fig. 4.8B). In agreement with this finding, a small increase in the expression of IFN-γ and Granzyme B was observed in $CD44^{high}CD8^+$ T cells with an effector phenotype among recipients of immune T cells without immune serum, a ~1.4-fold increase (data not shown).

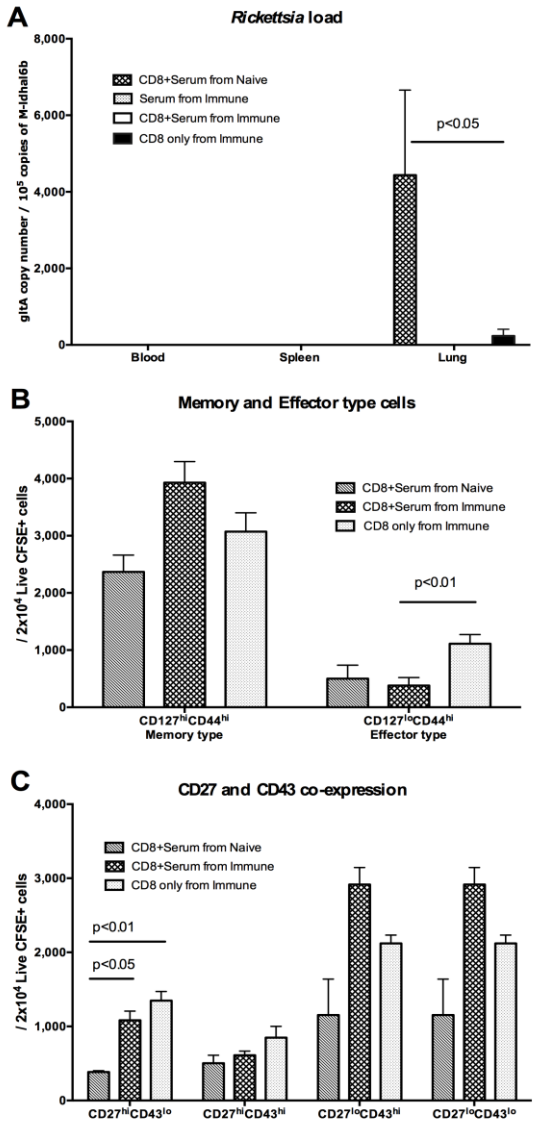

Figure 4.8 Adoptive transfer of immune serum and CD8$^+$ T cells. Serum and/or CD8$^+$ T cells labeled with CFSE from naïve or *Rikettsia*-immune mice were adoptively transferred into naïve C3H/HeN mice. Twenty-four hours after transfer, recipient mice were challenged with 10 LD_{50} of *R. typhi*. Forty hours after challenge, mice were injected with BFA and monensin, i.p., and 4 hours later they were sacrificed to obtain splenocytes for flow cytometric analysis and tissues for assessment of rickettsial load. (A) Rickettsial load was measured on blood, spleen and lung by Q-PCR. (B) Effector-type ($CD127^{low}CD44^{high}$) and memory-type ($CD127^{high}CD44^{high}$) subpopulations of transferred CD8$^+$ T cells. (C) Analysis of the expression of CD27 and CD43 among transferred $CD44^{high}$ CD8$^+$ T cells. Data represents mean ± SEM from three mice (receiving CD8$^+$ T cells and serum from naïve donors) or seven mice (receiving serum and/or CD8$^+$ T cells from immune donors) per group.

Next, the T_{CM} and T_{EM} status of the transferred cells, as well as their proliferative response to a secondary *Rickettsia* encounter was explored. In agreement with our previous results, upon recall, higher numbers of T_{CM} cells were detected in the spleen of mice that received immune cells; similarly, increased Ki67 expression was observed for both T_{CM} and T_{EM} subsets; however, the absence of anti-*Rickettsia* antibodies did not significantly improve the activation status of memory $CD8^+$ T cells (Fig 4.9).

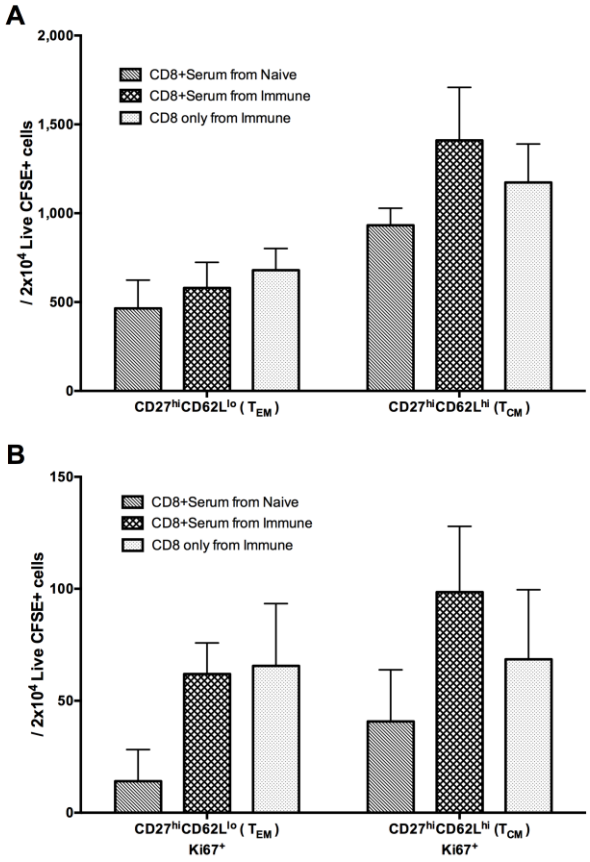

Figure 4.9 Dynamics of T_{CM} and T_{EM} subsets, and Ki67 expression on adoptively transferred $CD8^+$ T cells in the presence or absence of immune serum. (A) Numbers of T_{CM} ($CD27^{high}CD62L^{high}$) and T_{EM} ($CD27^{high}CD62L^{low}$) subsets gated on $CD127^{high}CD44^{high}$ $CD8^+$ T cells. (B) Expression of Ki67 on the T_{CM} and T_{EM} subsets. Mean ± SEM from three mice or seven mice per group are shown; each data point represents the mean value per 2×10^4 $CFSE^+$ cells. No statistically significant differences were observed.

On the contrary, when heterologous challenge experiments were performed, a slightly different scenario was observed. The rationale behind this experiment was that if anti-*R. typhi* antibodies are interfering with activation of quiescent memory $CD8^+$ T cell, and considering that antibodies are not cross-protective between phylogenetically distant *Rickettsia* groups (*R typhi* and SFG *Rickettsia*), we reasoned that the challenge of *R. conorii* immune mice (SFG *Rickettsia*) with *R. typhi* (typhus group *Rickettsia*) would allow $CD8^+$ T cells to become fully activated. As shown in figure 4.10, when *R. conorii* immune mice were challenged with $10LD_{50}$ of *R. typhi* and terminated 40 hpi, although not statistically significant, increased numbers of memory-type cells ($CD127^{high}CD44^{high}$, MPECs and T_{CM}) were observed compared to the homologous challenge scenario (*R. typhi* immune mice challenged with $10LD_{50}$ of *R. typhi*). In agreement with what was observed in the adoptive transfer experiments, an increase in $CD8^+CD44^+CD43^+$ effectors was also observed in mice heterologously challenged (data not shown). Efficiency of memory T cells in mediating *Rickettsia* clearance upon a secondary heterologous challenge is further supported by the rickettsia load results: compared to naïve animals, *R. conorii* immune mice significantly reduced *Rickettsia* load in the lungs, although less than *R. typhi* immune mice did. These data further supports the concept of T-cell mediated cross-protection (Fig 4.10D).

Although memory $CD8^+$ T cells are proven protectors against reinfection, our results showed that significant phenotypic changes (as assessed by the markers used here) are not detectable in memory $CD8^+$ T cells even in the absence of specific antibodies. This situation, at least for now, precludes the use of recall experiments for the validation cellular responses elicited by rickettsial protective antigens. My results might be

explained, at least in part, by our direct *ex vivo* approach without any *in vitro* re-stimulation, which reveals the tightly regulated and rapid kinetics of memory $CD8^+$ T cells *in vivo*. It is also quite possible that *Rickettsia*-infected endothelial cells respond very rapidly to circulating memory $CD8^+$ T cells to kill rickettsiae through oxidative stress- and IDO-related mechanisms [210], thus ceasing the antigenic stimulation for anti-*Rickettsia* $CD8^+$ T cells.

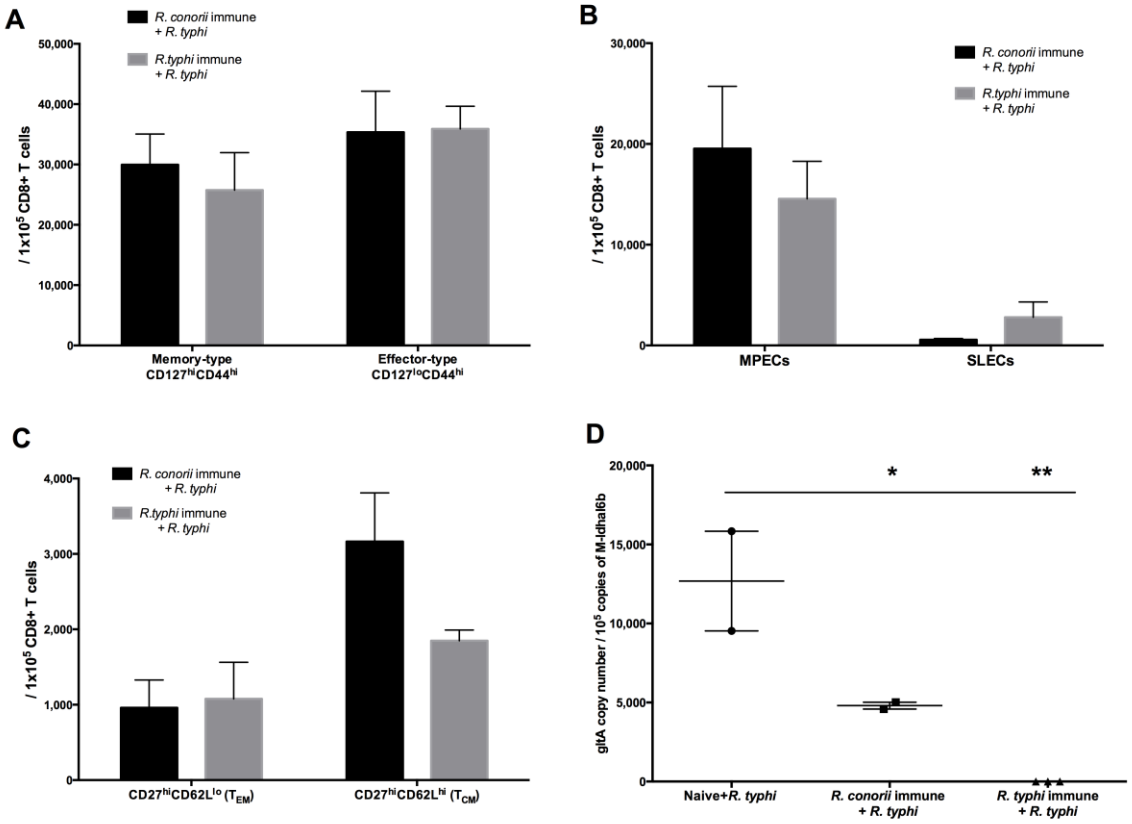

Figure 4.10 Dynamics of memory CD8$^+$ T cell subsets after heterologous challenge. *R. conorii* or *R. typhi* immune mice were challenged with 10 LD_{50} of *R. typhi*. Forty hours after challenge, mice were injected with BFA and monensin, i.p., and 4 hours later they were sacrificed to obtain splenocytes for flow cytometric analysis and tissues for assessment of rickettsial load. (A) Effector-type ($CD127^{low}CD44^{high}$) and memory-type ($CD127^{high}CD44^{high}$) subsets. (B) Numbers of MPECs ($CD127^{high}KLRG1^{low}$) and SLECs ($CD127^{low}KLRG1^{high}$) among $CD3^+CD8^+CD44^{high}$ antigen experienced cells. (C) Numbers of T_{CM} ($CD27^{high}CD62L^{high}$) and T_{EM} ($CD27^{high}CD62L^{low}$) subsets gated on $CD127^{high}CD44^{high}$ $CD8^+$ T cells. (D) *Rickettsia* load in the lungs. Each data point represents the mean value per 10^5 $CD8^+$ T cells ± SEM from two (naïve) or three mice per time point. p values are represented as follows: * $p<0.05$; ** $p<0.001$.

Induction of IFN-γ and Memory-Type $CD8^+$ T Cells Correlate with Protection against *R. typhi* Infection in Mice Immunized with Novel Protective Rickettsial Antigens.

Altogether, the data above indicate that the assessment of $CD8^+$ T cell responses 7 days after challenge provide the most appropriate time point for validation of the protective potential of those vaccine targets, firstly because rickettsiae are still detectable, and reduction of bacterial load can be used as a measure of protection, and secondly because this time point represents the peak of the $CD8^+$ T cell response after a first encounter with *R. typhi* including effector- and memory-type $CD8^+$T cells. Assessment at this time point after primary challenge is relevant because our platform for the discovery of rickettsial protective antigens involves a rapid prime and boost immunization followed shortly thereafter by a lethal challenge; further, this immunization strategy is known to result in the production of memory-type $CD8^+$ T cells within 5 to 7 days after immunization [106, 107].

To determine whether immunization with rickettsial protective antigens was inducing memory- and/or effector-type subsets, I studied $CD8^+$ T cell responses 7 days after a lethal challenge ($5LD_{50}$) with *R. typhi* in mice immunized with individual (RP778, RP739, RP403, and RP598) or pooled *R. prowazekii* protective antigens (RP884, RP739, RP403, and RP598); as controls, mice were immunized with an irrelevant protein (luciferase) or a weakly-protective rickettsial antigen (RP734). To confirm that immunization conferred protection, I measured the *Rickettsia* load in lung and liver. As shown in figure 4.11, mice immunized with the protective antigens showed reduced bacterial loads.

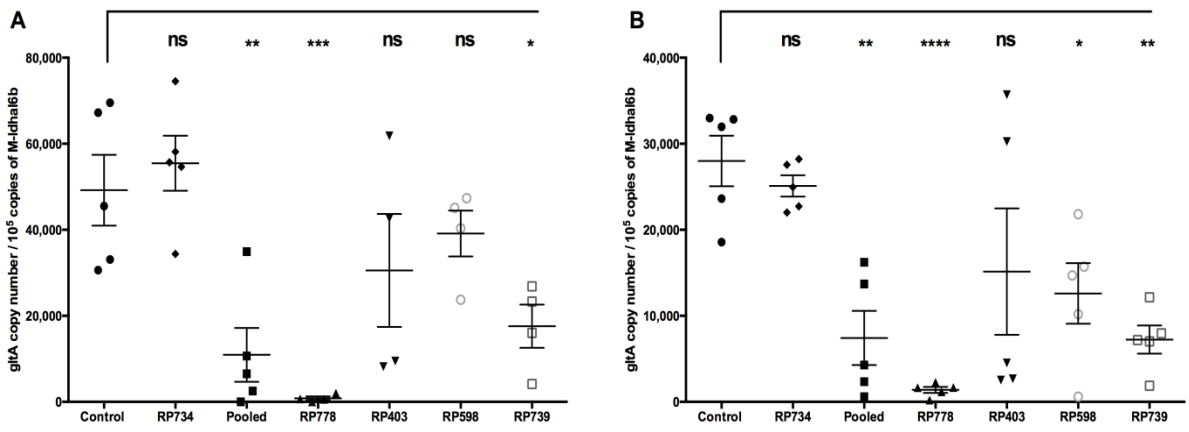

Figure 4.11 Assessment of protection after immunization with rickettsial protective antigens. Mice were immunized with APCs individually expressing selected *R. prowazekii* protective antigens RP778, RP739, RP598 or RP403 or pooled *Rickettsia* proteins (RP739, RP598, RP403 and RP884). Animals immunized with an irrelevant protein (luciferase) or with a weakly-protective rickettsial antigen (RP734) were used as controls. Seven days after immunization, mice were challenged with 5 × LD_{50} *R. typhi*. At 7 dpi, animals were terminated and rickettsia load in the lungs (A) and liver (B) was determined using quantitative real time PCR targeting the mouse gene *Idhal6b* and the rickettsial gene *gltA*. Individual data points with mean ± SEM are shown. p values for comparisons against control mice are represented as follows: *p<0.05; **p<0.01; ***p<0.001; ****p<0.0001; non-significant (ns).

Compared to mice immunized with non-protective proteins (luciferase or RP734), mice that received protective antigens had increased numbers of memory-type $CD8^+$ T cells ($CD44^{high}CD127^{high}CD43^{low}$) and reduced numbers of effector-type $CD8^+$ T cells ($CD44^{high}CD127^{low}CD43^{high}$); however, this differences were only statistically significant for RP778 (Fig. 4.12A and B). Memory-type $CD8^+$ T cells also had increased IFN-γ expression; at least a ~2-fold change was observed in mice immunized with RP778, RP403, or pooled protective antigens (Fig. 4.12C). In contrast, IFN-γ expression on effector-type cells was not different between groups (data not shown). In an independent experiment with only RP884, we observed a similar pattern (Fig. 4.13). For the most protective antigen, RP778, the CD127 vs. KLRG1 and CD27 vs. CD43 analyses also showed increased memory-type ($CD127^{high}KLRG1^{low}$ or $CD27^{high}CD43^{Low}$) $CD8^+$ T cells (Fig. 4.12D-F). Interestingly, similarly to my observations in recall responses, mice immunized with protective antigens also had increased numbers of $CD27^{low}CD43^{low}$and $CD127^{low}CD43^{low}$ cells but without an increase in the $CD127^{low}KLRG1^{low}$ subpopulation (Fig. .14A-C). In fact, increased IFN-γ production in groups immunized with protective antigens, particularly those receiving RP778, RP403, or pooled protective antigens, was also observed in $CD27^{low}CD43^{low}$ and $CD127^{low}CD43^{low}$ cells (Fig. 4.14D and E). Since effector-like memory $CD27^{low}CD43^{low}$ cells express Granzyme B, are cytolytic, and protect against *Listeria* [92, 117], we assessed Granzyme B expression in our model and observed increased expression in $CD27^{low}CD43^{low}$ cells from mice immunized with protective antigens (Fig. 4.14F).

Figure 4.12 Increased numbers of memory-type but not of effector-type $CD8^+$ T cells are induced in mice immunized with protective rickettsial antigens.

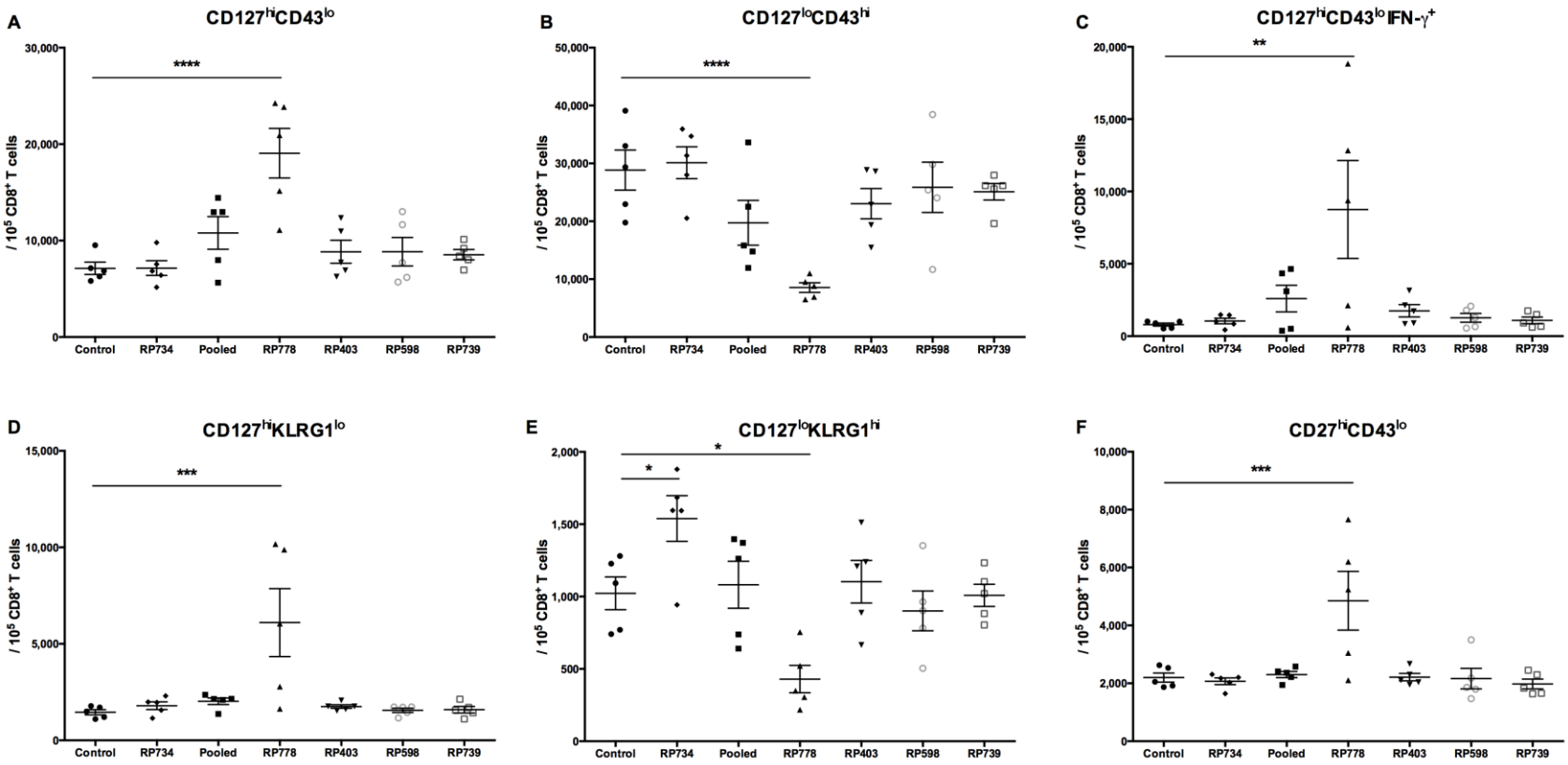

Figure 4.12 Increased numbers of memory-type but not of effector-type $CD8^+$ T cells are induced in mice immunized with protective rickettsial antigens. Mice were immunized with APCs individually expressing selected *R. prowazekii* protective antigens RP778, RP739, RP598 or RP403 or pooled *Rickettsia* proteins (RP739, RP598, RP403 and RP884). Animals immunized with an irrelevant protein (luciferase) or with a weakly-protective rickettsial antigen (RP734) were used as controls. Seven days after immunization, mice were challenged with $5 \times LD_{50}$ *R. typhi*. At 7 dpi, animals were sacrificed to obtain splenocytes for flow cytometric analysis. All analysis were performed on antigen experienced $CD3^+CD8^+CD44^{high}$cells. (A) Memory-type $CD127^{high}CD43^{low}$ cells. (B) Effector-type $CD127^{low}CD43^{high}$ cells. (C) IFN-γ expression in memory-type $CD127^{high}CD43^{low}$ cells. (D) Memory precursor effector cells (MPECs, $CD127^{high}KLRG1^{low}$). (E) Short-lived effector cells (SLECs, $CD127^{low}KLRG1^{high}$). (F) Memory-type $CD27^{high}CD43^{low}$ cells. Individual data points with mean ± SEM are shown. p values for comparisons against control mice are represented as follows: *p<0.05; **p<0.01; ***p<0.001; ****p<0.0001.

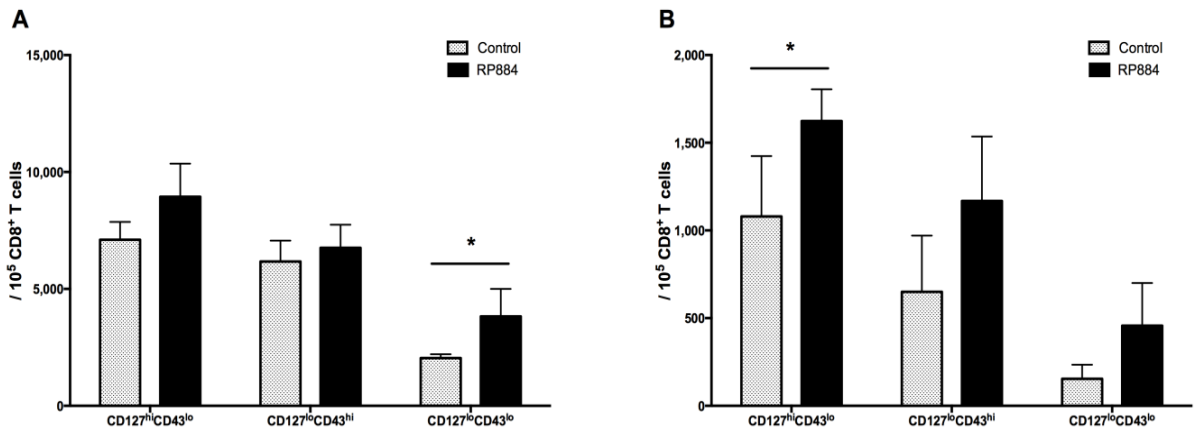

Figure 4.13 Number of $CD8^+$ T cells expressing different phenotypes in the CD127 vs. CD43 analysis, and expression of IFN-γ in the same subpopulations from RP884-immune mice. Splenocytes for flow cytometric analysis from RP884-immune animals and control mice were obtained as previously described. (A) Number of $CD127^{high}CD43^{low}$, $CD127^{low}CD43^{high}$ and $CD127^{low}CD43^{low}$ cells among $CD3^+CD8^+$ $CD44^{high}$ cells. (B) Expression of IFN-γ in the same subsets. Each bar represents the mean value ± SEM per 10^5 $CD8^+$T cells from five mice per group. p values for comparisons against control mice are represented as follows: *$p<0.05$.

Figure 4.14 $CD27^{low}CD43^{low}$ and $CD127^{low}CD43^{low}$ subsets, but not $CD127^{low}KLRG1^{low}$ cells, are increased in mice immunized with protective rickettsial antigens.

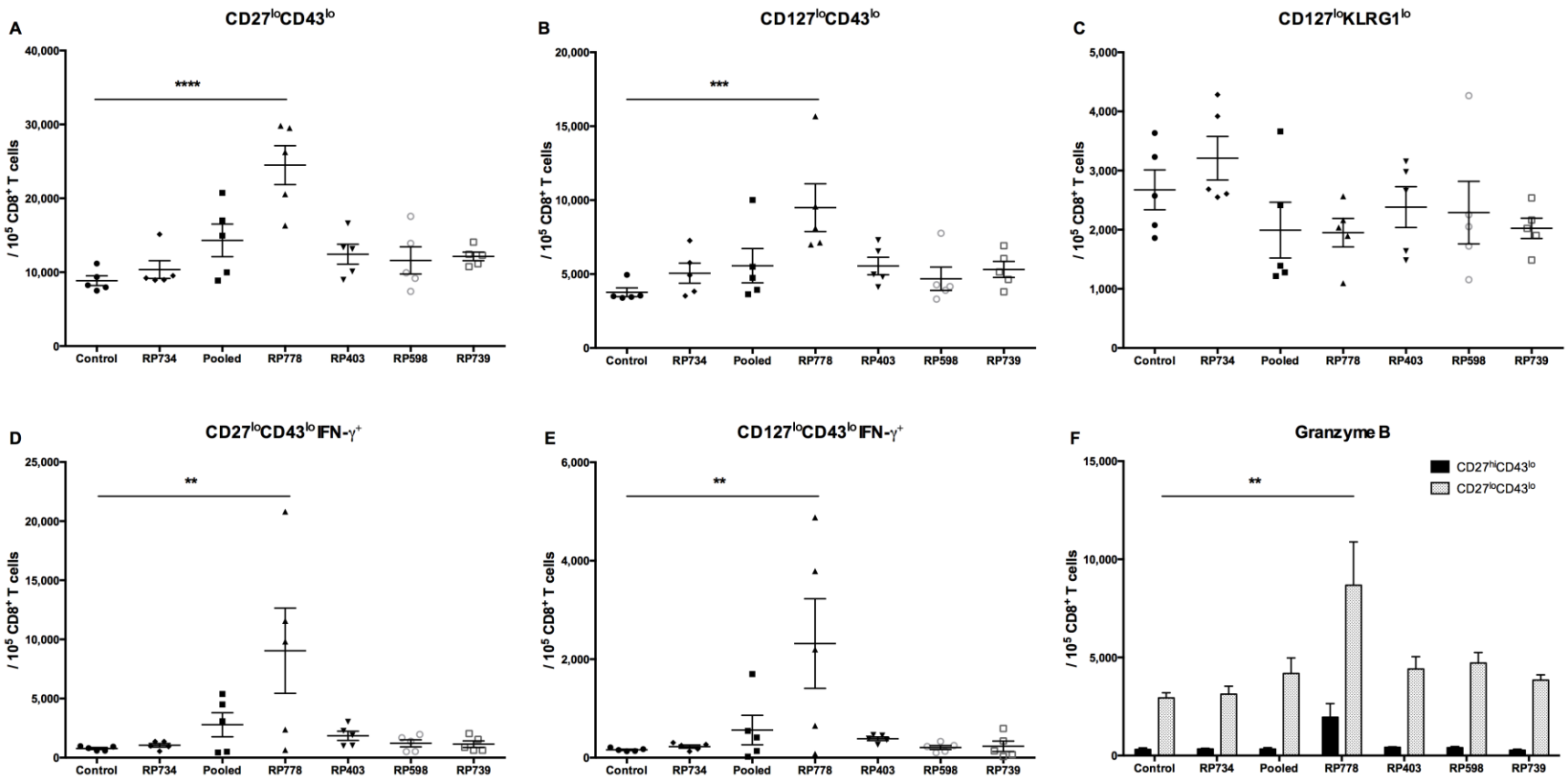

Figure 4.14 $CD27^{low}CD43^{low}$ and $CD127^{low}CD43^{low}$ subsets, but not $CD127^{low}KLRG1^{low}$ cells, are increased in mice immunized with protective rickettsial antigens. Mice were immunized and challenged with 5 × LD_{50} *R. typhi* as described. At 7 dpi, animals were sacrificed to obtain splenocytes for flow cytometric analysis. All analyses were performed on antigen experienced $CD3^{+}CD8^{+}CD44^{high}$cells. (A) $CD27^{low}CD43^{low}$ cells. (B) $CD127^{low}CD43^{low}$ cells. (C) $CD127^{low}KLRG1^{low}$ cells. (D) IFN-γ expression in $CD27^{low}CD43^{low}$ cells. (E) IFN-γ expression in $CD127^{low}CD43^{low}$ cells. (F) Granzyme B expression in $CD27^{high}$ and $CD27^{low}$ memory-type cells. Individual data points with mean ± SEM are shown. p values for comparisons against control mice are represented as follows: **p<0.01; ***p<0.001; ****p<0.0001.

I then asked if the level of protection achieved after immunization with protective antigens (as assessed by rickettsial load) would correlate with the number of memory-type cells, and/or the number of cells producing IFN-γ or Granzyme B (Fig. 4.15). Calculation of Pearson's correlation coefficient showed statistically significant correlations between reduction in *Rickettsia* load and the number of $CD3^{+}CD8^{+}CD44^{high}$ cells producing IFN-γ, or the number of cells with any of the following phenotypes: $CD127^{high}CD43^{low}$, $CD127^{low}CD43^{low}$, $CD127^{high}KLRG1^{low}$ (MPECs), $CD27^{high}CD43^{low}$, and $CD27^{low}CD43^{low}$, as well as with Granzyme B expression by $CD27^{low}CD43^{low}$ cells. In contrast, the induction of effector subsets such as $CD127^{low}CD43^{high}$ and $CD127^{low}KLRG1^{high}$ (SLECs) was correlated with increased *Rickettsia* loads.

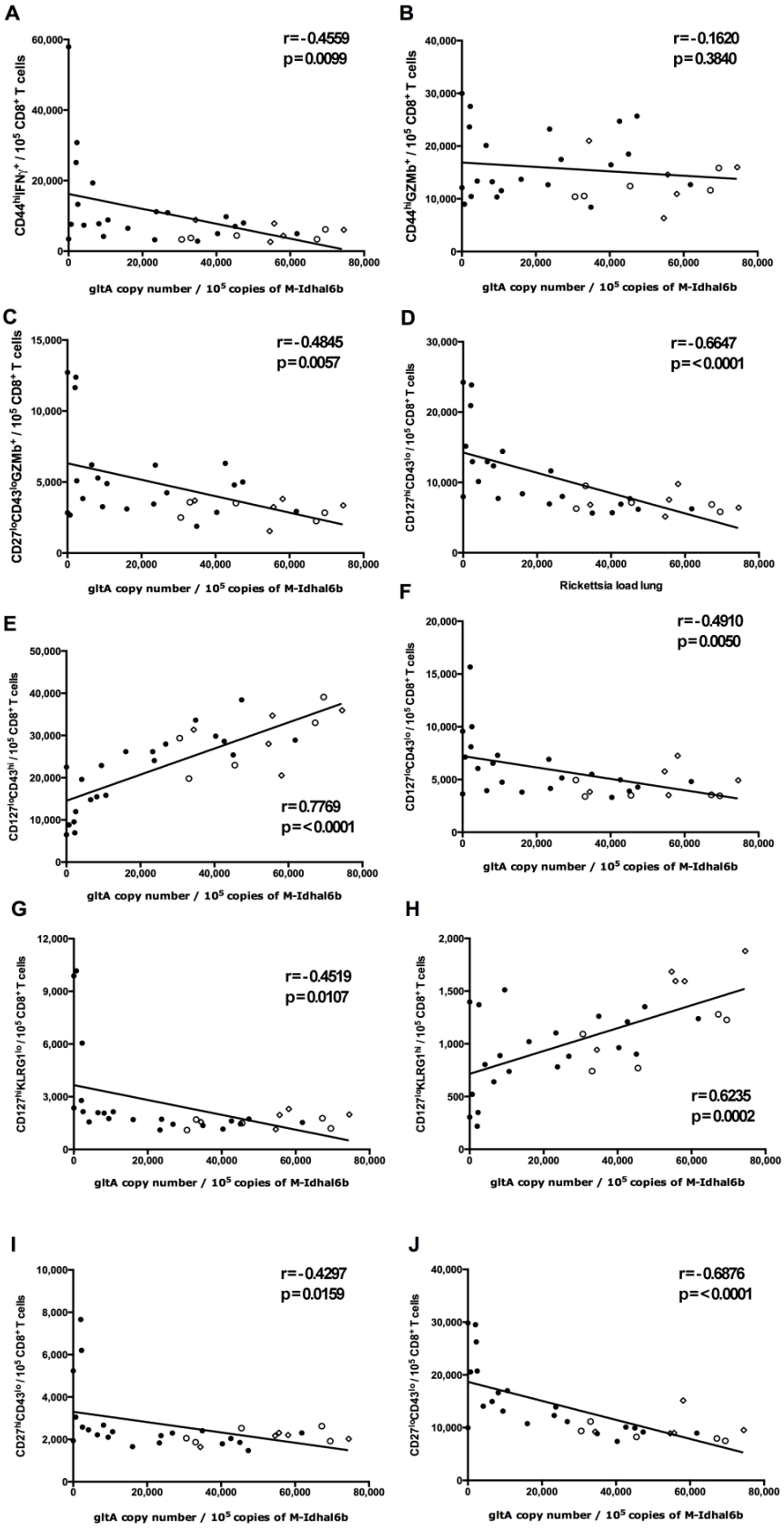
A
r=-0.4559
p=0.0099
CD44hiIFNγ+ / 10^5 CD8+ T cells
gltA copy number / 10^5 copies of M-Idhal6b
B
r=-0.1620
p=0.3840
CD44hiGZMb+ / 10^5 CD8+ T cells
gltA copy number / 10^5 copies of M-Idhal6b
C
r=-0.4845
p=0.0057
CD27loCD43loGZMb+ / 10^5 CD8+ T cells
gltA copy number / 10^5 copies of M-Idhal6b
D
r=-0.6647
p=<0.0001
CD127hiCD43lo / 10^5 CD8+ T cells
Rickettsia load lung
E
r=0.7769
p=<0.0001
CD127hiCD43hi / 10^5 CD8+ T cells
gltA copy number / 10^5 copies of M-Idhal6b
F
r=-0.4910
p=0.0050
CD127loCD43lo / 10^5 CD8+ T cells
gltA copy number / 10^5 copies of M-Idhal6b
G
r=-0.4519
p=0.0107
CD127hiKLRG1lo / 10^5 CD8+ T cells
gltA copy number / 10^5 copies of M-Idhal6b
H
r=0.6235
p=0.0002
CD127loKLRG1hi / 10^5 CD8+ T cells
gltA copy number / 10^5 copies of M-Idhal6b
I
r=-0.4297
p=0.0159
CD27hiCD43lo / 10^5 CD8+ T cells
gltA copy number / 10^5 copies of M-Idhal6b
J
r=-0.6876
p=<0.0001
CD27loCD43lo / 10^5 CD8+ T cells
gltA copy number / 10^5 copies of M-Idhal6b

Figure 4.15 Induction of memory-type $CD8^+$ T cells and $CD27^{low}CD43^{low}$ cells, and expression of IFN-γ correlate with protection against rickettsia challenge in mice immunized with protective antigens. Mice were immunized and challenged with 5 × LD_{50} *R. typhi* as described. At 7 dpi, animals were sacrificed to obtain splenocytes for flow cytometric analysis. All analysis were performed on antigen experienced $CD3^+CD8^+CD44^{high}$cells. The protective effect of immunization with rickettsial vaccine targets was assessed as reduction of the *Rickettsia* load. (A) $CD44^{high}$IFN-γ^+ cells. (B) $CD44^{high}GZMb^+$ cells. (C) $CD27^{low}CD43^{low}GZMb^+$ cells. (D) $CD127^{high}CD43^{low}$ cells. (E) $CD127^{low}CD43^{high}$ cells. (F) $CD127^{low}CD43^{low}$ cells. (G) $CD127^{high}KLRG1^{low}$ cells. (H) $CD127^{low}KLRG1^{high}$ cells. (I) $CD27^{high}CD43^{low}$ cells. (J) $CD27^{low}CD43^{low}$ cells. Pearson's correlation between rickettsial load (gltA copy number/10^5 copies of M-Idhal6b) and number of positive cells for each subset per10^5 $CD8^+$ T cells is shown. (○) Mice immunized with control protein (luciferase). (◇) Mice immunized with weakly-protective rickettsial antigen RP734. (●) Mice immunized with protective antigens.

DISCUSSION

$CD8^+$ T cells are critical effectors of immunity against rickettsial infections in pertinent mouse models that mimic the pathophysiology of severe human rickettsioses [35]; mice that survive a rickettsial infection become solidly immune against subsequent lethal challenges [40, 44]. In consequence, the definition and validation of potential correlates of protection for validation and testing of vaccine antigen candidates in these models is, in my opinion, justified. Although previous studies have examined anti-*Rickettsia* $CD8^+$ T cell responses [37, 38], there is still a large gap in the identification of antigens that provide strong protective T cell-mediated immunity and in the systematic definition of correlates or surrogates of protection in rickettsial diseases.

In this study, I analyzed the expression of activation markers and effector molecules that have been linked to the achievement of long-lasting protection after vaccination. First, I studied the kinetics of primary and memory $CD8^+$ T cell responses with the aim of identifying a combination of markers of cellular protective immunity that could be used for the validation of vaccine antigen candidates against *Rickettsia*. Then, I asked whether this marker combination could serve as an immune correlate of protection in mice immunized with protective antigens. The detailed kinetic analysis presented here showed that after a primary challenge with *R. typhi*, the peak of anti-*Rickettsia* $CD8^+$ T cell-mediated responses occurs at 7 dpi (Fig. 4.3 and 4.4). Interestingly, although memory $CD8^+$ T cells were effective in controlling *Rickettsia* infection upon a secondary challenge, direct *ex vivo* recall responses were rather discrete (Fig. 4.5, 4.6 and 4.7); only a small increase in the $CD27^{high}CD43^{low}$, T_{CM} subsets, and IL-2 production, without

changes in the expression of the proliferation marker Ki67 or the expression of the effector molecules IFN-γ and Granzyme B, was observed. The results from adoptive transfer and heterologous challenge experiments suggest that anti-*Rickettsia* antibodies might be playing a role in the paucity of recall responses by interfering with the activation of memory $CD8^+$ T cells (Fig. 4.8, 4.9 and 4.10). Another non-exclusive alternative explanation for this phenomenon is that memory immune responses mediated by $CD8^+$ T cells upon re-encounter with *R. typhi* are very efficient, tightly controlled, and self limited *in vivo*. In addition, the present study only interrogated memory $CD8^+$ T cells present in the circulating memory pool and there is a growing number of studies supporting the concept that tissue resident memory cells represent a distinct subset with functional properties different from those residing in lymphoid tissues [211, 212]; thus, it will be interesting to test if memory cells isolated from target organs such as liver and lung will show a different activation pattern upon recall. Since our laboratory experimental approach is aimed to directly measure what is occurring *in vivo* without further *in vitro* restimulation steps, other immunological tools, such as transgenic TCR mice or tetramer staining, which are not currently available for *Rickettsia*, will be required to further dissect the kinetics and breadth of the memory $CD8^+$ T cell responses against *Rickettsia*.

Thus, the present results support 7 dpi as a valid time point for assessing $CD8^+$ T cell responses in mice immunized with rickettsial vaccine antigens for two reasons: 1) both memory precursors and terminally differentiated effector cells can be detected at the peak of $CD8^+$ T cell responses in other models [104], and we observed this phenomenon here (Fig. 4.4); and 2) we are following a rapid immunization protocol that generates

memory-type $CD8^+$ T cells within 5 to 7 days after immunization [106, 107]. Based on the analysis of the anti-*R. typhi* $CD8^+$ T cell response, I propose four correlates of protection against *R. typhi* infection in animals immunized with novel protective rickettsial antigens: 1) production of IFN-γ by antigen experienced $CD3^+CD8^+CD44^{high}$ cells, 2) production of Granzyme B by $CD27^{low}CD43^{low}$ antigen-experienced $CD8^+$ T cells, 3) generation of memory-type $CD8^+$ T cells ($CD127^{high}CD43^{low}$, MPECs, and $CD27^{high}CD43^{low}$), and 4) generation of effector-like memory $CD8^+$ T cells ($CD27^{low}CD43^{low}$) (Fig. 4.15). These findings support the concept that protective antigens identified through our platform are good inducers of memory-type cells with appropriate relevant phenotypes. Interestingly, despite the lack of correlation between the number of cells producing Granzyme B among all antigen experienced cells ($CD3^+CD8^+CD44^{high}$) and reduction of *Rickettsia* load, we observed a correlation between decreased rickettsial load and increased expression of Granzyme B on effector-like memory $CD8^+$ T cells ($CD27^{low}CD43^{low}$). This finding is aligned with the concept that memory $CD8^+$ T cell subsets might have a specialized organization and distribution based on their effector functions and activation status [117].

It has been shown that the number of memory-type T cells generated after infection or vaccination strongly correlates with the degree of protection to subsequent challenge [107]. This study supports this correlation since the most protective antigen, as assessed by survival and rickettsial load (RP778), produced the largest increase in IFN-γ expression and generated the largest number of memory-type $CD8^+$ T cells. Moreover, when antigens that were not as strong individually were pooled (RP884, RP739, RP403 and RP598), they provided an overall superior protection in terms of reduction of the

Rickettsia load (Fig 4.11) and the induction of memory-type $CD8^+$ T cells (Fig. 4.12 and 4.13), suggesting that some degree of synergy was achieved. Interestingly, mice immunized with protective antigens had increased numbers of $CD27^{low}CD43^{low}$ and $CD127^{low}CD43^{low}$, but not of $CD127^{low}KLRG1^{low}$ antigen experienced $CD8^+$ T cells. Although $CD27^{low}CD43^{low}$ effector-like memory $CD8^+$ T cells were initially associated with inferior recall proliferation responses when compared to the $CD27^{high}$ pool [92], it was recently demonstrated that this subset efficiently protects against *Listeria* and vaccinia infection [117]. Even though it is currently unknown if protection provided by the $CD27^{low}CD43^{low}$ memory pool can be extended to other double negative memory $CD8^+$T cell subsets (such as $CD127^{low}CD43^{low}$ cells), the fact that a solid memory T cell response is generated after experimental sublethal infection with *Rickettsia* together with the findings presented here would support the speculation that rapid induction of the $CD127^{low}CD43^{low}$ or $CD27^{low}CD43^{low}$ subsets could mediate protection against *Rickettsia* infection in immunized animals. In fact, it has been proposed that $CD27^{low}CD43^{low}$ cells could represent the potential source of protection induced in rapid prime-boost vaccination approaches, which was used here, and that persistence of effector-like memory cells might account for immediate protection against acute infection [117, 123]. More studies are required in order to assess the protective capability of the $CD27^{low}CD43^{low}$ subset upon recall compared to the classical T_{CM} and T_{EM} or the $CD27^{high}CD43^{low}$ memory subsets that are known to mediate optimal protection in other models [92, 120–122].

In summary, this is the first report of a comprehensive characterization of the anti-*Rickettsia* $CD8^+$ T cell immune response with implications for the identification of

correlates of T cell-mediated protective immunity. Our findings provide useful paradigms for the validation of vaccine antigen candidates recognized by $CD8^+$ T cells and for the general assessment of the quality of the immune response induced by novel vaccine targets.

CHAPTER 5: Summary and Future Directions

In the present study, a reverse vaccinology approach for the identification of T cell rickettsial antigens was applied for the first time. Analysis of the complete *R. prowazekii* ORFeome allowed the identification of five novel protective antigens, namely RP884, RP778, RP739, RP598, and RP403. All, except for RP884, were predicted to encompass both MHC class-I and MHC class-II epitopes. RP884 was predicted to encompass only MHC class-I epitopes.

We implemented a $CD8^+$ T cell biased platform for antigen discovery because $CD8^+$ T cells are critical effectors of immunity against experimental rickettsial infections [37, 38], and $CD8^+$ T cells from patients that recovered from endemic typhus can recognize rickettsial antigens [75]. Mouse SVEC4-10 endothelial cells were modified to express the costimulatory molecules CD80 and CD137L, and transfected with rickettsial genes for stable expression of *in silico*-selected rickettsial proteins. Rapid proteasome processing of rickettsial proteins was induced by fusion to a destabilization (DD) domain; these endothelial cell lines were used as APCs in a rapid prime and boost immunization protocol [106], which resulted in $CD8^+$ T cell stimulation as expected. Although the aims of this study did not include determining which antigen presentation pathway(s) were involved in T cell priming, survival of SVEC4-10 cells expressing Luc2 inoculated into C3H/HeN mice was tested to determine whether these cells could function as direct APCs *in vivo*. Although i.v. injection produced rapid dilution and re-distribution of the cellular inoculum and the signal was not detectable, the injection of Luc2- expressing cells into a single anatomical space, namely i.p or i.m. injection, produced a signal that

was detectable and stable for 6 days. This result indicated that SVEC4-10 cells expressing a foreign antigen can persist up to the time when activated effector T-cells would start to emerge, indirectly suggesting that direct antigen presentation by the synthetic APCs used in this study was at least possible [174]. Future experiments using adoptively transferred naïve $CD8^+$ T-cells into MHC class I-deficient mice will directly address if direct antigen presentation is the mechanism of T-cell priming for this antigen-screening platform.

One interesting finding was that 4 protective rickettsial antigens out of 14 tested antigens (28.6%) discovered in the present study were predicted to encompass both MHC class-I and MHC class-II epitopes; in contrast, only 1 protective antigen was discovered when we tested 9 (11.1%) antigens predicted to encompass only MHC class-I epitopes. This suggests that antigens predicted to have both types of epitopes might have superior protective capabilities; future *in silico* studies will address if these protective antigens contain overlapping $CD4^+$ and $CD8^+$ T cell epitopes. Although not tested in the present study, it is tempting to speculate that the presence of $CD4^+$ T cell epitopes might improve antigen immunogenicity by providing help to $CD8^+$ T cells; if that is the case, two scenarios mediating $CD4^+$ T cell activation are possible: one involves the uptake of SVEC4-10 cells expressing rickettsial antigens by other APCs, probably DCs, to be further processed via the endocytic pathway; the other involves the potential upregulation of MHC class-II molecules on the SVEC4-10 cells for direct antigen presentation, which is possible given that MHC class-II upregulation on these cells can be induced in the presence of IFN-γ [213]. Future studies involving $CD4^+$ depletion might help elucidate the contribution of $CD4^+$ T cells to the protective mechanism of rickettsial antigens

encompassing both MHC class-I and MHC class-II epitopes. In addition, immunization with nonviable or fragmented SVEC4-10 cells expressing rickettsial antigens could provide insights about the role of these cells in direct antigen presentation for T cell priming.

Interestingly, the position in the ranking of the novel protective antigens after applying the HLA binding score for both MHC class I and class II did not exactly correlate with their protective capabilities. RP778, the strongest candidate of this set of proteins, was ranked in the middle (position 23 and 40 for MHC class I and MHC class II, respectively) for both systems; however, when only MHC class-I binding data is taken into consideration, all candidates found thus far are among the top 23 ranked proteins, suggesting that the HLA class I binding score applied here could indeed provide a very important component for the prioritization of $CD8^+$ T cell vaccine targets; testing of the remaining 40 *in silico*-defined vaccine candidates is required in order to further support this notion.

Considering that the C3H mouse model mimics the pathophysiology of severe human rickettsioses, the sublethal rickettsial infection in this model, which confers long-lasting cross-protective immunity, can be regarded as the paradigm for the definition of potential correlates of cellular immunity and for the validation of vaccine candidates. In this study, the kinetics of primary and memory $CD8^+$ T cell responses was analyzed from the perspective of activation markers and effector molecules expression with the aim of identifying $CD8^+$ T cell activation patterns that could be useful for the validation of rickettsial vaccine candidates.

Even though mice remained healthy and *Rickettsia* was undetectable at all tested time points (6-120h) after a secondary lethal challenge, the paucity of the $CD8^+$ T cell memory response was puzzling. In light of the prominent role of antibodies in protection against a secondary encounter with homologous *Rickettsia*, the interference of anti-*Rickettsia* antibodies with memory $CD8^+$ T cell activation was hypothesized as a potential explanation for this scenario. Even though, a series of experiments were performed in order to rule-out this possibility, such as adoptive transfer of immune $CD8^+$ T cells into naïve mice and heterologous challenge of *R. conorii* immune mice with *R. typhi*, the results obtained, although suggestive, did not fully support the antibody-interference hypothesis since the differences were small and not statistically significant. As opposed to the adoptive transfer, the heterologous challenge experiments showed a more consistent activation trend among different memory-type subsets suggesting that this approach could be useful for elucidating the role of anti-*Rickettsia* antibodies on the paucity of recall responses and that a new set of experiments increasing the number of animals per group might be informative. Also, in the future, when immunological tools that allow tracking of antigen-specific T cell responses become available for *Rickettsia*, a more detailed insight about recall responses could be attained. The capacity to assess and track anti-*Rickettsia* T-cell recall responses would be pivotal for further validation of the identified protective antigens since memory generation is one of the ultimate goals of vaccination and the T-cell component, mediator of cross-protection in rickettsial infections, will be critical for the development of a universal anti-*Rickettsia* vaccine.

On the other hand, the $CD8^+$ T cell response after a primary challenge with *R. typhi* was most informative from the perspectives of identifying critical time points and

marker combinations that could be used to evaluate the ability of the newly discovered protective antigens to induce protective $CD8^+$ T cell responses and for providing a rational for the prioritization of the novel candidates for further characterization. In the present study, four potential correlates of protective cellular immunity were identified when $CD8^+$ T cell responses were assessed 7 days after *R. typhi* challenge: 1) production of IFN-γ by antigen experienced $CD3^+CD8^+CD44^{high}$ cells, 2) production of Granzyme B by $CD27^{low}CD43^{low}$ antigen-experienced $CD8^+$ T cells, 3) generation of memory-type $CD8^+$ T cells [Memory Precursor Effector Cells (MPECs), as well as $CD127^{high}CD43^{low}$, and $CD27^{high}CD43^{low}$ $CD8^+$ T cells], and 4) generation of effector-like memory $CD8^+$ T cells ($CD27^{low}CD43^{low}$). The next step towards the further validation of this potential correlates of cellular immunity will be performing adoptive transfer of the specific memory-type subsets to test protection, which in turn will also contribute to the initial assessment of the immunological mechanisms involved in the protection conferred by the recently identified protective antigens.

The next question that needs to be addressed is whether these novel protective antigens can induce long-term memory; as discussed, the immunization strategy definitely will play a role in answering this question and long term experiments involving *Rickettsia* lethal challenge several months after immunization will be required. In our current strategy, immunophenotyping of $CD8^+$ T cells is performed after vaccination and challenge with virulent *Rickettsia*. An alternative approach towards obtaining insights about the capacity of the novel protective antigens to induce long-term memory might be attained through the use of *Rickettsia*-immune mice in order to establish if antigen-specific recall responses against protective antigens can be detected. One potential

drawback from this approach will be that antigens identified thus far might not be immunodominant, and consequently memory cells recognizing a given antigen might be absent or at low frequency; however, some preliminary data generated for RP884 support the viability of this approach: the i.v administration of APCs expressing RP884 to *R. typhi* immune mice followed by overnight *in vitro* re-stimulation with the same cells allowed the detection of increased frequencies of MPECs and $CD8^{low}CD11a^{high}CD44^{high}IFN\text{-}\gamma^{+}$ cells (Fig. 5.1). Although these preliminary results suggest that this approach could be viable, improvements to the tools available for assessing anti-*Rickettsia* specific T cell responses are required; in particular the identification of T cell epitopes that can induce robust T cell activation might be essential.

Interestingly, when novel protective antigens were pooled to test protection against a lethal challenge with the phylogenetically distant *R. conorii*, although mice were protected from the heterologous challenge to a similar extent than the ones challenged with *R. typhi,* the protection observed against *R. typhi* was less than the one attained when some of these proteins were tested individually. Some possible explanations for this observation include that one or more of the other antigens in the pool might be triggering suppressive responses or that this discrepancy might be related to changes in the immunodominance hierarchy of the most protective antigens when other antigens are also present. Some preliminary data offer support to the latter explanation since the exclusion of RP884 form the pool improved the survival (87.5% vs. 62.5%) to *R. typhi* lethal challenge (Fig. 5.2). Nonetheless, at this early stage of antigen discovery, it would be premature to discard antigens that afforded protection without a

more detailed characterization. This is an important aspect to be addressed in the future when formulating multi-subunit vaccines for *Rickettsia*. This finding also suggests that pool testing might not be the best option since antigen interactions could mask the protective potential of the individual proteins.

Another important aspect is how protective antigens are delivered, which could, in some cases, be as important as the antigen itself; this is why future improvements to the vector as well as to the immunization platform are important in order to take advantage of all the protective potential of the antigens identified. For instance, in malaria vaccines it has been observed that the vector selected for immunization play a role in determining if an effective cellular protective response will be generated [214]. The extrapolation of this observation to an antigen discovery approach that uses *in silico* predictions could imply that if the immunization platform is not appropriate for a given pathogen or antigen, regardless of how accurate the *in silico* predictions are, it might hinder the chances of finding protective antigens. In the course of this study, we found two scenarios that could potentially support this notion. First, RP778, which appears to be one of the most promising protective antigens found in this study, was also part of the original pool containing RP884; however, it failed to provide protection when APCs transiently expressing rickettsial proteins were used for immunization. On the other hand, when cell lines stably expressing RP778 were used for immunization, RP778 emerged as strong protective antigen. An alternative but not exclusive explanation for this discrepancy might be the fact that the pool containing RP884 was deconvoluted and analyzed using reduction of the *Rickettsia* load as readout; we now know that this endpoint does not always reflect the protective capabilities of rickettsial antigens and that

any *in vivo* assessment of protection needs to include survival studies. Second, preliminary results of the performance of a new vector being developed in our laboratory suggest that RP884 could confer even superior protection against a lethal challenge with *R. typhi* if the antigen is directly delivered to host DCs (Fig. 5.3). This new vector, instead of directing proteins for proteasome degradation, targets DEC-205 on DCs, an endocytic receptor and member of the C-type lectins family, by fusing rickettsial antigens to anti-DEC-205 antibodies; this approach was shown to elicit potent $CD8^+$ T cells responses [215]. Future studies will seek to address the potential advantages of this new vector for the screening of *in silico* defined *Rickettsia* vaccine targets.

Finally, with regard to the paradigm that surface or secreted proteins are potentially better vaccine antigens, in my studies, only 1 out 5 protective antigens have this subcellular localization (RP739, predicted as a cytoplasmic membrane antigen); thus, the present results are in agreement with the notion that for T cell antigens subcellular localization is not as critical as it is for B cell antigens.

Interestingly, among *in silico* targets predicted to contain T cell epitopes, there are 3 sca (surface cell antigens) proteins. *Sca* comprises a family of genes encoding putative outer membrane proteins; although many genes in the *sca* family are split, fragmented, or absent in many rickettsial species: *OmpA* (*sca0*), *OmpB* (*sca5*), *sca1*, *sca2*, and *sca4*, are present in the genomes of most rickettsiae [216]. Furthermore, the predicted proteins encoded by *ompA*, *sca1, sca2* and *ompB* share homology with autotransporters, a family of proteins in Gram-negative bacteria known for including virulence factors [217, 218]. The three sca proteins predicted as potential T cell antigens are RP498 (sca 4), RP451 (sca3), and RP704 (OmpB, sca5); the latter is known for mediating *Rickettsia* entry to

target cells and for being an immunodominant antigen for the humoral response that also contains T cell epitopes. Thus far, only RP498, the smallest of the three, has been tested and found non protective using the current screening platform; the remaining two, RP451 and RP704, are large proteins that have not been tested yet due to difficulties for cloning, transfecting and expressing them on SVEC4-10 cells; this is not unexpected since these proteins are predicted to contain several transmembrane domains, a parameter which now is used as an exclusion criteria for *in silico* approaches defining vaccine targets based on subcellular localization [219]. Despite these difficulties, the interest in testing these vaccine targets, especially RP704, persists in our laboratory; thus, future attempts will divide these proteins into overlapping fragments or domains for successful cloning and expression.

The general approach presented here might have a broader application, beyond the *Rickettsia* field, for the rational discovery of T cell protective antigens and for the assessment of the immune response and identification of markers that could serve as correlates/surrogates of T-cell immunity in other infections for which TCR-transgenic tools and/or tetramers are not yet available. Future experiments will seek to further characterize the five novel rickettsial vaccine targets identified here in order to generate tools such as MHC tetramers for tracking antigen-specific protective responses, and to identify protective epitopes relevant to humans that may be introduced in a future safe and effective universal T-cell-based anti-*Rickettsia* vaccine.

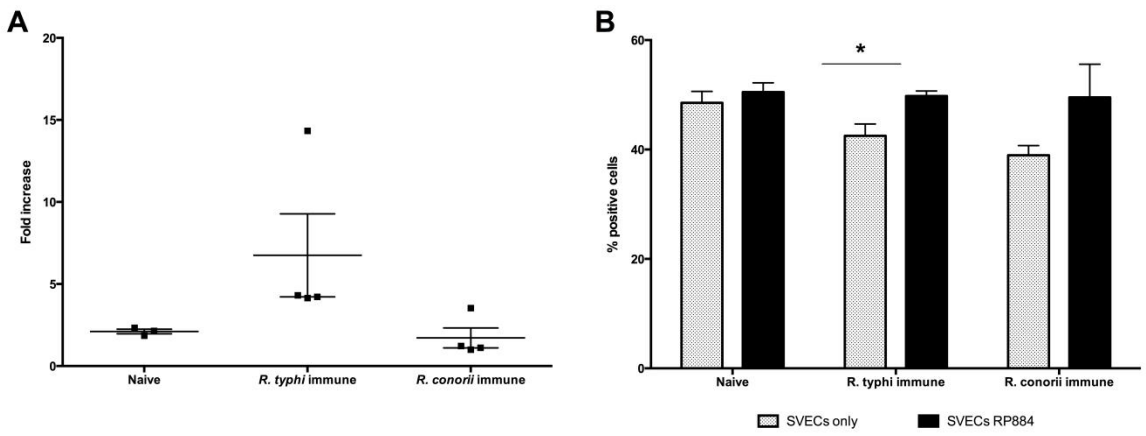

Figure 5.1 RP884 recall response: preliminary results. *R. typhi* immune mice were boosted with APCs expressing RP884 (1.5×10^6 cells i.p and 0.45×10^6 cells i.m) or with an irrelevant protein (luciferase). Splenocytes were obtained 72 hours after boost and mononuclear cells were obtained by gradient centrifugation. Mononuclear cells from boosted mice were incubated overnight with APCs expressing RP884 at a 10:1 ratio. Recovered cell were stained and processed for flow cytometric analysis. Naïve mice receiving the same treatment were used as controls. (A) Fold change of IFN-γ expression gated on $CD8^{low}CD11a^{high}CD44^{high}$ antigen experienced cells. (B) Frequency of MPECs, gated on $CD8^{+}CD44^{high}$ antigen experienced cells. Data in (A) was calculated as the ratio between mice boosted with RP884 and those that received the control protein; results are presented as individual data points and mean ±SEM (C). Data in (B) is presented as mean ± SEM from four mice per group. p values for comparisons against control protein are represented as follows: *$p<0.05$.

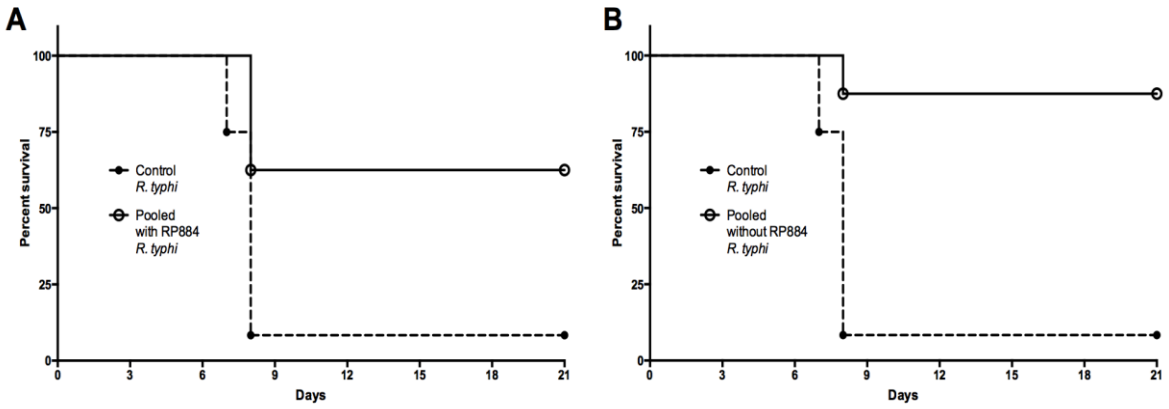

Figure 5.2 Protective rickettsial antigens pool comparison. APCs lines individually expressing selected *R. prowazekii* open reading frames (ORFs) were combined in 2 pools as follows: (A) RP884, RP778, RP739, RP598, RP403, and (B) RP778, RP739, RP598, RP403. Mice were immunized with pooled rickettsial proteins (n=8) or with APCs expressing luciferase (control, n=8) challenged with 5 × LD_{50} of *R. typhi* and followed for 21 days to determine survival. (A) p=0.0090 and (B) p=0.0008

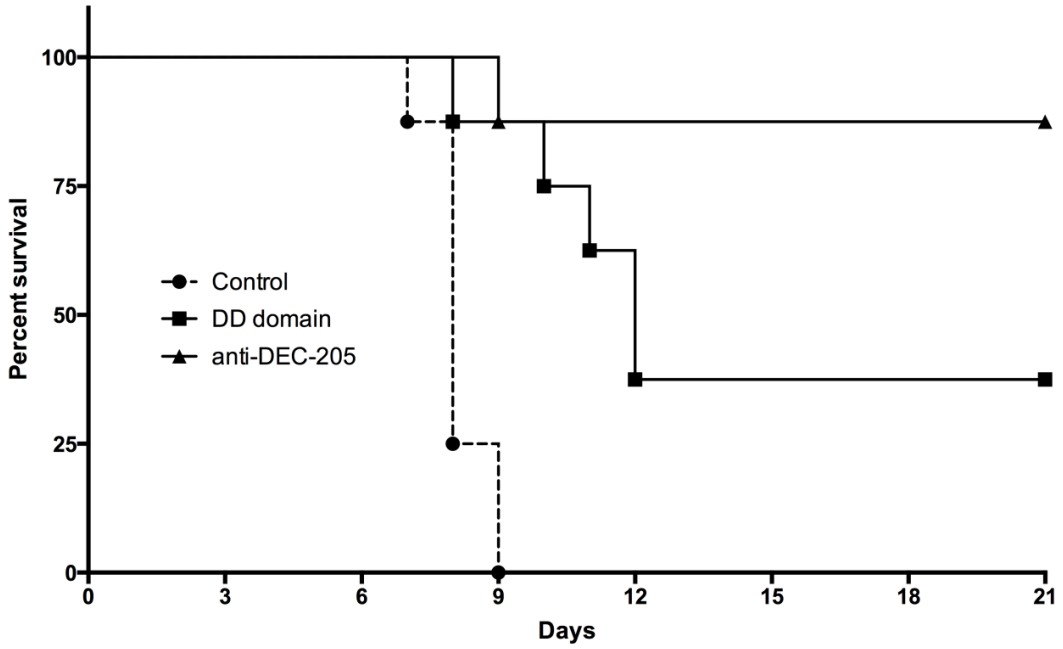

Figure 5.3 Vector comparison. Mice were immunized with APCs expressing RP884 in two different vectors (n=8): one targeting the proteasome via fusion of the rickettsial protein to the DD domain and other targeting DEC-205 via fusion of the rickettsial protein to anti-DEC-205 antibodies. APCs expressing luciferase were used as control. DD domain vector p=0.0005 and anti-DEC-205 vector p=0.0002.

APPENDIX

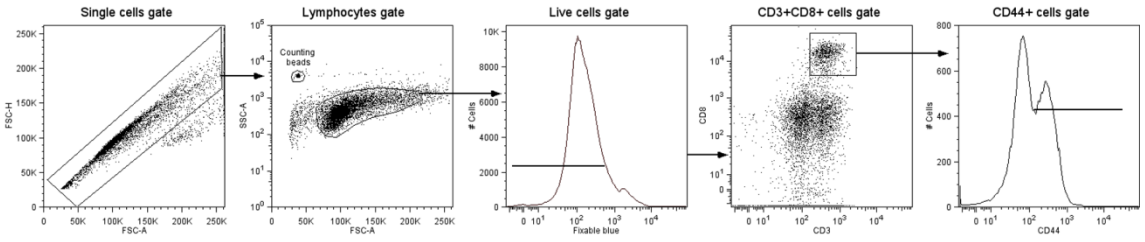

Figure A1 Representative gating strategy to identify and analyze antigen experienced $CD8^+$ T cells ($CD3^+CD8^+CD44^{high}$).

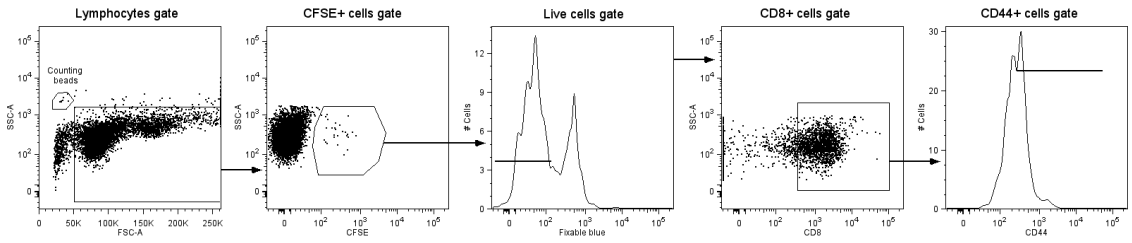

Figure A2 Representative gating for analyzing $CFSE^{+}$ cells after adoptive transfer.

REFERENCES

[1] X. Yu and D. H. Walker, “Family l. Rickettsiaceae,” in *Bergey’s Manual of Systematic Bacteriology*, 2nd ed., D. Brenner, N. Kreig, and J. Staley, Eds. New York: Springer Science+Business Media, Inc., 2005, pp. 96–116.

[2] J. J. Gillespie, M. S. Beier, M. S. Rahman, N. C. Ammerman, J. M. Shallom, A. Purkayastha, B. S. Sobral, and A. F. Azad, “Plasmids and rickettsial evolution: insight from Rickettsia felis.,” *PLoS One*, vol. 2, no. 3, p. e266, Jan. 2007.

[3] D. H. Walker and N. Ismail, “Emerging and re-emerging rickettsioses: endothelial cell infection and early disease events.,” *Nat. Rev. Microbiol.*, vol. 6, no. 5, pp. 375–86, May 2008.

[4] G. B. Schoeler, C. Morón, A. Richards, P. J. Blair, and J. G. Olson, “Human spotted fever rickettsial infections.,” *Emerg. Infect. Dis.*, vol. 11, no. 4, pp. 622–4, Apr. 2005.

[5] A. F. Azad, *Relationship of vector biology and epidemiology of louse- and flea-borne rickettsioses*. Boca Raton: CRC Press, 1988, pp. 51–62.

[6] D. H. Walker, “The realities of biodefense vaccines against Rickettsia.,” *Vaccine*, vol. 27 Suppl 4, pp. D52–5, Nov. 2009.

[7] A. F. Azad, “Pathogenic rickettsiae as bioterrorism agents.,” *Clin. Infect. Dis.*, vol. 45 Suppl 1, pp. S52–5, Jul. 2007.

[8] H. Zinsser and M. Castaneda, “On the isolation from a case of Brill’s disease of a typhus strain resembling the European type,” *N. Engl. J. Med*, vol. 209, pp. 815–819, 1933.

[9] H. Ogata, S. Audic, P. Renesto-Audiffren, P. E. Fournier, V. Barbe, D. Samson, V. Roux, P. Cossart, J. Weissenbach, J. M. Claverie, and D. Raoult, “Mechanisms of evolution in Rickettsia conorii and R. prowazekii.,” *Science*, vol. 293, no. 5537, pp. 2093–8, Sep. 2001.

[10] M. P. McLeod, X. Qin, S. E. Karpathy, J. Gioia, S. K. Highlander, G. E. Fox, T. Z. McNeill, H. Jiang, D. Muzny, L. S. Jacob, A. C. Hawes, E. Sodergren, R. Gill, J. Hume, M. Morgan, G. Fan, A. G. Amin, R. A. Gibbs, C. Hong, X.-J. Yu, D. H. Walker, and G. M. Weinstock, “Complete genome sequence of Rickettsia typhi and comparison with sequences of other rickettsiae.,” *J. Bacteriol.*, vol. 186, no. 17, pp. 5842–55, Sep. 2004.

[11] P. Renesto, H. Ogata, S. Audic, J.-M. Claverie, and D. Raoult, “Some lessons from Rickettsia genomics.,” *FEMS Microbiol. Rev.*, vol. 29, no. 1, pp. 99–117, Jan. 2005.

[12] S. G. Andersson and C. G. Kurland, “Reductive evolution of resident genomes.,” *Trends Microbiol.*, vol. 6, no. 7, pp. 263–8, Jul. 1998.

[13] D. E. Sonenshine, F. M. Bozeman, M. S. Williams, S. A. Masiello, D. P. Chadwick, N. I. Stocks, D. M. Lauer, and B. L. Elisberg, “Epizootiology of epidemic typhus (Rickettsia

prowazekii) in flying squirrels.," *Am. J. Trop. Med. Hyg.*, vol. 27, no. 2 Pt 1, pp. 339–49, Mar. 1978.

[14] D. H. Walker, G. A. Valbuena, and J. P. Olano, "Pathogenic mechanisms of diseases caused by Rickettsia.," *Ann. N. Y. Acad. Sci.*, vol. 990, pp. 1–11, Jun. 2003.

[15] J. J. Martinez, S. Seveau, E. Veiga, S. Matsuyama, and P. Cossart, "Ku70, a component of DNA-dependent protein kinase, is a mammalian receptor for Rickettsia conorii.," *Cell*, vol. 123, no. 6, pp. 1013–23, Dec. 2005.

[16] J. J. Martinez and P. Cossart, "Early signaling events involved in the entry of Rickettsia conorii into mammalian cells.," *J. Cell Sci.*, vol. 117, no. Pt 21, pp. 5097–106, Oct. 2004.

[17] Y. G. Y. Chan, M. M. Cardwell, T. M. Hermanas, T. Uchiyama, and J. J. Martinez, "Rickettsial outer-membrane protein B (rOmpB) mediates bacterial invasion through Ku70 in an actin, c-Cbl, clathrin and caveolin 2-dependent manner.," *Cell. Microbiol.*, vol. 11, no. 4, pp. 629–44, Apr. 2009.

[18] M. M. Cardwell and J. J. Martinez, "The Sca2 autotransporter protein from Rickettsia conorii is sufficient to mediate adherence to and invasion of cultured mammalian cells.," *Infect. Immun.*, vol. 77, no. 12, pp. 5272–80, Dec. 2009.

[19] M. Vellaiswamy, M. Kowalczewska, V. Merhej, C. Nappez, R. Vincentelli, P. Renesto, and D. Raoult, "Characterization of rickettsial adhesin Adr2 belonging to a new group of adhesins in α-proteobacteria.," *Microb. Pathog.*, vol. 50, no. 5, pp. 233–42, May 2011.

[20] T. Whitworth, V. L. Popov, X.-J. Yu, D. H. Walker, and D. H. Bouyer, "Expression of the Rickettsia prowazekii pld or tlyC gene in Salmonella enterica serovar Typhimurium mediates phagosomal escape.," *Infect. Immun.*, vol. 73, no. 10, pp. 6668–73, Oct. 2005.

[21] H.-M. Feng, T. Whitworth, V. Popov, and D. H. Walker, "Effect of antibody on the rickettsia-host cell interaction.," *Infect. Immun.*, vol. 72, no. 6, pp. 3524–30, Jun. 2004.

[22] H. Li and D. H. Walker, "rOmpA is a critical protein for the adhesion of Rickettsia rickettsii to host cells.," *Microb. Pathog.*, vol. 24, no. 5, pp. 289–98, May 1998.

[23] C. L. Wisseman, A. D. Waddell, and D. J. Silverman, "In vitro studies on Rickettsia-host cell interactions: lag phase in intracellular growth cycle as a function of stage of growth of infecting Rickettsia prowazeki, with preliminary observations on inhibition of rickettsial uptake by host cell fragments.," *Infect. Immun.*, vol. 13, no. 6, pp. 1749–60, Jun. 1976.

[24] C. L. Wisseman, E. A. Edlinger, A. D. Waddell, and M. R. Jones, "Infection cycle of Rickettsia rickettsii in chicken embryo and L-929 cells in culture.," *Infect. Immun.*, vol. 14, no. 4, pp. 1052–64, Oct. 1976.

[25] R. A. Heinzen, S. F. Hayes, M. G. Peacock, and T. Hackstadt, "Directional actin polymerization associated with spotted fever group Rickettsia infection of Vero cells.," *Infect. Immun.*, vol. 61, no. 5, pp. 1926–35, May 1993.

[26] D. H. Walker, “Pathology and pathogenesis of the vasculotropic rickettsioses,” in *Biology of rickettsial diseases*, D. H. Walker, Ed. Boca Raton: CRC Press, 1988, pp. 115–37.

[27] D. R. Clifton, E. Rydkina, R. S. Freeman, and S. K. Sahni, “NF-kappaB activation during Rickettsia rickettsii infection of endothelial cells involves the activation of catalytic IkappaB kinases IKKalpha and IKKbeta and phosphorylation-proteolysis of the inhibitor protein IkappaBalpha.,” *Infect. Immun.*, vol. 73, no. 1, pp. 155–65, Jan. 2005.

[28] D. R. Clifton, R. A. Goss, S. K. Sahni, D. van Antwerp, R. B. Baggs, V. J. Marder, D. J. Silverman, and L. A. Sporn, “NF-kappa B-dependent inhibition of apoptosis is essential for host cellsurvival during Rickettsia rickettsii infection.,” *Proc. Natl. Acad. Sci. U. S. A.*, vol. 95, no. 8, pp. 4646–51, Apr. 1998.

[29] M. Jensenius, T. Ueland, P.-E. Fournier, F. Brosstad, E. Stylianou, S. Vene, B. Myrvang, D. Raoult, and P. Aukrust, “Systemic inflammatory responses in African tick-bite fever.,” *J. Infect. Dis.*, vol. 187, no. 8, pp. 1332–6, Apr. 2003.

[30] M. T. Elghetany and D. H. Walker, “Hemostatic changes in Rocky Mountain spotted fever and Mediterranean spotted fever.,” *Am. J. Clin. Pathol.*, vol. 112, no. 2, pp. 159–68, Aug. 1999.

[31] G. Valbuena, W. Bradford, and D. H. Walker, “Expression analysis of the T-cell-targeting chemokines CXCL9 and CXCL10 in mice and humans with endothelial infections caused by rickettsiae of the spotted fever group.,” *Am. J. Pathol.*, vol. 163, no. 4, pp. 1357–69, Oct. 2003.

[32] L. A. Sporn, S. O. Lawrence, D. J. Silverman, and V. J. Marder, “E-selectin-dependent neutrophil adhesion to Rickettsia rickettsii-infected endothelial cells.,” *Blood*, vol. 81, no. 9, pp. 2406–12, May 1993.

[33] F. Dignat-George, N. Teysseire, M. Mutin, N. Bardin, G. Lesaule, D. Raoult, and J. Sampol, “Rickettsia conorii infection enhances vascular cell adhesion molecule-1- and intercellular adhesion molecule-1-dependent mononuclear cell adherence to endothelial cells.,” *J. Infect. Dis.*, vol. 175, no. 5, pp. 1142–52, May 1997.

[34] J. K. Damås, G. Davì, M. Jensenius, F. Santilli, K. Otterdal, T. Ueland, T. H. Flo, E. Lien, T. Espevik, S. S. Frøland, G. Vitale, D. Raoult, and P. Aukrust, “Relative chemokine and adhesion molecule expression in Mediterranean spotted fever and African tick bite fever.,” *J. Infect.*, vol. 58, no. 1, pp. 68–75, Jan. 2009.

[35] D. H. Walker, V. L. Popov, and H. M. Feng, “Establishment of a novel endothelial target mouse model of a typhus group rickettsiosis: evidence for critical roles for gamma interferon and CD8 T lymphocytes.,” *Lab. Invest.*, vol. 80, no. 9, pp. 1361–72, Sep. 2000.

[36] D. H. Walker, V. L. Popov, J. Wen, and H. M. Feng, “Rickettsia conorii infection of C3H/HeN mice. A model of endothelial-target rickettsiosis.,” *Lab. Invest.*, vol. 70, no. 3, pp. 358–68, Mar. 1994.

[37] D. H. Walker, J. P. Olano, and H. M. Feng, “Critical role of cytotoxic T lymphocytes in immune clearance of rickettsial infection.,” *Infect. Immun.*, vol. 69, no. 3, pp. 1841–6, Mar. 2001.

[38] H. Feng, V. L. Popov, G. Yuoh, and D. H. Walker, “Role of T lymphocyte subsets in immunity to spotted fever group Rickettsiae.,” *J. Immunol.*, vol. 158, no. 11, pp. 5314–20, Jun. 1997.

[39] H.-M. Feng, T. Whitworth, J. P. Olano, V. L. Popov, and D. H. Walker, “Fc-dependent polyclonal antibodies and antibodies to outer membrane proteins A and B, but not to lipopolysaccharide, protect SCID mice against fatal Rickettsia conorii infection.,” *Infect. Immun.*, vol. 72, no. 4, pp. 2222–8, Apr. 2004.

[40] H. Feng and D. H. Walker, “Cross-protection between distantly related spotted fever group rickettsiae.,” *Vaccine*, vol. 21, no. 25–26, pp. 3901–5, Sep. 2003.

[41] H. M. Feng, V. L. Popov, and D. H. Walker, “Depletion of gamma interferon and tumor necrosis factor alpha in mice with Rickettsia conorii-infected endothelium: impairment of rickettsicidal nitric oxide production resulting in fatal, overwhelming rickettsial disease.,” *Infect. Immun.*, vol. 62, no. 5, pp. 1952–60, May 1994.

[42] R. Fang, N. Ismail, L. Soong, V. L. Popov, T. Whitworth, D. H. Bouyer, and D. H. Walker, “Differential interaction of dendritic cells with Rickettsia conorii: impact on host susceptibility to murine spotted fever rickettsiosis.,” *Infect. Immun.*, vol. 75, no. 6, pp. 3112–23, Jun. 2007.

[43] J. M. Jordan, M. E. Woods, H.-M. Feng, L. Soong, and D. H. Walker, “Rickettsiae-stimulated dendritic cells mediate protection against lethal rickettsial challenge in an animal model of spotted fever rickettsiosis.,” *J. Infect. Dis.*, vol. 196, no. 4, pp. 629–38, Aug. 2007.

[44] G. Valbuena, J. M. Jordan, and D. H. Walker, “T cells mediate cross-protective immunity between spotted fever group rickettsiae and typhus group rickettsiae.,” *J. Infect. Dis.*, vol. 190, no. 7, pp. 1221–7, Oct. 2004.

[45] J. S. Dumler and D. H. Walker, “Rocky Mountain spotted fever--changing ecology and persisting virulence.,” *N. Engl. J. Med.*, vol. 353, no. 6, pp. 551–3, Aug. 2005.

[46] Y. Bechah, C. Capo, J.-L. Mege, and D. Raoult, “Epidemic typhus.,” *Lancet Infect. Dis.*, vol. 8, no. 7, pp. 417–26, Jul. 2008.

[47] P. Parola, C. D. Paddock, and D. Raoult, “Tick-borne rickettsioses around the world: emerging diseases challenging old concepts.,” *Clin. Microbiol. Rev.*, vol. 18, no. 4, pp. 719–56, Oct. 2005.

[48] J. A. Oteo and A. Portillo, “Tick-borne rickettsioses in Europe.,” *Ticks Tick. Borne. Dis.*, vol. 3, no. 5–6, pp. 271–8, Dec. 2012.

[49] J. J. Openshaw, D. L. Swerdlow, J. W. Krebs, R. C. Holman, E. Mandel, A. Harvey, D. Haberling, R. F. Massung, and J. H. McQuiston, "Rocky mountain spotted fever in the United States, 2000-2007: interpreting contemporary increases in incidence.," *Am. J. Trop. Med. Hyg.*, vol. 83, no. 1, pp. 174–82, Jul. 2010.

[50] C. M. Ripoll, C. E. Remondegui, G. Ordonez, R. Arazamendi, H. Fusaro, M. J. Hyman, C. D. Paddock, S. R. Zaki, J. G. Olson, and C. A. Santos-Buch, "Evidence of rickettsial spotted fever and ehrlichial infections in a subtropical territory of Jujuy, Argentina.," *Am. J. Trop. Med. Hyg.*, vol. 61, no. 2, pp. 350–4, Aug. 1999.

[51] E. R. de Lemos, F. B. Alvarenga, M. L. Cintra, M. C. Ramos, C. D. Paddock, T. L. Ferebee, S. R. Zaki, F. C. Ferreira, R. C. Ravagnani, R. D. Machado, M. A. Guimarães, and J. R. Coura, "Spotted fever in Brazil: a seroepidemiological study and description of clinical cases in an endemic area in the state of São Paulo.," *Am. J. Trop. Med. Hyg.*, vol. 65, no. 4, pp. 329–34, Oct. 2001.

[52] M. A. M. Galvâo, J. S. Dumler, C. L. Mafra, S. B. Calic, C. B. Chamone, G. Cesarino Filho, J. P. Olano, and D. H. Walker, "Fatal spotted fever rickettsiosis, Minas Gerais, Brazil.," *Emerg. Infect. Dis.*, vol. 9, no. 11, pp. 1402–5, Nov. 2003.

[53] J. E. Zavala-Castro, J. E. Zavala-Velázquez, D. H. Walker, E. E. Ruiz Arcila, H. Laviada-Molina, J. P. Olano, J. A. Ruiz-Sosa, M. A. Small, and K. R. Dzul-Rosado, "Fatal human infection with Rickettsia rickettsii, Yucatán, Mexico.," *Emerg. Infect. Dis.*, vol. 12, no. 4, pp. 672–4, Apr. 2006.

[54] J. E. Zavala-Velazquez, X. J. Yu, and D. H. Walker, "Unrecognized spotted fever group rickettsiosis masquerading as dengue fever in Mexico.," *Am. J. Trop. Med. Hyg.*, vol. 55, no. 2, pp. 157–9, Aug. 1996.

[55] M. Hidalgo, R. Sánchez, L. Orejuela, J. Hernández, D. H. Walker, and G. Valbuena, "Prevalence of antibodies against spotted fever group rickettsiae in a rural area of Colombia.," *Am. J. Trop. Med. Hyg.*, vol. 77, no. 2, pp. 378–80, Aug. 2007.

[56] M. Hidalgo, L. Orejuela, P. Fuya, P. Carrillo, J. Hernandez, E. Parra, C. Keng, M. Small, J. P. Olano, D. Bouyer, E. Castaneda, D. Walker, and G. Valbuena, "Rocky Mountain spotted fever, Colombia.," *Emerg. Infect. Dis.*, vol. 13, no. 7, pp. 1058–60, Jul. 2007.

[57] E. C. de RODANICHE and A. RODANICHE, "Spotted fever in Panama; isolation of the etiologic agent from a fatal case.," *Am. J. Trop. Med. Hyg.*, vol. 30, no. 4, pp. 511–7, Jul. 1950.

[58] J. McKiel, "The rodent and avian-borne diseases in Canada," *Can. J. Public Heal.*, vol. 51, pp. 220–225, 1950.

[59] L. Fuentes, "Primer caso de fiebre de las Montanas Rocosas en Costa Rica, America Central," *Rev. Latinoam. Microbiol*, vol. 21, pp. 167–172, 1979.

[60] V. Punda-Polić, Z. Klismanić, and V. Capkun, "Prevalence of antibodies to spotted fever group rickettsiae in the region of Split (southern Croatia).," *Eur. J. Epidemiol.*, vol. 18, no. 5, pp. 451–5, Jan. 2003.

[61] C. D. Paddock, J. W. Sumner, J. A. Comer, S. R. Zaki, C. S. Goldsmith, J. Goddard, S. L. F. McLellan, C. L. Tamminga, and C. A. Ohl, "Rickettsia parkeri: a newly recognized cause of spotted fever rickettsiosis in the United States.," *Clin. Infect. Dis.*, vol. 38, no. 6, pp. 805–11, Mar. 2004.

[62] C. D. Paddock, P. W. Greer, T. L. Ferebee, J. Singleton, D. B. McKechnie, T. A. Treadwell, J. W. Krebs, M. J. Clarke, R. C. Holman, J. G. Olson, J. E. Childs, and S. R. Zaki, "Hidden mortality attributable to Rocky Mountain spotted fever: immunohistochemical detection of fatal, serologically unconfirmed disease.," *J. Infect. Dis.*, vol. 179, no. 6, pp. 1469–76, Jun. 1999.

[63] T. E. Woodward, "Rickettsial vaccines with emphasis on epidemic typhus. Initial report of an old vaccine trial.," *S. Afr. Med. J.*, vol. Suppl, pp. 73–6, Oct. 1986.

[64] R. A. Mason, R. P. Wenzel, E. B. Seligmann, and R. K. Ginn, "A reference, inactivated, epidemic typhus vaccine: clinical trials in man.," *J. Biol. Stand.*, vol. 4, no. 3, pp. 217–24, Jan. 1976.

[65] N. M. Balayeva and V. N. Nikolskaya, "Analysis of lung culture of Rickettsia prowazekii E strain with regard to its capacity of increasing virulence in passages on the lungs of white mice.," *J. Hyg. Epidemiol. Microbiol. Immunol.*, vol. 17, no. 3, pp. 294–303, Mar. 1973.

[66] R. Spencer and R. Parker, "Rocky Mountain spotted fever: vaccination of monkeys and man," *Public Heal. Rep*, vol. 40, pp. 2159–67, 1925.

[67] H. L. DuPont, R. B. Hornick, A. T. Dawkins, G. G. Heiner, I. B. Fabrikant, C. L. Wisseman, and T. E. Woodward, "Rocky Mountain spotted fever: a comparative study of the active immunity induced by inactivated and viable pathogenic Rickettsia rickettsii.," *J. Infect. Dis.*, vol. 128, no. 3, pp. 340–4, Sep. 1973.

[68] R. H. Kenyon, L. S. Sammons, and C. E. Pedersen, "Comparison of three rocky mountain spotted fever vaccines.," *J. Clin. Microbiol.*, vol. 2, no. 4, pp. 300–4, Oct. 1975.

[69] M. L. Clements, C. L. Wisseman, T. E. Woodward, P. Fiset, J. S. Dumler, W. McNamee, R. E. Black, J. Rooney, T. P. Hughes, and M. M. Levine, "Reactogenicity, immunogenicity, and efficacy of a chick embryo cell-derived vaccine for Rocky Mountain spotted fever.," *J. Infect. Dis.*, vol. 148, no. 5, pp. 922–30, Nov. 1983.

[70] R. L. Anacker, R. H. List, R. E. Mann, S. F. Hayes, and L. A. Thomas, "Characterization of monoclonal antibodies protecting mice against Rickettsia rickettsii.," *J. Infect. Dis.*, vol. 151, no. 6, pp. 1052–60, Jun. 1985.

[71] R. A. Mason, E. Seligmann, and R. Ginn, "A reference, inactivated, epidemic typhus vaccine: laboratory evaluation of candidate vaccines," *J. Biol. Stand.*, vol. 4, pp. 209–216, 1976.

[72] M. Carl, S. Vaidya, F. M. Robbins, W. M. Ching, R. J. Hartzman, and G. A. Dasch, "Heterogeneity of CD4-positive human T-cell clones which recognize the surface protein antigen of Rickettsia typhi.," *Infect. Immun.*, vol. 57, no. 4, pp. 1276–80, Apr. 1989.

[73] J. W. Sumner, K. G. Sims, D. C. Jones, and B. E. Anderson, “Protection of guinea-pigs from experimental Rocky Mountain spotted fever by immunization with baculovirus-expressed Rickettsia rickettsii rOmpA protein.,” *Vaccine*, vol. 13, no. 1, pp. 29–35, Jan. 1995.

[74] P. A. Crocquet-Valdes, C. M. Díaz-Montero, H. M. Feng, H. Li, A. D. Barrett, and D. H. Walker, “Immunization with a portion of rickettsial outer membrane protein A stimulates protective immunity against spotted fever rickettsiosis.,” *Vaccine*, vol. 20, no. 5–6, pp. 979–88, Dec. 2001.

[75] A. Churilla, W. M. Ching, G. A. Dasch, and M. Carl, “Human T lymphocyte recognition of cyanogen bromide fragments of the surface protein of Rickettsia typhi.,” *Ann. N. Y. Acad. Sci.*, vol. 590, pp. 215–20, Jan. 1990.

[76] Z. Li, C. M. Díaz-Montero, G. Valbuena, X.-J. Yu, J. P. Olano, H.-M. Feng, and D. H. Walker, “Identification of CD8 T-lymphocyte epitopes in OmpB of Rickettsia conorii.,” *Infect. Immun.*, vol. 71, no. 7, pp. 3920–6, Jul. 2003.

[77] Y. G.-Y. Chan, S. P. Riley, E. Chen, and J. J. Martinez, “Molecular basis of immunity to rickettsial infection conferred through outer membrane protein B.,” *Infect. Immun.*, vol. 79, no. 6, pp. 2303–13, Jun. 2011.

[78] W. Pornwiroon, A. Bourchookarn, C. D. Paddock, and K. R. Macaluso, “Proteomic analysis of Rickettsia parkeri strain portsmouth.,” *Infect. Immun.*, vol. 77, no. 12, pp. 5262–71, Dec. 2009.

[79] Y. Qi, X. Xiong, C. Duan, J. Jiao, W. Gong, and B. Wen, “Recombinant protein YbgF induces protective immunity against Rickettsia heilongjiangensis infection in C3H/HeN mice.,” *Vaccine*, vol. 31, no. 48, pp. 5643–50, Nov. 2013.

[80] F. Zhou, J. Santoli, M. L. Messonnier, H. R. Yusuf, A. Shefer, S. Y. Chu, L. Rodewald, and R. Harpaz, “Economic evaluation of the 7-vaccine routine childhood immunization schedule in the United States, 2001.,” *Arch. Pediatr. Adolesc. Med.*, vol. 159, no. 12, pp. 1136–44, Dec. 2005.

[81] B. Pulendran and R. Ahmed, “Immunological mechanisms of vaccination.,” *Nat. Immunol.*, vol. 12, no. 6, pp. 509–17, Jun. 2011.

[82] M. N. Davies and D. R. Flower, “Harnessing bioinformatics to discover new vaccines.,” *Drug Discov. Today*, vol. 12, no. 9–10, pp. 389–95, May 2007.

[83] T. D. Jones, W. J. Phillips, B. J. Smith, C. A. Bamford, P. D. Nayee, T. P. Baglin, J. S. H. Gaston, and M. P. Baker, “Identification and removal of a promiscuous CD4+ T cell epitope from the C1 domain of factor VIII.,” *J. Thromb. Haemost.*, vol. 3, no. 5, pp. 991–1000, May 2005.

[84] R. Arens and S. P. Schoenberger, “Plasticity in programming of effector and memory CD8 T-cell formation.,” *Immunol. Rev.*, vol. 235, no. 1, pp. 190–205, May 2010.

[85] C.-A. Siegrist, “Vaccine immunology,” in *Vaccines*, 5th ed., S. Plotkin, W. Orenstein, and P. Offit, Eds. Philadelphia, PA: Saunders Elsevier, 2008, pp. 17–36.

[86] W. A. Hanekom, “The immune response to BCG vaccination of newborns.,” *Ann. N. Y. Acad. Sci.*, vol. 1062, pp. 69–78, Dec. 2005.

[87] J. E. McElhaney, D. Xie, W. D. Hager, M. B. Barry, Y. Wang, A. Kleppinger, C. Ewen, K. P. Kane, and R. C. Bleackley, “T cell responses are better correlates of vaccine protection in the elderly.,” *J. Immunol.*, vol. 176, no. 10, pp. 6333–9, May 2006.

[88] M. J. Levin, M. N. Oxman, J. H. Zhang, G. R. Johnson, H. Stanley, A. R. Hayward, M. J. Caulfield, M. R. Irwin, J. G. Smith, J. Clair, I. S. F. Chan, H. Williams, R. Harbecke, R. Marchese, S. E. Straus, A. Gershon, and A. Weinberg, “Varicella-zoster virus-specific immune responses in elderly recipients of a herpes zoster vaccine.,” *J. Infect. Dis.*, vol. 197, no. 6, pp. 825–35, Mar. 2008.

[89] A. M. Arvin, “Humoral and cellular immunity to varicella-zoster virus: an overview.,” *J. Infect. Dis.*, vol. 197 Suppl , pp. S58–60, Mar. 2008.

[90] F. Sallusto, A. Lanzavecchia, K. Araki, and R. Ahmed, “From vaccines to memory and back.,” *Immunity*, vol. 33, no. 4, pp. 451–63, Oct. 2010.

[91] D. F. Hoft, V. Brusic, and I. G. Sakala, “Optimizing vaccine development.,” *Cell. Microbiol.*, vol. 13, no. 7, pp. 934–42, Jul. 2011.

[92] H. Hikono, J. E. Kohlmeier, S. Takamura, S. T. Wittmer, A. D. Roberts, and D. L. Woodland, “Activation phenotype, rather than central- or effector-memory phenotype, predicts the recall efficacy of memory CD8+ T cells.,” *J. Exp. Med.*, vol. 204, no. 7, pp. 1625–36, Jul. 2007.

[93] S. Sarkar, V. Kalia, W. N. Haining, B. T. Konieczny, S. Subramaniam, and R. Ahmed, “Functional and genomic profiling of effector CD8 T cell subsets with distinct memory fates.,” *J. Exp. Med.*, vol. 205, no. 3, pp. 625–40, Mar. 2008.

[94] J. D. Ahlers and I. M. Belyakov, “Memories that last forever: strategies for optimizing vaccine T-cell memory.,” *Blood*, vol. 115, no. 9, pp. 1678–89, Mar. 2010.

[95] C. M. Smith, N. S. Wilson, J. Waithman, J. A. Villadangos, F. R. Carbone, W. R. Heath, and G. T. Belz, “Cognate CD4(+) T cell licensing of dendritic cells in CD8(+) T cell immunity.,” *Nat. Immunol.*, vol. 5, no. 11, pp. 1143–8, Nov. 2004.

[96] S. P. Schoenberger, R. E. Toes, E. I. van der Voort, R. Offringa, and C. J. Melief, “T-cell help for cytotoxic T lymphocytes is mediated by CD40-CD40L interactions.,” *Nature*, vol. 393, no. 6684, pp. 480–3, Jun. 1998.

[97] S. Johnson, Y. Zhan, R. M. Sutherland, A. M. Mount, S. Bedoui, J. L. Brady, E. M. Carrington, L. E. Brown, G. T. Belz, W. R. Heath, and A. M. Lew, “Selected Toll-like receptor ligands and viruses promote helper-independent cytotoxic T cell priming by upregulating CD40L on dendritic cells.,” *Immunity*, vol. 30, no. 2, pp. 218–27, Feb. 2009.

[98] V. Y. Taraban, T. F. Rowley, D. F. Tough, and A. Al-Shamkhani, “Requirement for CD70 in CD4+ Th cell-dependent and innate receptor-mediated CD8+ T cell priming.,” *J. Immunol.*, vol. 177, no. 5, pp. 2969–75, Sep. 2006.

[99] V. Y. Taraban, T. F. Rowley, and A. Al-Shamkhani, “Cutting edge: a critical role for CD70 in CD8 T cell priming by CD40-licensed APCs.,” *J. Immunol.*, vol. 173, no. 11, pp. 6542–6, Dec. 2004.

[100] F. Castellino, A. Y. Huang, G. Altan-Bonnet, S. Stoll, C. Scheinecker, and R. N. Germain, “Chemokines enhance immunity by guiding naive CD8+ T cells to sites of CD4+ T cell-dendritic cell interaction.,” *Nature*, vol. 440, no. 7086, pp. 890–5, Apr. 2006.

[101] Y. Nakanishi, B. Lu, C. Gerard, and A. Iwasaki, “CD8(+) T lymphocyte mobilization to virus-infected tissue requires CD4(+) T-cell help.,” *Nature*, vol. 462, no. 7272, pp. 510–3, Nov. 2009.

[102] C. Bourgeois, B. Rocha, and C. Tanchot, “A role for CD40 expression on CD8+ T cells in the generation of CD8+ T cell memory.,” *Science*, vol. 297, no. 5589, pp. 2060–3, Sep. 2002.

[103] A. K. Sewell, “Why must T cells be cross-reactive?,” *Nat. Rev. Immunol.*, vol. 12, no. 9, pp. 669–77, Sep. 2012.

[104] J. J. Obar and L. Lefrançois, “Early signals during CD8 T cell priming regulate the generation of central memory cells.,” *J. Immunol.*, vol. 185, no. 1, pp. 263–72, Jul. 2010.

[105] N.-L. L. Pham, V. P. Badovinac, and J. T. Harty, “A default pathway of memory CD8 T cell differentiation after dendritic cell immunization is deflected by encounter with inflammatory cytokines during antigen-driven proliferation.,” *J. Immunol.*, vol. 183, no. 4, pp. 2337–48, Aug. 2009.

[106] V. P. Badovinac, K. A. N. Messingham, A. Jabbari, J. S. Haring, and J. T. Harty, “Accelerated CD8+ T-cell memory and prime-boost response after dendritic-cell vaccination.,” *Nat. Med.*, vol. 11, no. 7, pp. 748–56, Jul. 2005.

[107] N.-L. L. Pham, L. L. Pewe, C. J. Fleenor, R. A. Langlois, K. L. Legge, V. P. Badovinac, and J. T. Harty, “Exploiting cross-priming to generate protective CD8 T-cell immunity rapidly.,” *Proc. Natl. Acad. Sci. U. S. A.*, vol. 107, no. 27, pp. 12198–203, Jul. 2010.

[108] C. Verheust, M. Goossens, K. Pauwels, and D. Breyer, “Biosafety aspects of modified vaccinia virus Ankara (MVA)-based vectors used for gene therapy or vaccination.,” *Vaccine*, vol. 30, no. 16, pp. 2623–32, Mar. 2012.

[109] S. A. Plotkin, “Correlates of protection induced by vaccination.,” *Clin. Vaccine Immunol.*, vol. 17, no. 7, pp. 1055–65, Jul. 2010.

[110] E. D. Williamson, M. G. Duchars, and R. Kohberger, “Predictive models and correlates of protection for testing biodefence vaccines.,” *Expert Rev. Vaccines*, vol. 9, no. 5, pp. 527–37, May 2010.

[111] V. Appay, D. C. Douek, and D. A. Price, "CD8+ T cell efficacy in vaccination and disease.," *Nat. Med.*, vol. 14, no. 6, pp. 623–8, Jun. 2008.

[112] B. Abel, M. Tameris, N. Mansoor, S. Gelderbloem, J. Hughes, D. Abrahams, L. Makhethe, M. Erasmus, M. de Kock, L. van der Merwe, A. Hawkridge, A. Veldsman, M. Hatherill, G. Schirru, M. G. Pau, J. Hendriks, G. J. Weverling, J. Goudsmit, D. Sizemore, J. B. McClain, M. Goetz, J. Gearhart, H. Mahomed, G. D. Hussey, J. C. Sadoff, and W. A. Hanekom, "The novel tuberculosis vaccine, AERAS-402, induces robust and polyfunctional CD4+ and CD8+ T cells in adults.," *Am. J. Respir. Crit. Care Med.*, vol. 181, no. 12, pp. 1407–17, Jun. 2010.

[113] P. A. Darrah, S. T. Hegde, D. T. Patel, R. W. B. Lindsay, L. Chen, M. Roederer, and R. A. Seder, "IL-10 production differentially influences the magnitude, quality, and protective capacity of Th1 responses depending on the vaccine platform.," *J. Exp. Med.*, vol. 207, no. 7, pp. 1421–33, Jul. 2010.

[114] P. A. Darrah, D. T. Patel, P. M. De Luca, R. W. B. Lindsay, D. F. Davey, B. J. Flynn, S. T. Hoff, P. Andersen, S. G. Reed, S. L. Morris, M. Roederer, and R. A. Seder, "Multifunctional TH1 cells define a correlate of vaccine-mediated protection against Leishmania major.," *Nat. Med.*, vol. 13, no. 7, pp. 843–50, Jul. 2007.

[115] S. N. Mueller, W. A. Langley, G. Li, A. García-Sastre, R. J. Webby, and R. Ahmed, "Qualitatively different memory CD8+ T cells are generated after lymphocytic choriomeningitis virus and influenza virus infections.," *J. Immunol.*, vol. 185, no. 4, pp. 2182–90, Aug. 2010.

[116] J. J. Obar, E. R. Jellison, B. S. Sheridan, D. A. Blair, Q.-M. Pham, J. M. Zickovich, and L. Lefrançois, "Pathogen-induced inflammatory environment controls effector and memory CD8+ T cell differentiation.," *J. Immunol.*, vol. 187, no. 10, pp. 4967–78, Nov. 2011.

[117] J. A. Olson, C. McDonald-Hyman, S. C. Jameson, and S. E. Hamilton, "Effector-like $CD8^+$ T cells in the memory population mediate potent protective immunity.," *Immunity*, vol. 38, no. 6, pp. 1250–60, Jun. 2013.

[118] N. S. Joshi, W. Cui, A. Chandele, H. K. Lee, D. R. Urso, J. Hagman, L. Gapin, and S. M. Kaech, "Inflammation directs memory precursor and short-lived effector CD8(+) T cell fates via the graded expression of T-bet transcription factor.," *Immunity*, vol. 27, no. 2, pp. 281–95, Aug. 2007.

[119] S. M. Kaech, J. T. Tan, E. J. Wherry, B. T. Konieczny, C. D. Surh, and R. Ahmed, "Selective expression of the interleukin 7 receptor identifies effector CD8 T cells that give rise to long-lived memory cells.," *Nat. Immunol.*, vol. 4, no. 12, pp. 1191–8, Dec. 2003.

[120] E. J. Wherry, V. Teichgräber, T. C. Becker, D. Masopust, S. M. Kaech, R. Antia, U. H. von Andrian, and R. Ahmed, "Lineage relationship and protective immunity of memory CD8 T cell subsets.," *Nat. Immunol.*, vol. 4, no. 3, pp. 225–34, Mar. 2003.

[121] M. F. Bachmann, P. Wolint, K. Schwarz, P. Jäger, and A. Oxenius, "Functional properties and lineage relationship of CD8+ T cell subsets identified by expression of IL-7 receptor alpha and CD62L.," *J. Immunol.*, vol. 175, no. 7, pp. 4686–96, Oct. 2005.

[122] A. Laouar, M. Manocha, V. Haridas, and N. Manjunath, “Concurrent generation of effector and central memory CD8 T cells during vaccinia virus infection.,” *PLoS One*, vol. 3, no. 12, p. e4089, Jan. 2008.

[123] R. S. Akondy, N. D. Monson, J. D. Miller, S. Edupuganti, D. Teuwen, H. Wu, F. Quyyumi, S. Garg, J. D. Altman, C. Del Rio, H. L. Keyserling, A. Ploss, C. M. Rice, W. A. Orenstein, M. J. Mulligan, and R. Ahmed, “The yellow fever virus vaccine induces a broad and polyfunctional human memory CD8+ T cell response.,” *J. Immunol.*, vol. 183, no. 12, pp. 7919–30, Dec. 2009.

[124] M. Prlic, J. A. Sacks, and M. J. Bevan, “Dissociating markers of senescence and protective ability in memory T cells.,” *PLoS One*, vol. 7, no. 3, p. e32576, Jan. 2012.

[125] D. Grubaugh, J. B. Flechtner, and D. E. Higgins, “Proteins as T cell antigens: methods for high-throughput identification.,” *Vaccine*, vol. 31, no. 37, pp. 3805–10, Aug. 2013.

[126] A. S. De Groot, J. McMurry, and L. Moise, “Prediction of immunogenicity: in silico paradigms, ex vivo and in vivo correlates.,” *Curr. Opin. Pharmacol.*, vol. 8, no. 5, pp. 620–6, Oct. 2008.

[127] M. Halling-Brown, R. Shaban, D. Frampton, C. E. Sansom, M. Davies, D. Flower, M. Duffield, R. W. Titball, V. Brusic, and D. S. Moss, “Proteins accessible to immune surveillance show significant T-cell epitope depletion: Implications for vaccine design.,” *Mol. Immunol.*, vol. 46, no. 13, pp. 2699–705, Aug. 2009.

[128] J. Tung and A. J. Sant, “Orchestration of CD4 T cell epitope preferences after multipeptide immunization.,” *J. Immunol.*, vol. 191, no. 2, pp. 764–72, Jul. 2013.

[129] J. M. Weaver, C. A. Lazarski, K. A. Richards, F. A. Chaves, S. A. Jenks, P. R. Menges, and A. J. Sant, “Immunodominance of CD4 T cells to foreign antigens is peptide intrinsic and independent of molecular context: implications for vaccine design.,” *J. Immunol.*, vol. 181, no. 5, pp. 3039–48, Sep. 2008.

[130] E.-J. Im, J. P. Hong, Y. Roshorm, A. Bridgeman, S. Létourneau, P. Liljeström, M. J. Potash, D. J. Volsky, A. J. McMichael, and T. Hanke, “Protective efficacy of serially up-ranked subdominant CD8+ T cell epitopes against virus challenges.,” *PLoS Pathog.*, vol. 7, no. 5, p. e1002041, May 2011.

[131] A. Gallimore, T. Dumrese, H. Hengartner, R. M. Zinkernagel, and H. G. Rammensee, “Protective immunity does not correlate with the hierarchy of virus-specific cytotoxic T cell responses to naturally processed peptides.,” *J. Exp. Med.*, vol. 187, no. 10, pp. 1647–57, May 1998.

[132] P. Riedl, A. Wieland, K. Lamberth, S. Buus, F. Lemonnier, K. Reifenberg, J. Reimann, and R. Schirmbeck, “Elimination of immunodominant epitopes from multispecific DNA-based vaccines allows induction of CD8 T cells that have a striking antiviral potential.,” *J. Immunol.*, vol. 183, no. 1, pp. 370–80, Jul. 2009.

[133] J. Liu, B. A. Ewald, D. M. Lynch, A. Nanda, S. M. Sumida, and D. H. Barouch, "Modulation of DNA vaccine-elicited CD8+ T-lymphocyte epitope immunodominance hierarchies.," *J. Virol.*, vol. 80, no. 24, pp. 11991–7, Dec. 2006.

[134] R. G. van der Most, R. J. Concepcion, C. Oseroff, J. Alexander, S. Southwood, J. Sidney, R. W. Chesnut, R. Ahmed, and A. Sette, "Uncovering subdominant cytotoxic T-lymphocyte responses in lymphocytic choriomeningitis virus-infected BALB/c mice.," *J. Virol.*, vol. 71, no. 7, pp. 5110–4, Jul. 1997.

[135] D. K. Kaushik and D. Sehgal, "Developing antibacterial vaccines in genomics and proteomics era.," *Scand. J. Immunol.*, vol. 67, no. 6, pp. 544–52, Jun. 2008.

[136] D. R. Flower, I. K. Macdonald, K. Ramakrishnan, M. N. Davies, and I. A. Doytchinova, "Computer aided selection of candidate vaccine antigens.," *Immunome Res.*, vol. 6 Suppl 2, p. S1, Jan. 2010.

[137] A. W. Purcell, J. McCluskey, and J. Rossjohn, "More than one reason to rethink the use of peptides in vaccine design.," *Nat. Rev. Drug Discov.*, vol. 6, no. 5, pp. 404–14, May 2007.

[138] A. Sette and R. Rappuoli, "Reverse vaccinology: developing vaccines in the era of genomics.," *Immunity*, vol. 33, no. 4, pp. 530–41, Oct. 2010.

[139] M. Halling-Brown, C. E. Sansom, M. Davies, R. W. Titball, and D. S. Moss, "Are bacterial vaccine antigens T-cell epitope depleted?," *Trends Immunol.*, vol. 29, no. 8, pp. 374–9, Aug. 2008.

[140] M. M. Giuliani, J. Adu-Bobie, M. Comanducci, B. Aricò, S. Savino, L. Santini, B. Brunelli, S. Bambini, A. Biolchi, B. Capecchi, E. Cartocci, L. Ciucchi, F. Di Marcello, F. Ferlicca, B. Galli, E. Luzzi, V. Masignani, D. Serruto, D. Veggi, M. Contorni, M. Morandi, A. Bartalesi, V. Cinotti, D. Mannucci, F. Titta, E. Ovidi, J. A. Welsch, D. Granoff, R. Rappuoli, and M. Pizza, "A universal vaccine for serogroup B meningococcus.," *Proc. Natl. Acad. Sci. U. S. A.*, vol. 103, no. 29, pp. 10834–9, Jul. 2006.

[141] T. M. Wizemann, J. H. Heinrichs, J. E. Adamou, A. L. Erwin, C. Kunsch, G. H. Choi, S. C. Barash, C. A. Rosen, H. R. Masure, E. Tuomanen, A. Gayle, Y. A. Brewah, W. Walsh, P. Barren, R. Lathigra, M. Hanson, S. Langermann, S. Johnson, and S. Koenig, "Use of a whole genome approach to identify vaccine molecules affording protection against Streptococcus pneumoniae infection.," *Infect. Immun.*, vol. 69, no. 3, pp. 1593–8, Mar. 2001.

[142] N. Ariel, A. Zvi, K. S. Makarova, T. Chitlaru, E. Elhanany, B. Velan, S. Cohen, A. M. Friedlander, and A. Shafferman, "Genome-based bioinformatic selection of chromosomal Bacillus anthracis putative vaccine candidates coupled with proteomic identification of surface-associated antigens.," *Infect. Immun.*, vol. 71, no. 8, pp. 4563–79, Aug. 2003.

[143] D. N. Chakravarti, M. J. Fiske, L. D. Fletcher, and R. J. Zagursky, "Application of genomics and proteomics for identification of bacterial gene products as potential vaccine candidates.," *Vaccine*, vol. 19, no. 6, pp. 601–12, Nov. 2000.

[144] B. C. Ross, L. Czajkowski, D. Hocking, M. Margetts, E. Webb, L. Rothel, M. Patterson, C. Agius, S. Camuglia, E. Reynolds, T. Littlejohn, B. Gaeta, A. Ng, E. S. Kuczek, J. S. Mattick, D. Gearing, and I. G. Barr, "Identification of vaccine candidate antigens from a genomic analysis of Porphyromonas gingivalis.," *Vaccine*, vol. 19, no. 30, pp. 4135–42, Jul. 2001.

[145] K. Al-Hasani, J. Boyce, V. P. McCarl, S. Bottomley, I. Wilkie, and B. Adler, "Identification of novel immunogens in Pasteurella multocida.," *Microb. Cell Fact.*, vol. 6, p. 3, Jan. 2007.

[146] S. Montigiani, F. Falugi, M. Scarselli, O. Finco, R. Petracca, G. Galli, M. Mariani, R. Manetti, M. Agnusdei, R. Cevenini, M. Donati, R. Nogarotto, N. Norais, I. Garaguso, S. Nuti, G. Saletti, D. Rosa, G. Ratti, and G. Grandi, "Genomic approach for analysis of surface proteins in Chlamydia pneumoniae.," *Infect. Immun.*, vol. 70, no. 1, pp. 368–79, Jan. 2002.

[147] D. Maione, I. Margarit, C. D. Rinaudo, V. Masignani, M. Mora, M. Scarselli, H. Tettelin, C. Brettoni, E. T. Iacobini, R. Rosini, N. D'Agostino, L. Miorin, S. Buccato, M. Mariani, G. Galli, R. Nogarotto, V. Nardi-Dei, V. Nardi Dei, F. Vegni, C. Fraser, G. Mancuso, G. Teti, L. C. Madoff, L. C. Paoletti, R. Rappuoli, D. L. Kasper, J. L. Telford, and G. Grandi, "Identification of a universal Group B streptococcus vaccine by multiple genome screen.," *Science*, vol. 309, no. 5731, pp. 148–50, Jul. 2005.

[148] C. Herrera-Najera, R. Piña-Aguilar, F. Xacur-Garcia, M. J. Ramirez-Sierra, and E. Dumonteil, "Mining the Leishmania genome for novel antigens and vaccine candidates.," *Proteomics*, vol. 9, no. 5, pp. 1293–301, Mar. 2009.

[149] S. Buus, "Description and prediction of peptide-MHC binding: the 'human MHC project'.," *Curr. Opin. Immunol.*, vol. 11, no. 2, pp. 209–13, Apr. 1999.

[150] A. S. De Groot, "Exploring the immunome: A brave new world for human vaccine development.," *Hum. Vaccin.*, vol. 5, no. 12, pp. 790–3, Dec. 2009.

[151] D. L. Doolan, J. C. Aguiar, W. R. Weiss, A. Sette, P. L. Felgner, D. P. Regis, P. Quinones-Casas, J. R. Yates, P. L. Blair, T. L. Richie, S. L. Hoffman, and D. J. Carucci, "Utilization of genomic sequence information to develop malaria vaccines.," *J. Exp. Biol.*, vol. 206, no. Pt 21, pp. 3789–802, Nov. 2003.

[152] S. L. Lauemøller, C. Kesmir, S. L. Corbet, A. Fomsgaard, A. Holm, M. H. Claesson, S. Brunak, and S. Buus, "Identifying cytotoxic T cell epitopes from genomic and proteomic information: 'The human MHC project.'.," *Rev. Immunogenet.*, vol. 2, no. 4, pp. 477–91, Jan. 2000.

[153] D. D. Chaplin, "1. Overview of the human immune response.," *J. Allergy Clin. Immunol.*, vol. 117, no. 2 Suppl Mini-Primer, pp. S430–5, Feb. 2006.

[154] D. R. Flower, "Towards in silico prediction of immunogenic epitopes.," *Trends Immunol.*, vol. 24, no. 12, pp. 667–74, Dec. 2003.

[155] C. Lundegaard, O. Lund, C. Kesmir, S. Brunak, and M. Nielsen, “Modeling the adaptive immune system: predictions and simulations.,” *Bioinformatics*, vol. 23, no. 24, pp. 3265–75, Dec. 2007.

[156] C. Delisi, J. Cornette, H. Margalit, K. Cease, J. Spouge, and J. A. Berzofsky, “The role of amphipathicity as an indicator of T cell antigenic sites on proteins,” in *mmunogenicity of Protein Antigens: Repertoire and Regulation*, E. Sercarz and J. A. Berzofsky, Eds. Boca Raton: CRC Press, 1987, pp. 35–42.

[157] J. C. Tong, T. W. Tan, and S. Ranganathan, “Methods and protocols for prediction of immunogenic epitopes.,” *Brief. Bioinform.*, vol. 8, no. 2, pp. 96–108, Mar. 2007.

[158] P. Oyarzún, J. J. Ellis, M. Bodén, and B. Kobe, “PREDIVAC: CD4+ T-cell epitope prediction for vaccine design that covers 95% of HLA class II DR protein diversity.,” *BMC Bioinformatics*, vol. 14, p. 52, Jan. 2013.

[159] F. A. Chaves, A. H. Lee, J. L. Nayak, K. A. Richards, and A. J. Sant, “The utility and limitations of current Web-available algorithms to predict peptides recognized by CD4 T cells in response to pathogen infection.,” *J. Immunol.*, vol. 188, no. 9, pp. 4235–48, May 2012.

[160] T. J. Yuen, I. E. A. Flesch, N. A. Hollett, B. M. Dobson, T. A. Russell, A. M. Fahrer, and D. C. Tscharke, “Analysis of A47, an immunoprevalent protein of vaccinia virus, leads to a reevaluation of the total antiviral CD8+ T cell response.,” *J. Virol.*, vol. 84, no. 19, pp. 10220–9, Oct. 2010.

[161] C. A. Weber, P. J. Mehta, M. Ardito, L. Moise, B. Martin, and A. S. De Groot, “T cell epitope: friend or foe? Immunogenicity of biologics in context.,” *Adv. Drug Deliv. Rev.*, vol. 61, no. 11, pp. 965–76, Sep. 2009.

[162] C. Donati and R. Rappuoli, “Reverse vaccinology in the 21st century: improvements over the original design.,” *Ann. N. Y. Acad. Sci.*, vol. 1285, pp. 115–32, May 2013.

[163] J. M. Calvo-Calle, I. Strug, M.-D. Nastke, S. P. Baker, and L. J. Stern, “Human CD4+ T cell epitopes from vaccinia virus induced by vaccination or infection.,” *PLoS Pathog.*, vol. 3, no. 10, pp. 1511–29, Oct. 2007.

[164] G. Sánchez-Burgos, J. Ramos-Castañeda, R. Cedillo-Rivera, and E. Dumonteil, “Immunogenicity of novel Dengue virus epitopes identified by bioinformatic analysis.,” *Virus Res.*, vol. 153, no. 1, pp. 113–20, Oct. 2010.

[165] D. L. Doolan, S. Southwood, D. A. Freilich, J. Sidney, N. L. Graber, L. Shatney, L. Bebris, L. Florens, C. Dobano, A. A. Witney, E. Appella, S. L. Hoffman, J. R. Yates, D. J. Carucci, and A. Sette, “Identification of Plasmodium falciparum antigens by antigenic analysis of genomic and proteomic data.,” *Proc. Natl. Acad. Sci. U. S. A.*, vol. 100, no. 17, pp. 9952–7, Aug. 2003.

[166] D. L. Bolton and M. Roederer, “Flow cytometry and the future of vaccine development.,” *Expert Rev. Vaccines*, vol. 8, no. 6, pp. 779–89, Jun. 2009.

[167] A. C. Hobeika, M. A. Morse, T. Osada, M. Ghanayem, D. Niedzwiecki, R. Barrier, H. K. Lyerly, and T. M. Clay, "Enumerating antigen-specific T-cell responses in peripheral blood: a comparison of peptide MHC Tetramer, ELISpot, and intracellular cytokine analysis.," *J. Immunother.*, vol. 28, no. 1, pp. 63–72.

[168] J. D. Altman, P. A. Moss, P. J. Goulder, D. H. Barouch, M. G. McHeyzer-Williams, J. I. Bell, A. J. McMichael, and M. M. Davis, "Phenotypic analysis of antigen-specific T lymphocytes.," *Science*, vol. 274, no. 5284, pp. 94–6, Oct. 1996.

[169] Y. Bechah, C. Capo, J.-L. Mege, and D. Raoult, "Epidemic typhus.," *Lancet Infect. Dis.*, vol. 8, no. 7, pp. 417–26, Jul. 2008.

[170] M. Moutaftsi, H.-H. Bui, B. Peters, J. Sidney, S. Salek-Ardakani, C. Oseroff, V. Pasquetto, S. Crotty, M. Croft, E. J. Lefkowitz, H. Grey, and A. Sette, "Vaccinia virus-specific CD4+ T cell responses target a set of antigens largely distinct from those targeted by CD8+ T cell responses.," *J. Immunol.*, vol. 178, no. 11, pp. 6814–20, Jun. 2007.

[171] M. Moutaftsi, D. C. Tscharke, K. Vaughan, D. M. Koelle, L. Stern, M. Calvo-Calle, F. Ennis, M. Terajima, G. Sutter, S. Crotty, I. Drexler, G. Franchini, J. W. Yewdell, S. R. Head, J. Blum, B. Peters, and A. Sette, "Uncovering the interplay between CD8, CD4 and antibody responses to complex pathogens.," *Future Microbiol.*, vol. 5, no. 2, pp. 221–39, Feb. 2010.

[172] K. Sykes, "Progress in the development of genetic immunization.," *Expert Rev. Vaccines*, vol. 7, no. 9, pp. 1395–404, Nov. 2008.

[173] K. Stemke-Hale, B. Kaltenboeck, F. J. DeGraves, K. F. Sykes, J. Huang, C. Bu, and S. A. Johnston, "Screening the whole genome of a pathogen in vivo for individual protective antigens.," *Vaccine*, vol. 23, no. 23, pp. 3016–25, Apr. 2005.

[174] M. Gazi, E. Caro-Gomez, Y. Goez, M. A. Cespedes, M. Hidalgo, P. Correa, and G. Valbuena, "Discovery of a protective Rickettsia prowazekii antigen recognized by CD8+ T cells, RP884, using an in vivo screening platform.," *PLoS One*, vol. 8, no. 10, p. e76253, Jan. 2013.

[175] D. H. Walker and B. G. Cain, "The rickettsial plaque. Evidence for direct cytopathic effect of Rickettsia rickettsii.," *Lab. Invest.*, vol. 43, no. 4, pp. 388–96, Oct. 1980.

[176] T. J. Ruckwardt, C. Luongo, A. M. W. Malloy, J. Liu, M. Chen, P. L. Collins, and B. S. Graham, "Responses against a subdominant CD8+ T cell epitope protect against immunopathology caused by a dominant epitope.," *J. Immunol.*, vol. 185, no. 8, pp. 4673–80, Oct. 2010.

[177] M. Nielsen, C. Lundegaard, P. Worning, S. L. Lauemøller, K. Lamberth, S. Buus, S. Brunak, and O. Lund, "Reliable prediction of T-cell epitopes using neural networks with novel sequence representations.," *Protein Sci.*, vol. 12, no. 5, pp. 1007–17, May 2003.

[178] M. Nielsen, C. Lundegaard, P. Worning, C. S. Hvid, K. Lamberth, S. Buus, S. Brunak, and O. Lund, "Improved prediction of MHC class I and class II epitopes using a novel Gibbs sampling approach.," *Bioinformatics*, vol. 20, no. 9, pp. 1388–97, Jun. 2004.

[179] H. H. Lin, S. Ray, S. Tongchusak, E. L. Reinherz, and V. Brusic, “Evaluation of MHC class I peptide binding prediction servers: applications for vaccine research.,” *BMC Immunol.*, vol. 9, p. 8, Jan. 2008.

[180] H. Rammensee, J. Bachmann, N. P. Emmerich, O. A. Bachor, and S. Stevanović, “SYFPEITHI: database for MHC ligands and peptide motifs.,” *Immunogenetics*, vol. 50, no. 3–4, pp. 213–9, Nov. 1999.

[181] P. A. Reche and E. L. Reinherz, “Prediction of peptide-MHC binding using profiles.,” *Methods Mol. Biol.*, vol. 409, pp. 185–200, Jan. 2007.

[182] N. Y. Yu, J. R. Wagner, M. R. Laird, G. Melli, S. Rey, R. Lo, P. Dao, S. C. Sahinalp, M. Ester, L. J. Foster, and F. S. L. Brinkman, “PSORTb 3.0: improved protein subcellular localization prediction with refined localization subcategories and predictive capabilities for all prokaryotes.,” *Bioinformatics*, vol. 26, no. 13, pp. 1608–15, Jul. 2010.

[183] L. A. Banaszynski, L.-C. Chen, L. A. Maynard-Smith, A. G. L. Ooi, and T. J. Wandless, “A rapid, reversible, and tunable method to regulate protein function in living cells using synthetic small molecules.,” *Cell*, vol. 126, no. 5, pp. 995–1004, Sep. 2006.

[184] A. Sette, M. Moutaftsi, J. Moyron-Quiroz, M. M. McCausland, D. H. Davies, R. J. Johnston, B. Peters, M. Rafii-El-Idrissi Benhnia, J. Hoffmann, H.-P. Su, K. Singh, D. N. Garboczi, S. Head, H. Grey, P. L. Felgner, and S. Crotty, “Selective CD4+ T cell help for antibody responses to a large viral pathogen: deterministic linkage of specificities.,” *Immunity*, vol. 28, no. 6, pp. 847–58, Jun. 2008.

[185] L. Jing, D. H. Davies, T. M. Chong, S. Chun, C. L. McClurkan, J. Huang, B. T. Story, D. M. Molina, S. Hirst, P. L. Felgner, and D. M. Koelle, “An extremely diverse CD4 response to vaccinia virus in humans is revealed by proteome-wide T-cell profiling.,” *J. Virol.*, vol. 82, no. 14, pp. 7120–34, Jul. 2008.

[186] B. Foster, C. Prussin, F. Liu, J. K. Whitmire, and J. L. Whitton, “Detection of intracellular cytokines by flow cytometry.,” *Curr. Protoc. Immunol.*, vol. Chapter 6, p. Unit 6.24, Aug. 2007.

[187] M. M. Hufford, T. S. Kim, J. Sun, and T. J. Braciale, “Antiviral CD8+ T cell effector activities in situ are regulated by target cell type.,” *J. Exp. Med.*, vol. 208, no. 1, pp. 167–80, Jan. 2011.

[188] H. Li, T. R. Jerrells, G. L. Spitalny, and D. H. Walker, “Gamma interferon as a crucial host defense against Rickettsia conorii in vivo.,” *Infect. Immun.*, vol. 55, no. 5, pp. 1252–5, May 1987.

[189] D. Mason, “A very high level of crossreactivity is an essential feature of the T-cell receptor.,” *Immunol. Today*, vol. 19, no. 9, pp. 395–404, Sep. 1998.

[190] C. Stuehler, N. Khanna, S. Bozza, T. Zelante, S. Moretti, M. Kruhm, S. Lurati, B. Conrad, E. Worschech, S. Stevanović, S. Krappmann, H. Einsele, J.-P. Latgé, J. Loeffler, L. Romani, and M. S. Topp, “Cross-protective TH1 immunity against Aspergillus fumigatus and Candida albicans.,” *Blood*, vol. 117, no. 22, pp. 5881–91, Jun. 2011.

[191] N. Pica and P. Palese, “Toward a universal influenza virus vaccine: prospects and challenges.,” *Annu. Rev. Med.*, vol. 64, pp. 189–202, Jan. 2013.

[192] M. Wiesel and A. Oxenius, “From crucial to negligible: functional $CD8^+$ T-cell responses and their dependence on $CD4^+$ T-cell help.,” *Eur. J. Immunol.*, vol. 42, no. 5, pp. 1080–8, May 2012.

[193] L. E. Brown and A. Kelso, “Prospects for an influenza vaccine that induces cross-protective cytotoxic T lymphocytes.,” *Immunol. Cell Biol.*, vol. 87, no. 4, pp. 300–8.

[194] J. E. Kohlmeier and D. L. Woodland, “Immunity to respiratory viruses.,” *Annu. Rev. Immunol.*, vol. 27, pp. 61–82, Jan. 2009.

[195] M. Kremer, Y. Suezer, A. Volz, T. Frenz, M. Majzoub, K.-M. Hanschmann, M. H. Lehmann, U. Kalinke, and G. Sutter, “Critical role of perforin-dependent CD8+ T cell immunity for rapid protective vaccination in a murine model for human smallpox.,” *PLoS Pathog.*, vol. 8, no. 3, p. e1002557, Jan. 2012.

[196] C. R. Li, P. D. Greenberg, M. J. Gilbert, J. M. Goodrich, and S. R. Riddell, “Recovery of HLA-restricted cytomegalovirus (CMV)-specific T-cell responses after allogeneic bone marrow transplant: correlation with CMV disease and effect of ganciclovir prophylaxis.,” *Blood*, vol. 83, no. 7, pp. 1971–9, Apr. 1994.

[197] P. J. R. Goulder and D. I. Watkins, “Impact of MHC class I diversity on immune control of immunodeficiency virus replication.,” *Nat. Rev. Immunol.*, vol. 8, no. 8, pp. 619–30, Aug. 2008.

[198] J. E. Epstein, K. Tewari, K. E. Lyke, B. K. L. Sim, P. F. Billingsley, M. B. Laurens, A. Gunasekera, S. Chakravarty, E. R. James, M. Sedegah, A. Richman, S. Velmurugan, S. Reyes, M. Li, K. Tucker, A. Ahumada, A. J. Ruben, T. Li, R. Stafford, A. G. Eappen, C. Tamminga, J. W. Bennett, C. F. Ockenhouse, J. R. Murphy, J. Komisar, N. Thomas, M. Loyevsky, A. Birkett, C. V Plowe, C. Loucq, R. Edelman, T. L. Richie, R. A. Seder, and S. L. Hoffman, “Live attenuated malaria vaccine designed to protect through hepatic $CD8^+$ T cell immunity.,” *Science*, vol. 334, no. 6055, pp. 475–80, Oct. 2011.

[199] J. S. Woodworth, Y. Wu, and S. M. Behar, “Mycobacterium tuberculosis-specific CD8+ T cells require perforin to kill target cells and provide protection in vivo.,” *J. Immunol.*, vol. 181, no. 12, pp. 8595–603, Dec. 2008.

[200] P. Gilchuk, C. T. Spencer, S. B. Conant, T. Hill, J. J. Gray, X. Niu, M. Zheng, J. J. Erickson, K. L. Boyd, K. J. McAfee, C. Oseroff, S. R. Hadrup, J. R. Bennink, W. Hildebrand, K. M. Edwards, J. E. Crowe, J. V Williams, S. Buus, A. Sette, T. N. M. Schumacher, A. J. Link, and S. Joyce, “Discovering naturally processed antigenic determinants that confer protective T cell immunity.,” *J. Clin. Invest.*, vol. 123, no. 5, pp. 1976–87, May 2013.

[201] D. Ou, L. A. Mitchell, D. Décarie, S. Gillam, and A. J. Tingle, “Characterization of an overlapping CD8+ and CD4+ T-cell epitope on rubella capsid protein.,” *Virology*, vol. 235, no. 2, pp. 286–92, Sep. 1997.

[202] B. M. Carreno, R. V Turner, W. E. Biddison, and J. E. Coligan, “Overlapping epitopes that are recognized by CD8+ HLA class I-restricted and CD4+ class II-restricted cytotoxic T lymphocytes are contained within an influenza nucleoprotein peptide.,” *J. Immunol.*, vol. 148, no. 3, pp. 894–9, Feb. 1992.

[203] A. M. Wertheimer, C. Miner, D. M. Lewinsohn, A. W. Sasaki, E. Kaufman, and H. R. Rosen, “Novel CD4+ and CD8+ T-cell determinants within the NS3 protein in subjects with spontaneously resolved HCV infection.,” *Hepatology*, vol. 37, no. 3, pp. 577–89, Mar. 2003.

[204] H. Ponta, L. Sherman, and P. A. Herrlich, “CD44: from adhesion molecules to signalling regulators.,” *Nat. Rev. Mol. Cell Biol.*, vol. 4, no. 1, pp. 33–45, Jan. 2003.

[205] B. J. G. Baaten, C.-R. Li, M. F. Deiro, M. M. Lin, P. J. Linton, and L. M. Bradley, “CD44 regulates survival and memory development in Th1 cells.,” *Immunity*, vol. 32, no. 1, pp. 104–15, Jan. 2010.

[206] D. Rai, N.-L. L. Pham, J. T. Harty, and V. P. Badovinac, “Tracking the total CD8 T cell response to infection reveals substantial discordance in magnitude and kinetics between inbred and outbred hosts.,” *J. Immunol.*, vol. 183, no. 12, pp. 7672–81, Dec. 2009.

[207] K. L. Doll, N. S. Butler, and J. T. Harty, “Tracking the total CD8 T cell response following whole Plasmodium vaccination.,” *Methods Mol. Biol.*, vol. 923, pp. 493–504, Jan. 2013.

[208] W. Cui, N. S. Joshi, A. Jiang, and S. M. Kaech, “Effects of Signal 3 during CD8 T cell priming: Bystander production of IL-12 enhances effector T cell expansion but promotes terminal differentiation.,” *Vaccine*, vol. 27, no. 15, pp. 2177–87, Mar. 2009.

[209] V. P. Badovinac and J. T. Harty, “Programming, demarcating, and manipulating CD8+ T-cell memory.,” *Immunol. Rev.*, vol. 211, pp. 67–80, Jun. 2006.

[210] H. M. Feng and D. H. Walker, “Mechanisms of intracellular killing of Rickettsia conorii in infected human endothelial cells, hepatocytes, and macrophages.,” *Infect. Immun.*, vol. 68, no. 12, pp. 6729–36, Dec. 2000.

[211] L. M. Wakim, A. Woodward-Davis, R. Liu, Y. Hu, J. Villadangos, G. Smyth, and M. J. Bevan, “The molecular signature of tissue resident memory CD8 T cells isolated from the brain.,” *J. Immunol.*, vol. 189, no. 7, pp. 3462–71, Oct. 2012.

[212] S.-W. Tse, I. A. Cockburn, H. Zhang, A. L. Scott, and F. Zavala, “Unique transcriptional profile of liver-resident memory CD8+ T cells induced by immunization with malaria sporozoites.,” *Genes Immun.*, vol. 14, no. 5, pp. 302–9.

[213] K. A. O’Connell and M. Edidin, “A mouse lymphoid endothelial cell line immortalized by simian virus 40 binds lymphocytes and retains functional characteristics of normal endothelial cells.,” *J. Immunol.*, vol. 144, no. 2, pp. 521–5, Jan. 1990.

[214] A. Reyes-Sandoval, D. H. Wyllie, K. Bauza, A. Milicic, E. K. Forbes, C. S. Rollier, and A. V. S. Hill, "CD8+ T effector memory cells protect against liver-stage malaria.," *J. Immunol.*, vol. 187, no. 3, pp. 1347–57, Aug. 2011.

[215] L. Bozzacco, C. Trumpfheller, F. P. Siegal, S. Mehandru, M. Markowitz, M. Carrington, M. C. Nussenzweig, A. G. Piperno, and R. M. Steinman, "DEC-205 receptor on dendritic cells mediates presentation of HIV gag protein to CD8+ T cells in a spectrum of human MHC I haplotypes.," *Proc. Natl. Acad. Sci. U. S. A.*, vol. 104, no. 4, pp. 1289–94, Jan. 2007.

[216] G. Blanc, M. Ngwamidiba, H. Ogata, P.-E. Fournier, J.-M. Claverie, and D. Raoult, "Molecular evolution of rickettsia surface antigens: evidence of positive selection.," *Mol. Biol. Evol.*, vol. 22, no. 10, pp. 2073–83, Oct. 2005.

[217] I. R. Henderson and J. P. Nataro, "Virulence functions of autotransporter proteins.," *Infect. Immun.*, vol. 69, no. 3, pp. 1231–43, Mar. 2001.

[218] F. Jacob-Dubuisson, R. Fernandez, and L. Coutte, "Protein secretion through autotransporter and two-partner pathways.," *Biochim. Biophys. Acta*, vol. 1694, no. 1–3, pp. 235–57, Nov. 2004.

[219] M. Pizza, V. Scarlato, V. Masignani, M. M. Giuliani, B. Aricò, M. Comanducci, G. T. Jennings, L. Baldi, E. Bartolini, B. Capecchi, C. L. Galeotti, E. Luzzi, R. Manetti, E. Marchetti, M. Mora, S. Nuti, G. Ratti, L. Santini, S. Savino, M. Scarselli, E. Storni, P. Zuo, M. Broeker, E. Hundt, B. Knapp, E. Blair, T. Mason, H. Tettelin, D. W. Hood, A. C. Jeffries, N. J. Saunders, D. M. Granoff, J. C. Venter, E. R. Moxon, G. Grandi, and R. Rappuoli, "Identification of vaccine candidates against serogroup B meningococcus by whole-genome sequencing.," *Science*, vol. 287, no. 5459, pp. 1816–20, Mar. 2000.

VITA

Erika Caro Gomez was born in Medellin, Colombia on April 2, 1977. She is the first-born daughter of Maria Dolores Gomez Restrepo and Antonio Jose Caro Rueda. Erika graduated from Liceo Nacional Femenino Javiera Londono in 1994. In 1999 she earned her B.Sc. in Bacteriology and Clinical Laboratory Sciences from Universidad de Antioqiuia in Medellin. As an undergraduate she was involved in clinical research studying the complications of the Crotalinae subfamily snakebites. Erika began her graduate training after joining the Medical and Experimental Mycology Laboratory at the Corporacion para Investigaciones Biologicas in Medellin; in 2003 she received her M.Sc. in Biomedical Basic Sciences. Her thesis research was focused on the study of the mechanisms of adherence of *Paracoccidioides brasiliensis* conidia to extracellular matrix proteins and type II alveolar cells. After joining Dr. Gustavo Valbuena's laboratory, Erika began her doctoral training at the University of Texas Medical Branch in Galveston, TX, in 2009. Her dissertation research is focused in the identification of rickettsial protective antigens using a reverse vaccinology approach for developing a T-cell based vaccine.

Education

B.Sc., Bacteriology and Clinical Laboratory, Universidad de Antioquia, Medellin, Colombia. July, 1999.

M.Sc., Biomedical Basic Science: Immunology, Universidad de Antioquia, Medellin, Colombia. November, 2003.

Peer-Reviewed Publications

Gazi M, **Caro-Gomez E**, Goez Y, Cespedes MA, Hidalgo M, Correa P, Valbuena G. 2013. Discovery of a Protective *Rickettsia prowazekii* Antigen Recognized by CD8+ T Cells, RP884, Using an *In Vivo* Screening Platform. PLoS ONE 8:e76253.

Caro E, González A, Muñoz C, Urán ME, Restrepo A, Hamilton AJ, Cano LE. 2008. Recognition of laminin by *Paracoccidioides brasiliensis* conidia: a possible mechanism of adherence to human type II alveolar cells. Med Mycol. 46:795-804

González A, **Caro E**, Muñoz C, Restrepo A, Hamilton AJ, Cano LE. 2008. *Paracoccidioides brasiliensis* conidia recognize fibronectin and fibrinogen which subsequently participate in adherence to human type II alveolar cells: Involvement of a specific adhesin. Microb Pathog. 44:389-401.

González A, Aristizábal BH, **Caro-Gomez E**, Restrepo A, Cano LE. 2004. Short report: Inhibition by tumor necrosis factor-alpha-activated macrophages of the transition of *Paracoccidioides brasiliensis* conidia to yeast cells through a mechanism independent of nitric oxide. Am J Trop Med Hyg. 71:828-30.

González A, Aristizábal BH, **Caro E**, Restrepo A, Cano LE. 2003. Production of nitric oxide and TNF-α, and expression of iNOS and NFκB in peritoneal macrophages activated with interferon gamma. Ann Rev Biomed Sci, 4: 133-139.

Otero R, Gutiérrez J, Mesa MB, Duque E, Rodríguez O, Arango JL, Gómez F, Toro A, Cano F, Rodríguez LM, **Caro E**, Martínez J, Cornejo W, Gómez LM, Uribe FL, Cárdenas S, Núñez V, Díaz A. 2002. Complications of *Bothrops, Porthidium* and *Bothriechis* snakebites in Colombia. A clinical and epidemiological study of 39 cases attended in a universitary hospital. Toxicon, 40: 1107-1114.

Caro-Gomez E, Gazi M, Cespedes MA, Goez Y, Texeira B, Valbuena G. 2014. Phenotype of the Anti-*Rickettsia* $CD8^+$ T cell response suggests cellular correlates of protection for the assessment of novel antigens. Vaccine, in press.

Caro-Gomez E, Gazi M, Goez Y, Valbuena G. 2014. Discovery of novel cross-protective *Rickettsia prowazekii* T-cell antigens using a combined reverse vaccinology and *in vivo* screening approach. Vaccine, in press.

Abstracts

Caro-Gomez E, Cespedes MA, Texeira B, Gazi M, Valbuena G. Characterization of the CD8+ T cell response in rickettsial infections. American Association of Immunologists Annual Meeting. Poster. Honolulu, Hawaii, USA. May 3-7, 2013.

Cespedes MA, **Caro-Gomez E**, Gazi M, Valbuena G. Characterization of the CD8+ T cell response in rickettsial infections. 25th Meeting of the American Society for Rickettsiology. Poster. Park City, Utah, USA. July 28-31, 2012.

Caro-Gomez E, Gazi M, Cespedes MA, Valbuena G. Identification of rickettsial vaccine candidates encompassing T cell epitopes using an *in silico* approach. 25th Meeting of the American Society for Rickettsiology. Poster. Park City, Utah, USA. July 28-31, 2012.

Caro-Gomez E, Wikel SK, Boppana VD, Cespedes MA, Goez-Rivillas Y, Saito T, Gazi M, Valbuena G. Humanized mice for the study of rickettsial infection. 24th Meeting of the American Society for Rickettsiology. Poster. Stevenson, Washington, USA. July 31- August 3, 2010.

Correa P, **Caro E**, Valbuena G. Bone marrow chimeric mice and humanized mice for the study of Rickettsial pathophysiology and immunology. 23rd Meeting of the American Society for Rickettsiology. Poster. Hilton Head Island, South Carolina, USA. August 15-18, 2009.

Keng C, Orejuela L, **Caro-Gómez E**, Correa P, Valbuena G. Realible methods to quantify Typhus group Rickettsiae. 21st Meeting of the American Society for Rickettsiology. Poster. Colorado Springs, Colorado, USA. September 8-11, 2007.

Caro-Gómez E, Urán Jiménez M, Restrepo A, Cano L. Nitrogen and oxygen radicals contribute to the fungistatic and fungicidal activity exerted by macrophages against *Paracoccidioides brasiliensis*. 16th Congress of the International Society of Human and Animal Mycology (ISHAM). Poster. Paris, France. July 23-27, 2006.

González A, **Caro E**, Gómez B, Díez S, Hernández O, Restrepo A, Hamilton AJ, Cano LE. Interactions of extracellular matrix proteins with *Paracoccidioides brasiliensis.* IX International

Meeting on Paracoccidioidomycosis. Oral presentation. Aguas de Lindóia, Sao Paulo, Brazil. October 2-5, 2005.

Caro, Martha Urán, Claudia Vanegas, Angela Restrepo, Andrew John Hamilton and Luz Elena Cano. Interaction between *Paracoccidioides brasiliensis* conidia and type II alveolar cells: Preliminary results. 12th International Congress of Immunology. Poster. Montreal, Canadá. July 18-23, 2004.

Caro E, Hamilton AJ, Restrepo A, Cano LE. Interactions between laminin and *Paracoccidioides brasiliensis* conidia. 15th Congress of the International Society of Human and Animal Mycology (ISHAM). Oral presentation. San Antonio, Texas, USA. May 25-29, 2003.

González A, **Caro E**, Hamilton AJ, Ortiz B, Restrepo A, Cano LE. Interactions between fibronectin and *Paracoccidioides brasiliensis*: evidence for the presence of a binding molecule on the surface of mycelial but not on the yeast form cells. 15th Congress of the International Society of Human and Animal Mycology (ISHAM). Poster. San Antonio, Texas, USA. May 25-29, 2003.

Caro E, Hamilton AJ, Restrepo A, Cano LE. Adherence of *Paracoccidioides brasiliensis* conidia to extracellular matrix proteins. VIII International Meeting on Paracoccidioidomycosis, "Prof. Carlos da Silva Lacaz". Poster. In: ARBS, Annual Review of Biomedical Sciences, pp 66. Pirenópolis, Goiás, Brazil. June 25-28, 2002.

Urán ME, **Caro E**, González A, Barrera LF, Restrepo A, Cano LE. Th1-Th2 cytokine expression in the lungs of BALB/c mice infected intranasally with *Paracoccidioides brasiliensis* conidia. Relation to the inducible nitric oxide synthase. VIII International Meeting on Paracoccidioidomycosis, "Prof. Carlos da Silva Lacaz". Poster. In: ARBS, Annual Review of Biomedical Sciences, pp 100. Pirenópolis, Goiás, Brazil. June 25-28, 2002.

González A, Urán ME, Aristizabal BH, **Caro E**, Sahaza JH, Restrepo A, Cano LE. "Production and expresión of TNF-α, iNOS and NFκB in peritoneal macrophages and in mice with *Paracoccidioides brasiliensis* conidia". VIII International Meeting on Paracoccidioidomycosis, "Prof. Carlos da Silva Lacaz". Poster. In: ARBS, Annual Review of Biomedical Sciences, pp 97. Pirenópolis, Goiás, Brazil. June 25-28, 2002.

Caro E, Cock AM, Ruíz AC, Jiménez R, Alvarez DL, Restrepo A, Cano LE. Expression of Inducible Nitric Oxide Synthase (iNOS) in Murine Paraccoccidioidomycosis (PCM). Poster. American Society for Microbiology, 102nd General Meeting. Salt Lake City, Utah, USA. May 19-23, 2002.

Otero R, Gutiérrez J, Rodríguez O, Mesa MB, Duque E, Arango JL, Gómez F, Toro A, Cano F, Rodríguez LM, **Caro E**, Martínez J, Cornejo W, Gómez LM, Uribe FL, Cárdenas S, Núñez V, Díaz A. Complicaciones del accidente bothrópico en Colombia. Estudio clínico y epidemiológico de 39 casos atendidos durante un año en un hospital universitario. Oral presentation. V Reunión de expertos en envenenamiento por animales ponzoñosos. Puebla de los Angeles, México. March 29-31, 2001.

Otero R, Galeano A, Bolívar J, Gutiérrez J, Rodríguez O, Mesa MB, Duque E, Arango JL, Gómez F, Toro A, Miranda E, Pinto M, Buendía H, Cano F, Rodríguez LM, **Caro E**, Martínez J, Cornejo W, Gómez LM, Uribe FL, Cárdenas S. Current aspects of snakebites in Colombia. Proposal of intervention for a serious health public problem in Antioquia and Chocó. Poster. XV International Congress for Tropical Medicine and Malaria. Cartagena, Colombia. August 20-25, 2000.

This dissertation was typed by Erika Caro Gomez.